INVESTIGATION OF ATMOSPHERIC REACTIVITIES OF SELECTED CONSUMER PRODUCT VOCs

Final Report to California Air Resources Board
Contract 95-308

By

William P. L. Carter, Dongmin Luo, and Irina L. Malkina

May 30, 2000

College of Engineering
Center for Environmental Research and Technology
University of California
Riverside, California 92521

00-AP-RT4P-002-FR

ABSTRACT

A series of environmental chamber experiments and computer model calculations were carried out to assess the atmospheric ozone formation potentials of selected organic compounds representative of those emitted from consumer products. This information is needed to reduce the uncertainties of ozone reactivity scales for stationary source emissions. The compounds studied were cyclohexane, cyclohexane, isopropyl alcohol, the three octanol isomers, diethyl ether, methyl ethyl ketone, cyclohexanone, methyl isobutyl ketone, ethyl acetate, methyl isobutyrate, n-butyl acetate, and propylene glycol methyl ether acetate. "Incremental reactivity" experiments were carried out to determine the effect of each compound on O_3 formation, NO oxidation and integrated OH radical levels when added to irradiations of reactive organic gas (ROG) - NO_x mixtures representing simplified polluted urban atmospheres. Differing ROG surrogates and ROG/NO_x ratios were employed to test how the impacts of the compounds vary with chemical conditions. In addition, single compound - NO_x irradiations were carried out for the various ketones, OH radical rate constants were measured for the octanol isomers and propylene glycol methyl ether acetate, and the yields of the C_8 carbonyl products were determined for each of the octanol isomers.

The results of these experiments were used in the development and testing of the SAPRC-99 mechanism that is documented in detail in a separate report (Carter, 2000). The data obtained, in conjunction with results of industry-funded studies of related compounds, has resulted in significantly reduced uncertainties in estimates of ozone impacts of the wide variety of oxygenated compounds present in consumer product emissions inventories. However, uncertainties still remain, and information is still inadequate to estimate ozone impacts for other classes of emitted compounds, such as amines and halogenated organics.

ACKNOWLEDGEMENTS

The authors wish to acknowledge the major role played by Randy Pasek of California Air Resources Board (CARB) and the CARB's Reactivity Research Advisory Committee in overseeing this project and providing input on the choices of compounds to be studied. Helpful contributions and support by Eileen McCauley of the CARB during the later periods of this project are also gratefully acknowledged. The authors also thank Roger Atkinson of the Air Pollution Research Center at the University of California at Riverside (UCR) for helpful discussions and also for generously providing the methyl nitrite used in the kinetic and product yield studies.

The following people contributed significantly to the experiments discussed in this report. Dennis Fitz provided major assistance to the administration of this program and oversight of the laboratory and the experiments. Kurt Bumiller assisted with the maintenance of the instrumentation and carrying out of many of the experiments. Jodi Powell did most of the experimental work on the kinetic and product yield studies. Kathalena M.Smihula, Amy Lishan Ng, Thomas Cheng assisted in carrying out the experiments at various times during the course of this project.

This work was carried out under funding by the California Air Resources Board through Contract 95-308. However, the opinions and conclusions in this document are entirely those of the first author. Mention of trade names and commercial products does not constitute endorsement or recommendation for use.

TABLE OF CONTENTS

LIST OF TABLES vi
LIST OF FIGURES vii
EXECUTIVE SUMMARY ix

I. INTRODUCTION 1
A. Background and Objectives 1
B. Compounds Chosen for Study 2

II. METHODS 5
A. Overall Experimental Approach 5
1. Incremental Reactivity Experiments 5
a. Mini-Surrogate Experiments 5
b. Full Surrogate Experiments 5
c. Low NO_x Full Surrogate Experiments 6
2. Single compound - NO_x Experiments 6
3. Control and Characterization Runs 6
4. Kinetic and Product Yield Experiments 7
B. Environmental Chambers 8
C. Experimental Procedures 9
1. Environmental Chamber Experiments 9
2. Kinetic Experiments 10
3. Product Yield Experiments 11
D. Analytical Methods 11
E. Characterization Methods 12
1. Temperature 12
2. Xenon Arc Light Source 12
3. Blacklight Light Source 12
4. Dilution 14
F. Reactivity Data Analysis Methods 14
G. Modeling Methods 15
1. Gas-Phase Mechanism 15
2. Environmental Chamber Simulations 16

III. RESULTS AND DISCUSSION 19
A. Kinetic and Product Yield Studies 19
1. Relative Rate Constant Measurements 20
2. Octanol Product Yield Measurements 25
B. Environmental Chamber Results 27
1. Characterization Results 27
a. Light Characterization Results for the DTC 27
b. Light Characterization Results for the CTC 28
c. Radical Source Characterization Results 32
d. Results of Other Characterization and Control Runs 33

2. Mechanism Evaluation Results 35
a. Cyclohexane 36
b. Methyl Ethyl Ketone 39
c. Cyclohexanone 42
d. Methyl Isobutyl Ketone 44
e. Isopropyl Alcohol 44
f. Octanol Isomers 45
g. Diethyl Ether 47
h. Ethyl Acetate 47
i. Methyl Isobutyrate 51
j. Butyl Acetate 53
k. Propylene Glycol Methyl Ether Acetate 55
l. Diacetone Alcohol 55

IV. CONCLUSIONS 57

V. REFERENCES 59

APPENDIX A. MECHANISM AND DATA TABULATIONS 63

LIST OF TABLES

Table 1. List of gas chromatographic instruments used in this program and compounds used to monitor each. 13

Table 2. Chamber wall effect and background characterization parameters used in the environmental chamber model simulations for mechanism evaluation 17

Table 3. Summary of results of the OH radical rate constant measurements, and comparison with literature and estimated rate constants. 24

Table 4. Summary of octanol product yields measured in this work, and comparison with the estimated product yields. 27

Table 5. Codes used to designate types of experiments in tabulations of results. 29

Table 6. Results of ozone dark decay experiments. 38

Table A-1. Listing of the mechanisms used to represent the test VOCs when modeling the experiments carried out for this project. See Carter (2000) for a full listing of the base mechanism and the mechanisms used to represent the VOCs in the base case and control and characterization experiments. 63

Table A-2. Tabulation of data obtained in the relative rate constant determination experiments. 66

Table A-3. Measured reactant and measured and corrected product data obtained during the experiments to determine the octanal yields from 1-octanol and the 2-octanone yields from 2-octanol. 69

Table A-4. Measured reactant and measured and corrected product data obtained during the experiments to determine the 3-octanone yields from 3-octanol. 69

Table A-5. Measured reactant and measured and corrected product data obtained during the experiments to determine the 4-octanone yields from 4-octanol. 70

Table A-6. Chronological listing of the DTC experiments carried out for this program. 71

Table A-7. Chronological listing of the CTC experiments carried out for this program. 74

Table A-8. Summary of the conditions and results of the environmental chamber experiments carried out for this program. 75

Table A-9. Summary of experimental incremental reactivity results. 80

LIST OF FIGURES

Figure 1. Plots of Equation (IV) for the relative rate constant measurements for the octanol isomers. 21

Figure 2. Plots of Equation (IV) for the relative rate constant measurements for the octanol products. 22

Figure 3. Plots of Equation (IV) for the relative rate constant measurements for propylene glycol methyl ether (PGME) acetate, methyl isobutyrate, n-octane, and o-xylene. 23

Figure 4. Plots of corrected product yields versus amounts of octanol reacted in the octanol product yield determination experiments. 26

Figure 5. Plots of results of actinometry experiments against DTC run number, showing NO_2 photolysis rate assignments used for modeling purposes. 30

Figure 6. Plots of results of light intensity measurements against CTC run number for all experiments carried out to date in this chamber. 31

Figure 7. Plots of Representative average spectral distributions for the CTC chamber, and ratios of the relative intensities for the latest CTC runs relative to those for the initial experiments, against wavelength. 32

Figure 8. Radical source parameters that gave the best fits to the results of the n-butane - NO_x and CO - NO_x experiments used to characterize the conditions of the DTC during the period of this project. 34

Figure 9. Radical source parameters that gave the best fits to the results of the n-butane - NO_x and CO - NO_x experiments used to characterize the conditions of the CTC during the period of this project. 35

Figure 10. Experimental and calculated concentration-time plots for the $\Delta([O_3]-[NO])$ and propene data in the propene - NO_x control experiments in the DTC. 36

Figure 11. Experimental and calculated concentration-time plots for the $\Delta([O_3]-[NO])$ and propene or formaldehyde data for the propene - NO_x and formaldehyde - NO_x control experiments in the CTC. 37

Figure 12. Experimental and calculated concentration-time plots for the $\Delta([O_3]-[NO])$ and m-xylene data in the surrogate - NO_x side equivalency test experiments. 37

Figure 13. Experimental and calculated concentration-time plots for the O_3 data for the pure air and the acetaldehyde - air irradiations carried out during this program. 38

Figure 14. Plots of experimental and calculated results of the incremental reactivity experiments with cyclohexane. 39

Figure 15. Plots of experimental and calculated $\Delta([O_3]-[NO])$, formaldehyde, and acetaldehyde data for the methyl ethyl ketone (MEK) - NO_x experiments. 40

Figure 16. Plots of experimental and calculated results of the incremental reactivity experiments with methyl ethyl ketone. 41

Figure 17. Plots of experimental and calculated $\Delta([O_3]-[NO])$ results for the cyclohexanone - NO_x experiments. 42

Figure 18. Plots of experimental and calculated results of the incremental reactivity experiments with cyclohexanone. 43

Figure 19. Plots of experimental and calculated $\Delta([O_3]-[NO])$ and formaldehyde data for the methyl isobutyl ketone - NO_x experiments 45

Figure 20. Plots of experimental and calculated results of the incremental reactivity experiments with methyl isobutyl ketone 46

Figure 21. Plots of experimental and calculated results of the incremental reactivity experiments with isopropyl alcohol. 46

Figure 22. Plots of experimental and calculated results of the incremental reactivity experiments with 1-, 2-, and 3-octanols. 48

Figure 23. Plots of experimental and calculated results of the incremental reactivity experiments with diethyl ether. 49

Figure 24. Plots of experimental and calculated results of the incremental reactivity experiments with ethyl acetate. 50

Figure 25. Plots of experimental and calculated results of the incremental reactivity experiments with methyl isobutyrate. 51

Figure 26. Plots of experimental and calculated formaldehyde and acetone data for the incremental reactivity experiments with methyl isobutyrate. 52

Figure 27. Plots of experimental and calculated results of the incremental reactivity experiments with butyl acetate. 54

Figure 28. Plots of experimental and calculated results of the incremental reactivity experiments with propylene glycol methyl ether acetate. 55

EXECUTIVE SUMMARY

Background

Control strategies that take into account the fact that volatile organic compounds (VOCs) can differ significantly in their effects on ground-level ozone formation can potentially achieve ozone reductions in a more cost-effective manner than those that treat all VOCs equally. Such regulations require a means to quantify relative ozone impacts of VOCs. Because of the complexity of the atmospheric reactions of most VOCs and the fact that their ozone impacts depend on environmental conditions, the only practical way to do this is to develop chemical mechanism for them and use them in airshed models to calculate these impacts. Environmental chamber experiments play an essential role in providing the data necessary to test and verify the predictive capabilities of the mechanisms used in such models. However, until recently most such research has focused on the types of VOCs that are present in mobile sources, and the many other classes of VOCs in stationary sources have not been adequately studied. Because of this, the CARB contracted us to carry out an experimental and modeling study to reduce the uncertainties in estimations of atmospheric reactivities of VOCs present in consumer product emissions. The compounds studied were chosen in consultation with the CARB and the CARB's Reactivity Research Advisory Committee. The data obtained provided major input to the development of the SAPRC-99 mechanism, which was used to derive an updated Maximum Incremental Reactivity (MIR) scale that the CARB plans to use in its consumer product regulations.

Methods

For each compound studied, a series of environmental chamber experiments were carried out to determine their effects on O_3 formation, NO oxidation and integrated OH radical levels. Large volume dual reactor environmental chambers with either blacklight or xenon arc light sources were used for the 6-hour irradiations. The compounds monitored included O_3, NO, NO_x, the organic reactants, and simple oxygenated products. Control and characterization runs were carried out to characterize the conditions of the experiments for mechanism evaluation. OH radical rate constants were measured for the octanol isomers and propylene glycol methyl ether acetate, and the yields of the C_8 carbonyl products were determined for the octanol isomers. The results were used in the development and evaluation of the SAPRC-99 mechanism as documented by Carter (2000).

Results

Cyclohexane was studied because cyclic alkanes are important in the inventory and because mechanism evaluation data for them were limited. Isopropyl alcohol was studied because if its importance in the inventory and because of inconsistent results of previous reactivity experiments. Diethyl ether was studied not only because it is present in stationary source inventories but also to evaluate general estimation methods for reactions involving ether groups. In all these cases the model performance in simulating the data was generally satisfactory and no adjustments to the mechanism were made.

Methyl ethyl ketone, methyl isobutyl ketone and cyclohexanone were studied because ketones are important in the inventory, and previously all higher ketones were represented in the model using a highly approximate treatment. Satisfactory fits of the model to the data were obtained after adjusting overall photolysis quantum yields. These data, combined with data for 2-pentanone and 2-heptanone obtained

under separate funding, indicate that the ketone photolysis quantum yields decrease with the size of the molecule. Fair fits of model simulations to the cyclohexanone data were obtained after some adjustments to the mechanism, but mechanistic studies may be needed to reduce the uncertainties.

The octanol isomers were studied because higher C_{8+} compounds with alcohol groups are important in the inventory and data were needed to evaluate mechanism estimation methods for these compounds. The OH radical rate constants and the octanone yield data indicate that the current rate constant estimation methods for these compounds may need to be refined. The model fit the reactivity data reasonably well after incorporating the kinetic and product data obtained in this study. The fact that no adjustments were needed concerning overall nitrate yield tends to support the validity of current nitrate yield estimates, which is important because previous mechanisms had inconsistencies in this regard.

Ethyl acetate, n-butyl acetate and methyl isobutyrate were studied because data on reactivities of esters are limited. The data for ethyl acetate could only be explained if a previously unknown reaction, of the type RCH(O·)-O-C(O)-R' → RC(O)· + R-C(O)OH, was invoked. This hypothesis was subsequently confirmed by Tuazon et al (1998). Once this reaction, was incorporated, good fits of model simulations to the ethyl and butyl acetate data were obtained without further adjustment, though some adjustments had to be made for methyl isobutyrate. Because n-butyl acetate has a relatively complex mechanism with a number of uncertain branching ratios, it was one of the compounds chosen for a comprehensive uncertainty analysis by Milford and co-workers (Wang et al, 2000).

Propylene Glycol Methyl Ether Acetate was studied because it is in the inventories and mechanisms for compounds with multiple functional groups needed to be evaluated. The OH radical rate constant was measured was found to be a factor of 1.6 lower than estimated by structure-reactivity methods. The model using this rate constant fit the reactivity data reasonably well without further adjustment, which tends to validate the performance of the estimation methods for such compounds.

Conclusions

This project was successful in generating useful data to reduce uncertainties in ozone reactivity impacts for major classes of stationary source VOCs. Its particular utility has been to provide data needed for higher molecular weight oxygenated compounds. It has permitted the development and evaluation of mechanism estimation methods that now can be used to estimate ozone impacts for a wide variety of such compounds for which no data are available (Carter, 2000). In general, these data tended to verify that the estimation and mechanism generally performs surprisingly well considering all the uncertainties involved.

Although the data from this project has reduced uncertainties in overall reactivity predictions, significant uncertainties remain. Results suggest that refinements are needed to the structure-reactivity methods for estimating OH reaction rate constants. Recent data where ketone photolysis rates were measured directly indicate that the present model for ketone photolysis is an oversimplification. The nitrate yield estimates that affect reactivity predictions for many compounds are based on adjustments to fit chamber data, and compensating errors due to other uncertainties are a concern. Many of the estimates for the alkoxy radical reactions are uncertain and further research to refine current estimation methods is clearly needed. This study has also not eliminated the need for studies of additional classes of compounds, such as amines and halogenated organics, for which reactivity data are unavailable or inadequate.

I. INTRODUCTION

A. Background and Objectives

Many different types of volatile organic compounds (VOCs) are emitted into the atmosphere, each reacting at different rates and with different mechanisms. Because of this, VOCs can differ significantly in their effects on ozone formation, or their "reactivities". Therefore, VOC control strategies that take reactivity into account can potentially achieve ozone reductions in a more cost-effective manner than strategies that treat all non-exempt VOCs equally. Reactivity-based control strategies have already been implemented in the California Clean Fuel/Low Emissions Vehicle (CF/LEV) regulations (CARB, 1993), and the California Air Resources Board (CARB) is now in the process of developing reactivity-based controls for consumer product emissions.

Implementation of reactivity-based controls requires some means to quantify relative ozone impacts of different VOCs. This can be done using "reactivity scales", where each individual VOC is assigned a number which represents its ozone impact. However, deriving such numbers is not a straightforward matter, and there are a number of uncertainties involved. One source of uncertainty in reactivity scales comes from the fact that ozone impacts of VOCs depend on the environment where the VOC is emitted. The CARB has chosen to use the "Maximum Incremental Reactivity" (MIR) scale in its regulations because it reflects ozone impacts under conditions where VOCs have their greatest impact on ozone (Carter, 1994; CARB, 1993). In addition, the MIR scale has been shown to correspond reasonably well to relative impacts based on integrated ozone or ozone exposure (Carter, 1994; McNair et. al., 1994). A second source of uncertainty is variability or uncertainty in the chemical composition of the VOC source being considered. This is a particular concern in the case of the vehicle regulations because vehicle exhausts are complex mixtures of variable compositions, but is less of a concern for consumer products or stationary sources that involve individual compounds or simple, well-characterized mixtures. Although these factors need to be taken into account when implementing reactivity-based regulations, further discussion of these issues is beyond the scope of this report.

The third source of uncertainty comes from the complexity and uncertainties in the atmospheric processes by which emitted VOCs react to form ozone. Because ozone impacts depend on environmental conditions, the only practical means to assess atmospheric reactivity, and in particular to assess its variability with conditions, is to develop a chemical mechanism for the VOC and use it in an airshed model to calculate its incremental reactivities under various conditions. However, such calculations are no more reliable than the chemical mechanisms upon which they are based. Although the initial atmospheric reaction rates for most VOCs are reasonably well known or at least can be estimated, in many (or most) cases the subsequent reactions are complex and have uncertainties which can significantly affect predictions of atmospheric impacts. Laboratory studies have reduced these uncertainties for many VOCs, and have provided data that can be used to estimate mechanisms for VOCs where mechanistic information is unknown, but significant uncertainties remain. Environmental chamber experiments play an essential role in reactivity quantification by providing the data necessary to test and verify the predictive capabilities of the mechanisms, and in some cases provide the only available means to derive mechanisms for VOCs where available laboratory data or estimation methods are inadequate. However, not all types of VOCs have mechanisms that have been experimentally evaluated, and thus estimates of atmospheric ozone impacts of such VOCs are either not available or are highly uncertain. This makes it difficult to incorporate emissions sources containing such VOCs under reactivity-based regulations.

Until recently, most research on atmospheric reaction mechanisms and reactivities have focused on the types of VOCs that are present in vehicle emissions, which consist primarily of relatively low molecular weight alkanes and alkenes and aromatics, and the simplest oxygenated compounds such as formaldehyde, acetaldehyde, and methanol. This is because of the importance of vehicle emissions in affecting the total VOC burden, and because these compounds tend to be the dominant reactive organic species observed in ambient air samples (e.g., see Jeffries et al, 1989). However, implementation plan modeling has shown that for many urban areas (especially the California South Coast Air Basin) it will not be possible to achieve the ozone standard with controls of vehicle emissions alone, and substantial controls of VOCs from stationary sources such as consumer products will also be necessary. This presents a problem from a reactivity perspective because stationary sources contain many classes of VOCs that are not present in vehicle exhausts, and whose atmospheric reactivities have not been adequately studied. This includes a number of species such as esters, glycols, glycol ethers, higher molecular weight ethers, etc. Unless atmospheric ozone impacts of such compounds can be more reliably predicted, extending reactivity-based controls to stationary sources will be problematic.

Because of this, the CARB contracted the College of Engineering Center of Environmental Research and Technology (CE-CERT) at the University of California to carry out an experimental and modeling study to reduce the uncertainties in estimations of atmospheric reactivities of consumer product VOCs. This project had two major tasks. The first was to carry out environmental chamber and other experiments on selected representatives of consumer product VOCs that have not been adequately studied in order to obtain data needed to derive and evaluate mechanisms for predicting their atmospheric reactivities. The second was to use the results of those experiments and other relevant data (including results of studies on other stationary source compounds we have carried out under private sector funding) to derive chemical mechanisms to estimate atmospheric ozone impacts of these and other stationary source VOCs. To address the second objective, the SAPRC-97 mechanism we developed under previous CARB funding was completely updated, and explicit mechanisms were developed to represent a much wider variety of VOCs than has previously been the case. This updated mechanism is referred to as the SAPRC-99 mechanism, and it is extensively documented in a separate report (Carter, 2000). The SAPRC-99 mechanism was then used to derive updated reactivity scales that incorporate most of the major types of VOCs emitted from stationary sources (Carter, 2000). This includes the updated MIR scale that the CARB plans to use in its consumer product regulations (CARB, 1999).

The purpose of this report is to document the experimental work carried out for this program. Although the experimental results from this project were used in the process of developing and evaluating the SAPRC-99 mechanism, and the report of Carter (2000) indicates how the data were used in mechanism development and the results of the mechanism evaluation, it does not fully document these experiments. This report discusses why the specific compounds studied were chosen, the experimental and data analysis approach, discusses the results obtained, and summarizes the conclusions that were drawn from them.

B. Compounds Chosen for Study

As indicated above, the objectives of the experimental portion of the project was to obtain reactivity data on representative compounds that would be the most useful in reducing uncertainties in reactivity estimates for consumer product VOCs. This would necessarily include compounds that have not been adequately studied previously, and that are either important in current or anticipate future emissions inventories, or will provide data useful for reducing uncertainties in mechanisms for other compounds important in such inventories. Therefore, when choosing the representative compounds to study we

looked not only at their relative contribution to the emissions inventory, but also the extent to which the data obtained would be useful for developing and evaluating general estimation methods needed to derive mechanisms for compounds where such data are not available. The choices for the compounds were made in consultation with the CARB staff and the members of the CARB's Reactivity Research Advisory Committee.

The specific compounds that were judged to be most important for near-term research in reducing uncertainties in reactivity estimates for consumer product emissions are briefly summarized below. Note that some of these were not studied in this project because the necessary near-term research is already covered by other projects.

- Cyclohexane was studied because cyclic alkanes are present in the inventory and mechanism evaluation data for such compounds were limited prior to this project. Cyclohexane was chosen as the simplest representative cycloalkane, and reactivity data for this compound complement data obtained on separate funding on higher molecular weight alkyl cyclohexanes (unpublished data from this laboratory; see also Carter, 2000).

- Esters are given priority because they are also important in the inventory, and until recently there has been essentially no data on their atmospheric reactivity. Data on esters also complement results of studies on glycol ethers being carried out under separate CMA funding because they have similar mechanistic uncertainties and may assist in the development of general estimation methods. Esters of different structures need to be studied to obtain sufficient data to evaluate mechanism estimation methods. Methyl acetate (Carter et al, 1996), t-butyl acetate (Carter et al, 1997a), and methyl pivalate (unpublished results from our laboratory, see Carter, 2000) have been studied under separate funding. Ethyl acetate, n-butyl acetate and methyl isobutyrate were studied for this project to provided needed information on compounds with differing structures.

- Isopropyl alcohol was studied because if its importance in the inventory and because of the inconsistencies between the current model and the existing reactivity data.

- Methyl ethyl ketone (MEK) was studied because it is the most important of the ketones in the inventory, and because the results with acetone suggest that current mechanisms for ketones in general may need to be refined. In addition, MEK is an important surrogate species in the base SAPRC mechanism, and Gery (1991) had recommended that its mechanism needed to better evaluated.

- Higher Ketones are also important in emissions inventories and mechanism evaluation data for ketones other than acetone (which was studied previously by Carter et al, 1993a) and MEK are necessary to develop and evaluate general estimation methods for such compounds. Cyclohexanone was studied to provide data for a representative cyclic ketone, and methyl isobutyl ketone (MIBK) was studied to provide data on an acyclic higher molecular weight ketone. These data were complimented by studies of methyl propyl ketone and 2-pentanone carried out under separate funding (unpublished results from this laboratory; see also Carter, 2000).

- The isomers of octanol were studied because data for such compounds should be useful indicators of the extent to which simple alcohol mechanisms can be estimated from those for the corresponding alkane. Data to evaluate estimation of nitrate yields from the reaction of NO with the hydroxy-substituted peroxy radicals formed in the oxidations of these higher molecular weight alcohols is of particular interest. This is because such peroxy radicals are expected to be formed in the oxidations of alkanes and a wide variety of other VOCs, and in previous versions of

the SAPRC mechanism it had to be assumed that nitrate yields from these radicals was much less than was estimated. In addition to environmental chamber experiments, separate kinetic and mechanistic studies were carried out to obtain the information needed to assess the mechanisms of these compounds and of hydroxy-substituted peroxy radicals they are expected to form.

- Diethyl ether was studied not only because it is present in stationary source inventories but also because it provides a means to evaluate general estimation methods for the effects of ether groups on the mechanisms and reactivities of relatively high molecular weight compounds. Evaluation of nitrate yields from the reactions of NO with peroxy radicals with ether linkages was of particular interest since it is applicable to estimations of reactivities of a wide variety of oxygenated compounds, including glycol ethers.
- Propylene Glycol Methyl Ether Acetate was studied because it is present in emissions inventories and because it provides an example of a compound with more than one type of functional group that is different from glycol ethers. A variety of compounds present in stationary source inventories have more than one functional groups, and the ability of estimation methods based on data for simpler compounds to derive mechanisms for such compounds needs to be better evaluated.
- Diacetone Alcohol (4-methyl, 4-hydroxy-2-pentanone) was chosen for study because it is present in the stationary source inventory and it provides a representation of another type of compound with more than one functional group, for which mechanism evaluation data would be useful. Unfortunately, it was not possible to obtain useful mechanism evaluation data for this compound because of its low volatility combined with its thermal instability.

Despite their importance to the emissions inventory, this project did not include studies of glycols and glycol ethers. Glycol ethers were not studied because fairly comprehensive studies of several representative glycol ethers were being carried out under separate CMA funding, including kinetic and product studies as well as environmental chamber reactivity experiments (unpublished results from this laboratory, see Carter, 2000). Propylene glycol was studied under separate funding (Carter et al, 1997b), and the data obtained tended to validate its relatively straightforward mechanism, once its OH radical rate constant was remeasured. Ethylene glycol was not studied because of its relatively simple estimated mechanism and because of anticipated experimental difficulties. Based on these considerations, and after consultations with the CARB staff and the CARB's Reactivity Research Advisory Committee, it was decided that studies of the compounds listed above were the best use of the resources available for this project.

II. METHODS

A. Overall Experimental Approach

Most of the experiments carried out for this project consisted of environmental chamber experiments designed to provide data to test the ability of model predictions to simulate chemical transformations occurring under controlled simulated atmospheric conditions. In addition, a limited number of experiments were carried out to measure the OH radical rate constants for a few of the compounds studied in this program, and to determine the yields of some of the major products formed in these reactions. The purposes and major features of the various types of experiments employed in this program are summarized below, and the methods employed are discussed in more detail in the following sections.

1. Incremental Reactivity Experiments

Most of the experiments for this program consisted of environmental chamber runs to measure the "incremental reactivities" of the subject VOCs under various conditions. These involve two types of irradiations of model photochemical smog mixtures. The first is a "base case" experiment where a mixture of reactive organic gases (ROGs) representing those present in polluted atmospheres (the "ROG surrogate") is irradiated in the presence of oxides of nitrogen (NO_x) in air. The second is the "test" experiment that consists of repeating the base case irradiation except that the VOC whose reactivity is being assessed is added. The differences between the results of these experiments provide a measure of the atmospheric impact of the test compound, and the difference relative to the amount added is a measure of its reactivity.

To provide data concerning the reactivities of the test compound under varying atmospheric conditions, three types of base case experiments were carried out:

a. Mini-Surrogate Experiments

The "mini-surrogate" experiments employed a simplified ROG surrogate and relatively low ROG/NO_x ratios. Low ROG/NO_x ratios represent "maximum incremental reactivity" (MIR) conditions, which are most sensitive to VOC effects. This is useful because it provides a sensitive test for the model, and also because it is most important that the model correctly predict a VOC's reactivity under conditions where the atmosphere is most sensitive to the VOCs. The ROG mini-surrogate mixture employed consisted of ethene, n-hexane, and m-xylene. (N-octane was used in places of n-hexane in experiments employing methyl ethyl ketone as the test compound because of gas chromatographic interferences.) This surrogate was employed in our previous studies (Carter et al, 1993a,b; 1995a, 1997c), and was found to provide a more sensitive test of the mechanism than the more complex surrogates which more closely represent atmospheric conditions (Carter et al, 1995a). This high sensitivity to mechanistic differences makes the mini-surrogate experiments most useful for mechanism evaluation.

b. Full Surrogate Experiments

The "full surrogate" experiments employed a more complex ROG surrogate under somewhat higher, though still relatively low, ROG/NO_x conditions. While less sensitive to the mechanism

employed, experiments with a more representative ROG surrogate are needed to evaluate the mechanism under conditions that more closely resembling the atmosphere. The ROG surrogate employed was the same as the 8-component "lumped molecule" surrogate as employed in our previous study (Carter et al. 1995a), and consists of n-butane, n-octane, ethene, propene, trans-2-butene, toluene, m-xylene, and formaldehyde. Calculations have indicated that use of this 8-component mixture will give essentially the same results in incremental reactivity experiments as actual ambient mixtures (Carter et al. 1995a).

c. Low NO_x Full Surrogate Experiments

This base case employing the same 8-component "lumped molecule" surrogate as the full surrogate experiments described above, except that lower NO_x levels (higher ROG/NO_x ratios) were employed to represent NO_x-limited conditions. Such experiments are necessary to assess the ability of the model to properly simulate reactivities under conditions where NO_x is low. The initial ROG and NO_x reactant concentrations were comparable to those employed in our previous studies (Carter et al. 1995a).

2. Single compound - NO_x Experiments

For the ketones that were studied for this program, several ketone – NO_x – air experiments were also carried out. Such experiments provide a means to test mechanisms for VOCs with internal radical sources without the complications and uncertainties involved with modeling the reactions of the base ROG surrogate components. These experiments are not useful for evaluating mechanism of VOCs, such as most of the other compounds studied in this program, that do not have significant radical sources in their mechanisms or tend to act as radical inhibitors (Carter and Lurmann, 1990).

3. Control and Characterization Runs

Since the major objective for carrying out the environmental chamber experiments for this program is to provide data to test model predictions using chemical mechanisms, it is essential that the conditions of the experiment, such as light intensity, temperature, dilution, wall effects, etc, be adequately characterized by the model. Otherwise, unsuccessful model simulations of the data may be the result of incorrect characterization of conditions rather than errors in the mechanism being evaluated, or, worse, apparently successful simulations may be caused by incorrect characterization of conditions compensating for errors in the mechanism. Characterization of chamber conditions includes not only making measurements of physical parameters such as temperature, as discussed below in the "Characterization Methods" section, but also periodically carrying out various types of characterization runs (Carter et al, 1995b). These are carried out to determine chamber effects parameters that can not be determined by direct measurement, or to evaluate or verify models for chamber effects that are assumed or derived from other types of experiments. The following types of characterization experiments were carried out during this project:

- Actinometry experiments are carried out to measure light intensity. For this program, these consisted primarily of NO_2 actinometry runs using the quartz tube method of Zafonte et al (1977) modified as discussed by Carter et al (1995b), and Cl_2 actinometry experiments as discussed by Carter et al (1995b,c, 1997c).
- N-Butane - NO_x or CO - NO_x experiments are carried out to measure the chamber radical source (Carter et al, 1982; 1995b,c). The NO oxidation rates observed in these experiments are highly sensitive to the input or radicals from wall effects (presumed to be primarily due to light-induced formation of HONO from NO_2). Modeling the results of these experiments provide the most

reliable method currently available to determine the magnitude of this radical input, which varies from chamber to chamber and from time to time for a given chamber (Carter et al, 1995b,c).

- Ozone dark decay experiments are carried out to measure the rate of loss of ozone to the chamber walls, which is slow but not entirely negligible in the chambers employed in this study. For this program, these experiments were usually carried out with CO present in the chamber as well, so its rate of decay, if any, could be used to determine dilution, which then is used to correct the O_3 decay data to determine the actual wall loss.
- Pure air irradiations are carried out to test the model for background effects. The results of these experiments are sensitive to NO_x offgasing, offgasing of reactive VOC species, and, to a lesser extent, the chamber radical source (Carter et al, 1995b).
- Acetaldehyde - Air irradiations are carried out to determine the NO_x offgasing rates in the chamber. O_3 and PAN formation in these experiments is highly sensitive to any NO_x offgasing that occurs, since they cannot be formed if NO_x is absent. The PAN analysis method was not reliable during the period of this project, so the O_3 data were used as the primary method to evaluate the NO_x offgasing model.
- Standard propene - NO_x experiments are carried out for control purposes. These provide a means to evaluate reproducibility of conditions that affect results of high reactivity ozone forming VOC - NO_x experiments. The results are compared with the large existing body of such experiments carried out in this and other chambers to assure that consistent results are obtained when this standard mixture is irradiated. The same mixture is irradiated in both sides of the dual chamber (see below for a discussion of the chamber design) to test for side equivalency.
- Standard reactive organic gas (ROG) surrogate - NO_x experiments are also carried out for control purposes and to assure reproducibility of conditions. As discussed in the following section, these serve as simplified representations of photochemical smog mixtures and are used as the "base case" in the "incremental reactivity" experiments designed to test the effects of adding various compounds to irradiations of these mixtures. Most of these are carried out in conjunction with the incremental reactivity experiments discussed below, but occasionally such runs are carried out with the base case mixture on both sides of the dual chamber, to assess side equivalency. As discussed below, results of such experiments have turned out to be useful in assessing light characterization problems.
- Formaldehyde - NO_x experiments are also carried out from time to time for control purposes. These are simple chemical systems that are sensitive to the model for light intensity and spectrum.

The results of these experiments were generally consistent with such experiments carried out previously, as discussed later in this report.

4. Kinetic and Product Yield Experiments

Several experiments were carried out during the course of this project to measure the rate constants for reactions of some of the compounds studied in this program with OH radicals. This included the four octanol isomers, propylene glycol methyl ether acetate, and the octanol products octanal and the octanone isomers. This information is needed to develop mechanisms for the atmospheric reactions of these compounds and to evaluate estimation methods used to derive OH rate constants for similar compounds in cases where no data are available. Only limited information on OH rate constants for these

compounds could be found in the literature. The relative rate constant method employed is well described in the literature (see Atkinson, 1989, and references therein). It involves generating OH radicals by the photolysis of methyl nitrite, and simultaneously monitoring the consumption of the test compound and a reference compound whose OH radical rate constant is known due to their reactions with OH radicals. Plots of ln ([test compound]$_0$/[test compound]$_t$) vs ln ([reference compound]$_0$/[reference compound]$_t$) should yield a straight line whose slope is the ratio of rate constants. M-xylene was used as the reference compound, and relative rate constants for n-octane and o-xylene were also determined for control purposes.

In addition, several experiments were conducted to determine the yields of octanal from the reaction of OH with 1-octanol and of 2-, 3-, or 4-octanone from 2-, 3-, or 4-octanol. This information is necessary to derive mechanisms for the reactions of OH with these compounds under atmospheric conditions, and to evaluate estimation methods used when deriving these mechanisms for such compounds when no product data are available.

As discussed below, the experiments were carried out using a similar blacklight-irradiated environmental chamber as that used in the reactivity and ketone - NO_x runs, but with methyl nitrite present to serve as an OH radical source.

B. Environmental Chambers

Three environmental chambers were employed in this program, two for the mechanism evaluation experiments and a separate chamber for the kinetic and product yield studies. The two chambers used for mechanism evaluation differed primarily in the type of light source employed. Most of the mechanism evaluation experiments were carried out using the CE-CERT "Dividable Teflon Chamber" (DTC) with a blacklight light source. This consists of two ~6000-liter 2-mil heat-sealed FEP Teflon reaction bags located adjacent to each other and fitted inside an 8' x 8' x 8' framework, and which uses two diametrically opposed banks of 32 Sylvania 40-W BL black lights as the light source. The lighting system in the DTC was found to provide so much intensity that only half the lights were used for irradiation. The air conditioner for the chamber room was turned on before and during the experiments. Four air blowers that are located in the bottom of the chamber were used to help cool the chamber as well as mix the contents of the chamber. The CE-CERT DTC is very similar to the SAPRC DTC and is described in detail elsewhere (Carter et al, 1995b).

The blacklight light source has the advantage of being relatively inexpensive to operate and provides a reasonably good simulation of natural sunlight in the region of the spectrum that is important in affecting most photolysis reactions of importance for non-aromatic VOCs (Carter et al, 1995c). This is therefore appropriate for studies of reactivities of compounds that are not photoreactive and are not believed to form significant yields of photoreactive products whose action spectra are not well characterized. However, for photoreactive compounds such as the ketones studied in this program, it is better to use a chamber with a light source such as xenon arcs, which give a better simulation of sunlight throughout the full spectral range. Therefore, the CE-CERT xenon arc Teflon Chamber (CTC) was used in the experiments to study the reactivities of those compounds.

The CE-CERT CTC consists of two ~3500 –liter 4' x 4' x 8' FEP Teflon reaction bags located adjacent to each other at one end of an 8' x 12' room with reflective aluminum paneling on all surfaces to maximize light intensity and homogeneity. Four 6.5 KW xenon arc lights were mounted on the wall opposite the reaction bags. As discussed elsewhere (Carter et al. 1995c), this light source gives the closest

approximation available of the ground-level solar spectrum for an indoor chamber. The room with the chamber has a sufficiently powerful air conditioning system to remove the heat input caused by the lights to maintain an approximately constant ambient temperature of ~25°C. A movable panel is used to block the lights when they are first turned on and warming up, which is raised to begin the irradiation. The chamber was very similar to the Statewide Air Pollution Research Center's Xenon arc Teflon Chamber (SAPRC XTC) which is described in detail elsewhere (Carter et al. 1995b,c).

Both the DTC and CTC are designed to allow simultaneous irradiations of experiments with and without added test reactants under the same reaction conditions. Since the chambers are actually two adjacent FEP Teflon reaction bags, two mixtures can be simultaneously irradiated using the same light source and with the same temperature control system. These two reaction bags are referred to as the two "sides" of the chambers (Side A and Side B) in the subsequent discussion. The sides are interconnected with two ports, each with a box fan, which rapidly exchange their contents to assure that base case reactants have equal concentrations in both sides. In addition, a fan is located in each of the reaction bags to rapidly mix the reactants within each chamber. The ports connecting the two reactors can then be closed to allow separate injections on each side, and separate monitoring of each side.

A separate blacklight-irradiated chamber was used in the kinetic and product yield experiments. This consists of a single ~3200-liter, 2-mil thick FEP Teflon reaction bag fitted inside an aluminum frame of dimensions of 8 ft x 4 ft x 4 ft. This chamber is similar to the ETC chamber described by Carter et al (1993b, 1995b), except for the orientation of the lights. The light source for the chamber consisted of two diametrically opposed banks of 30 Sylvania 40-W BL blacklamps.

C. Experimental Procedures

1. Environmental Chamber Experiments

The reaction bags were flushed with dry air produced by an Aadco air purification system for 14 hours (6pm-8am) on the nights before experiments. The continuous monitors were connected prior to reactant injection and the data system began logging data from the continuous monitoring systems. The reactants were injected as described below (see also Carter et al, 1993b, 1995b). The common reactants were injected in both sides simultaneously using a three-way (one inlet and two outlets connected to side A and B respectively) bulb of 2 liters in the injection line and were well mixed before the chamber was divided. The contents of each side were blown into the other using two box fans located between them. Mixing fans were used to mix the reactants in the chamber during the injection period, but these were turned off prior to the irradiation. The procedures for injecting the various types of reactants were as follows:

- The NO and NO_2 were prepared for injection using a high vacuum rack. Known pressures of NO, measured with MKS Baratron capacitance manometers, were expanded into Pyrex bulbs with known volumes, which were then filled with nitrogen (for NO) or oxygen (for NO_2). The contents of the bulbs were then flushed into the chamber with nitrogen.
- The gaseous reactants were prepared for injections either using a high vacuum rack or gas-tight syringes. The gas reactants in a gas-tight syringe were usually diluted to 100-ml with nitrogen in a syringe. A MKS Baratron capacitance manometer was used to quantify the amount injected in cases where the vacuum rack was employed.

- To simplify the procedure for the injection of the gaseous organic components of the full surrogate mixture, a cylinder containing n-butane, ethene, propene, and trans-2-butene in the appropriate ratios was purchased for this purpose from Liquid Carbonic Specialty Gases. For full surrogate experiments the desired pressures introduced into a 2.2 liter Pyrex bulb using high vacuum rack, whose contents were then flushed into the chamber.
- The volatile liquid reactants were injected, using a micro syringe, into a 1-liter Pyrex bulb equipped with stopcocks on each end and a port for the injection of the liquid. Then one end of the bulb was attached to the injection port of the chamber and the other to a nitrogen source. The stopcocks were then opened, and the contents of the bulb were flushed into the chamber with a combination of nitrogen and heat gun for approximately 5 minutes.
- A liquid mixture of toluene, n-octane and m-xylene in the appropriate ratios was used simplify the procedure for the injection of the liquid reactants in the full surrogate experiments. Appropriate volumes of this mixture were measured using a microsyringe and injected using the same procedure as discussed above for pure liquids.
- Low volatility liquids such as propylene glycol methyl ether acetate, octanal, and the octanol and octanone isomers were injected by placing the desired quantities of the compound into a heated tube using a microsyringe. Those compounds were then flushed into the chamber, after reaching an elevated temperature with nitrogen leading into the chamber. Longer flushing times were employed for the less volatile compounds.
- Formaldehyde was prepared in a vacuum rack system by heating paraformaldehyde in an evacuated bulb until the pressure corresponded to the desired amount of formaldehyde. The bulb was then closed and detached from the vacuum system and its contents were flushed into the chamber with dry air through the injection port.

After injection of the common reactants and mixing, the fans were turned off to allow their pressures to equalize in the dual reactors, and then they were then separated by closing the ports that connected them. After that, reactants for specific reactors (generally the test compound in the case of reactivity experiments) were injected and mixed. In case of CTC chamber the lights are turned on after lowering a metal baffle between the lights and the reactors, and the lights are allowed to warm up for at least 30 minutes. Irradiation in the chamber is begun by raising the baffle between the lights and the reactors, and the irradiation proceeds for 6 hours. After the run, the contents of the chamber were emptied by allowing the bags to collapse, and then the chamber was flushed with purified air. The contents of the reactors were vented into a fume hood.

2. Kinetic Experiments

The experiments to measure the relative OH radical rate constants were all carried out in separate ~3200-liter blacklight-irradiated chamber. The procedures employed were generally as discussed above for the mechanism evaluation experiments except as noted. The reactants employed usually consisted of ~ 0.5 ppm each of the VOCs whose OH rate constants are being measured and the reference compound (m-xylene), and ~2 ppm of methyl nitrite. The methyl nitrate was synthesized at Roger Atkinson's laboratory at the Air Pollution Research Center (APRC) as described previously (Atkinson et al, 1981), and was transferred to our laboratory in the gas phase using ~0.6 liter Pyrex bulb covered with the black tape. The methyl nitrite was prepared for injection using a high vacuum rack as described above. The contents of the bulb were then flushed into the chamber with the Aadco air after all the reactants were already injected. After the reactants were injected and mixed, the concentrations of the VOC reactants were

monitored by gas chromatography until reproducible concentrations were measured. Then the lights were turned on for brief periods (initially 2.0 - 2.5 minutes, then longer as the experiment progressed) and then turned off. The reactant concentrations were measured between each irradiation. This continued until subsequent irradiations resulted in no change in reactant VOC concentrations. Typically, ~20 minutes of irradiations were carried out during a kinetic experiment.

The experiments typically employed more than one of the test VOCs at a time, though not all could be used in the same experiment because of GC interferences. For example, 2- and 3-octanols had the same GC retention time, so their relative rate constants could not be determined in the same experiment.

3. Product Yield Experiments

The product yield experiments were carried out using the same general procedures as the kinetic runs, except that only a single organic compound was injected, and product as well as reactant concentrations were measured by gas chromatography. A typical experiment employed ~0.5 ppm of octanol and ~2 ppm of methyl nitrite.

D. Analytical Methods

Ozone and nitrogen oxides (NO_x) were continuously monitored using commercially available continuous analyzers with Teflon sample lines inserted directly into the chambers. The sampling lines from each side of the chamber were connected to solenoids that switched from side to side every 10 minutes, so the instruments alternately collected data from each side. Ozone was monitored using a Dasibi Model 1003-AH UV absorption ozone analyzer and NO and total oxides of nitrogen (including HNO_3 and organic nitrates) were monitored using a Teco Model 42 chemilluminescent NO/NO_x monitor. The output of these instruments, along with that from the temperature sensors and the formaldehyde instrument, were attached to a computer data acquisition system, which recorded the data at 10 minutes intervals for ozone, NOx and temperature (and at 15 minutes for formaldehyde), using 30 second averaging times. This yielded a sampling interval of 20 minutes for taking data from each side.

The Teco instrument and Dasibi CO analyzer were calibrated with a certified NO and CO source and CSI gas-phase dilution system. It was done prior to chamber experiment for each run. The NO_2 converter efficiency check was carried out in regular intervals. The Dasibi ozone analyzer was calibrated against transfer standard ozone analyzer using transfer standard method in an interval of three months and was checked with CSI ozone generator for each experiment to assure that the instrument worked properly. The details were discussed elsewhere (Carter et al, 1995b)

Organic reactants other than formaldehyde were measured by gas chromatography with FID detection as described elsewhere (Carter et al. 1993b, 1995b). GC samples were taken for analysis at intervals from 20 minutes to 30 minutes either using 100-ml gas-tight glass syringes or by collecting the 100-ml sample from the chamber onto Tenax-GC solid adsorbent cartridge. These samples were taken from ports directly connected to the chamber after injection, before irradiation, and at regular intervals after the irradiation was started. The sampling method employed for injecting the sample onto the GC column depended on the volatility or "stickiness" of the compound. For analysis of the more volatile species, the contents of the syringe were flushed through a 10-ml and 5-ml stainless steel or 1/8' Teflon tube loop and subsequently injected onto the column by turning a gas sample valve. For analysis of less volatile species, the Tenax GC solid adsorbent cartridges were used, which were then placed into the

injector of the GC to be heated and desorbed onto the head of the cooled column, which was then temperature programmed for analysis.

The compounds monitored by GC during this program and the instruments used are listed on Table 1. In some cases, a given compound can be measured by one instrument. In those cases the data from the "priority" instrument that is judged to give more reliable or higher precision data than the other is used for determining initial concentrations or providing evaluation data for modeling purposes. The priority measurements are indicated on Table 1 by the compound's name being underlined in the list of compounds the instrument is used to monitor.

The calibrations for the GC analyses for most compounds were carried out by sampling from chambers or vessels of known volume into which known amounts of the reactants were injected, as described previously (Carter et al, 1995b).

E. Characterization Methods

1. Temperature

Three temperature thermocouples were used to monitor the chamber temperature, two of which were located in the sampling line of continuous analyzers to monitor the temperature in each side. The third one was located in the outlet of the air conditioning system used to control the chamber temperature. The temperature range in these experiments was typically 25-30 C.

2. Xenon Arc Light Source

The spectrum of the xenon arc light source was measured several (usually five) times during each CTC experiment using a LiCor LI-1800 spectroradiometer. The absolute light intensity in this chamber was measured by "photostationary state" NO_2 actinometry experiments and by Cl_2 actinometry, which in both cases were carried out prior to the period of the experiments discussed in this report. The photostationary state experiments consisted of simultaneous measurements of photostationary state concentrations of NO, NO_2, and O_3 in otherwise pure air, with the NO_2 photolysis rate being calculated from the $[NO][O_3]/[NO_2]$ ratio (Carter et al. 1997c). The Cl_2 actinometry experiments consisted of photolyzing ~0.1 ppm of Cl_2 in ~1 ppm of n-butane, calculating the Cl_2 photolysis rate from the rate of consumption of n-butane, and then calculating the corresponding NO_2 photolysis rate from the absorption cross sections and quantum yields for NO_2 and Cl_2 (assuming unit quantum yields for Cl_2) and the spectral distribution of the light source (Carter et al, 1997c).

Relative trends in light intensity with time are obtained using the quartz tube method of Zafonte et al. (1977), modified as discussed by Carter et al. (1995b; 1997c), and from absolute intensities of spectra taken several times during each run using a Li-Cor LI-1800 spectroradiometer. The results of these experiments were analyzed to determine the NO_2 photolysis rates for modeling as discussed later in this report.

3. Blacklight Light Source

The light intensity in the DTC chamber was monitored by periodic NO_2 actinometry experiments utilizing the quartz tube method of Zafonte et al (1977), with the data analysis method modified as discussed by Carter et al. (1995b). The spectrum of the blacklight light source is periodically measured

Table 1. List of gas chromatographic instruments used in this program and compounds used to monitor each.

Description	Compounds monitored [a]
A Hewlett-Packard 5890 Series II GC with a FID detector and injection system equipped for the Tenax cartridge sampling method. 30 m x 0.53 mm megabore DB-5 column used. Used for experiments prior to July 25, 1997.	n-Octane, Toluene, m-Xylene, 1-Octanol, 2-Octanol, 3-Octanol, Diacetone Alcohol, Propylene Glycol Methyl Ethyl Ether Acetate.
Same as above, but with a 30 m x 0.53 mm megabore DB-1701 column. Used for experiments after July 27, 1997.	n-Octane, Toluene, m-Xylene, 1-Octanol, 2-Octanol, 3-Octanol, 4-Octanol, 2-Octanone, 3-Octanone, 4-Octanone, Propylene Glycol Methyl Ethyl Ether Acetate, Cyclohexanone.
A Hewlett-Packard 5890 Series II GC with a FID detector and an injector set up for loop sampling. 15 m x 0.53 mm DB-5 column used. Used for experiments from April to June 14,1996 and from Oct.3, 1996 to Jan. 27, 1997.	n-Hexane, n-Octane, Cyclohexane, Toluene, m-Xylene, Methyl Ethyl Ketone, Isopropyl Alcohol, Ethyl Acetate, n-Butyl Acetate, Methyl Isobutyl Ketone.
Same as above but with a 30 m x 0.53 mm DB-WAX megabore column. Used between June 14 and September 17, 1996.	n-Octane, Toluene, m-Xylene, Ethyl Acetate, Butyl Acetate, Methyl Isobutyl Ketone, Isopropyl Alcohol.
Same as above but with a 30 m x 0.53 mm GS-Q megabore column. Used between September 17 and October 3, 1996 and after January 27, 1997.	n-Butane, Ethene, Propene, Acetaldehyde, Acetone.
The HP 5890 Series II GC with an ECD detector and a 15 m x 0.53 mm megabore DB-5 column; Loop method was employed	Peroxyacetylnitrate (PAN)
The HP 5890 Series II GC with a FID detector and injector set up for loop sampling method. A 30 m x 0.53 mm megabore GS-Alumina column was employed	n-Butane, n-Hexane, Cyclohexane, Ethene, Propene, trans-2-Butene.
The HP 5890 Series II GC with a FID detector and an injector set up for the loop sampling method. A 15 m x 0.53 mm megabore DB-5 column was employed. Used for runs prior to Sept. 22,1996.	n-Butane, n-Hexane, n-Octane, Cyclohexane, Toluene, m-Xylene, Isopropyl Alcohol, Diethyl Ether, Ethyl Acetate, Methyl Isobutyrate, n-Butyl Acetate, Acetaldehyde, Methyl Ethyl Ketone, Cyclohexanone, Methyl Isobutyl Ketone, 4-Methyl-2-Pentanone.
Same as above but with a 30 m x 0.53 mm megabore DB-5 column. Used for runs after September 22, 1996.	n-Butane, n-Hexane, n-Octane, Cyclohexane, Toluene, m-Xylene, Isopropyl Alcohol, Diethyl Ether, Ethyl Acetate, Methyl Isobutyrate, n-Butyl Acetate, Acetaldehyde, Methyl Ethyl Ketone, Cyclohexanone, Methyl Isobutyl Ketone, 4-Methyl-2-Pentanone, Diacetone Alcohol.

[a] If a compound can be measured on more than one instrument, the compounds name is underlined in the list where the measurement is given priority for analysis or modeling purposes.

using a LiCor LI-1200 spectroradiometer, and found to be essentially the same as the general blacklight spectrum recommended by Carter et al (1995b) for use in modeling blacklight chamber experiments.

4. Dilution

The dilution of the chambers due to sampling is expected to be small because the flexible reaction bags can collapse as samples are withdrawn for analysis. Also, the chamber was designed to operate under slightly positive pressure, so any small leaks would result in reducing the bag volume rather than diluting the contents of the chamber. Information concerning dilution in an experiment can be obtained from relative rates of decay of added VOCs which react with OH radicals with differing rate constants (Carter et al. 1993b; 1995b). Most experiments had a more reactive compounds such as m-xylene and n-octane present either as a reactant or added in trace amounts to monitor OH radical levels. Trace amounts (~0.1 ppm) of n-butane were also added to experiments if needed to provide a less reactive compound for monitoring dilution. In addition, specific dilution check experiments such as CO irradiations were carried out. Based on these results, the dilution rate was found to be negligible in this chamber during this period, being less than 0.3% per hour in all runs, and usually less than 0.1% per hour.

F. Reactivity Data Analysis Methods

As indicated above, most of the experiments for this program consisted of simultaneous irradiation of a "base case" reactive organic gas (ROG) surrogate - NO_x mixture in one of the dual reaction chambers, together with an irradiation, in the other reactor, of the same mixture with added. The results are analyzed to yield two measures of VOC reactivity: the effect of the added VOC on the amount of NO reacted plus the amount of ozone formed, and integrated OH radical levels. These are discussed in more detail below.

The first measure of reactivity is the effect of the VOC on the change in the quantity $[O_3]$-[NO], or $([O_3]_t$-$[NO]_t)$-$([O_3]_0$-$[NO]_0)$, which is abbreviated as $\Delta([O_3]$-[NO]) in the subsequent discussion. As discussed elsewhere (e.g., Johnson, 1983; Carter and Atkinson, 1987; Carter and Lurmann, 1990, 1991, Carter et al, 1993b), this gives a direct measure of the amount of conversion of NO to NO_2 by peroxy radicals formed in the photooxidation reactions, which is the process that is directly responsible for ozone formation in the atmosphere. (Johnson calls it "smog produced" or "SP".) The incremental reactivity of the VOC relative to this quantity, which is calculated for each hour of the experiment, is given by

$$IR[\Delta([O_3]-[NO])]_t^{VOC} = \frac{\Delta([O_3]-[NO])_t^{Test} - \Delta([O_3]-[NO])_t^{Base}}{[VOC]_0} \qquad (I)$$

where $\Delta([O_3]-[NO])_t^{Test}$ is the $\Delta([O_3]$-[NO]) measured at time t from the experiment where the test VOC was added, $\Delta([O_3]-[NO])_t^{Base}$ is the corresponding value from the corresponding base case run, and $[VOC]_0$ is the amount of test VOC added. An estimated uncertainty for IR[$\Delta([O_3]$-[NO])] is derived based on assuming an ~3% uncertainty or imprecision in the measured $\Delta([O_3]$-[NO]) values. This is consistent with the results of the side equivalency test, where equivalent base case mixtures are irradiated on each side of the chamber.

Note that reactivity relative to $\Delta([O_3]$-[NO]) is essentially the same as reactivity relative to O_3 in experiments where O_3 levels are high, because under such conditions $[NO]_t^{Base} \approx [NO]_t^{Test} \approx 0$, so a

change $\Delta([O_3]-[NO])$ caused by the test compound is due to the change in O_3 alone. However, $\Delta([O3]-[NO])$ reactivity has the advantage that it provides a useful measure of the effect of the VOC on processes responsible for O_3 formation even in experiments where O_3 formation is suppressed by relatively high NO levels.

The second measure of reactivity is the effect of the VOC on integrated hydroxyl (OH) radical concentrations in the experiment, which is abbreviated as "IntOH" in the subsequent discussion. This is an important factor affecting reactivity because radical levels affect how rapidly all VOCs present, including the base ROG components, react to form ozone. If a compound is present in the experiment that reacts primarily with OH radicals, then the IntOH at time t can be estimated from (Carter et al, 1993b)

$$\mathrm{IntOH}_t = \frac{\ln([\mathrm{tracer}]_0/[\mathrm{tracer}]_t) - \mathrm{Dt}}{\mathrm{kOH}^{\mathrm{tracer}}} \qquad \text{(II)}$$

where $[\mathrm{tracer}]_0$ and $[\mathrm{tracer}]_t$ are the initial and time t concentrations of the tracer compound, $\mathrm{kOH}^{\mathrm{tracer}}$ its OH rate constant, and D is the dilution rate in the experiments. The latter was found to be small and was neglected in our analysis. The concentration of tracer at each hourly interval was determined by linear interpolation of the experimentally measured values. M-xylene was used as the OH tracer in these experiments because it is a surrogate component present in all experiments, its OH rate constant is known (the value used was 2.36×10^{-11} cm^3 $molec^{-1}$ s^{-1} [Atkinson, 1989]), and it reacts relatively rapidly.

The effect of the VOC on OH radicals can thus be measured by its IntOH incremental reactivity, which is defined as

$$\mathrm{IR[IntOH]}_t = \frac{\mathrm{IntOH}_t^{\mathrm{Test}} - \mathrm{IntOH}_t^{\mathrm{Base}}}{[\mathrm{VOC}]_0} \qquad \text{(III)}$$

where $\mathrm{IntOH}^{\mathrm{Test}}$ and $\mathrm{IntOH}^{\mathrm{Base}}$ are the IntOH values measured at time t in the added VOC and the base case experiment, respectively (Carter et al, 1993b). The results are reported in units of 10^6 min. The uncertainties in IntOH and IR[IntOH] are estimated based on assuming an ~2% imprecision in the measurements of the m-xylene concentrations. This is consistent with the observed precision of results of replicate analyses of this compound.

G. Modeling Methods

1. Gas-Phase Mechanism

The model simulations shown in this report were all carried out using the "SAPRC-99" mechanism, which is documented in detail by Carter (2000). This mechanism represents a complete update of the SAPRC-90 mechanism of Carter (1990), and incorporates recent reactivity data from a wide variety of VOCs, including, but not limited to, those discussed in this report. This includes assignments for ~400 types of VOCs, and can be used to estimate reactivities for ~550 VOC categories. A unique feature of this mechanism is the use of a computerized system to estimate and generate complete reaction schemes for most non-aromatic hydrocarbons and oxygenates in the presence of NO_x, from which condensed mechanisms for the model can be derived. This includes the mechanisms for all the VOCs discussed in this report except for methyl ethyl ketone, which is represented explicitly in the base mechanism. The mechanisms for the more reactive organic products of such VOC are also adjusted based on the generated reactions of the specific products predicted to be formed (Carter, 2000).

The mechanism was evaluated against the results of almost 1700 environmental chamber experiments carried out at the University of California at Riverside, including experiments to test ozone reactivity predictions for over 80 types of VOCs. The experiments discussed in this report comprise an important part of this database, particularly for those types of oxygenated compounds for which evaluation data have been limited.

A listing of the base SAPRC-99 mechanism is given by Carter (2000) and is not reproduced here. However, Table A-1 in Appendix A gives the mechanisms used for the test VOCs that were evaluated in this study, except for methyl ethyl ketone, which is explicitly represented in the base mechanism. Note that most of these species were derived using the "adjusted product" approach, where the mechanisms used to represent the more reactive were derived based on the estimated mechanisms for the specific compounds predicted to be formed. These are represented using the PRD1, PRD2, etc., model species, whose mechanisms in general are different for each VOC whose reactivity is being assessed. The report of Carter (2000) should be consulted for documentation, and for the mechanisms used when representing these VOCs when present in mixtures.

2. Environmental Chamber Simulations

The methods used to conduct the simulations of the environmental chamber experiments discussed in this report are based on those discussed in detail by Carter and Lurmann (1990, 1991), updated as discussed by Carter (1995) and Carter et al (1997c). The photolysis rates were derived from results of NO_2 actinometry experiments and measurements of the relative spectra of the light source, derived as discussed below. The thermal rate constants were calculated using the temperatures measured during the experiments, with the small variations in temperature with time during the experiment being taken into account. The computer programs and modeling methods employed are discussed in more detail elsewhere (Carter et al, 1995b).

In order to use chamber experiments for mechanism evaluation, it is necessary that the model appropriately represent various chamber effects such as O_3 wall loss, the chamber radical source (Carter et al, 1992) and other factors (Carter et al, 1995b). The chamber model and the chamber effects parameters used in this study are the same as those employed by Carter (2000), and are summarized in Table 2. The previous reports of Carter et al (1995b, 1997c) should be consulted for a more detailed discussion of these parameters. Note that the radical source parameters given on Table 2 are based primarily on the results of the radical source characterization experiments discussed below in Section III.B.1.c.

Table 2. Chamber wall effect and background characterization parameters used in the environmental chamber model simulations for mechanism evaluation.

Cham.	Set(s)	Value	Discussion
RN-I (ppb)			Ratio of the rate of wall + hv -> HONO to the NO_2 photolysis rate.
DTC	11	0.080	Average of value of RS-I that gave best fits to n-butane - NO_x or CO - NO_x chamber experiments carried out in this chamber. The initial HONO was optimized at the same time. Although this parameter is expected to depend on temperature (Carter et al, 1995b), but the temperature variation for these experiments is small compared to the run-to-run variability in the best fit RN-I values.
	14	0.082	
	15	0.057	
CTC	1-8	0.064	Same procedure as DTC
	9	0.097	
RS-S (unitless)			Ratio of the rate of NO_2 + hv -> 0.5 HONO + 0.5 wall NO_x to the NO_2 photolysis rate.
DTC and CTC		0	Any dependence of apparent radical source on initial NOx levels in Teflon bag chambers was found to be much less than the run-to-run variability.
HONO-F (unitless)			Ratio of the initial HONO concentration to the measured initial NO2. [The initial NO_2 in the experiment is reduced by a factor of 1 - (HONO-F)]. Unless the characterization data indicate otherwise, it is assumed that the initial HONO is introduced with the NO_2 injection, so is it is assumed to be proportional to the initial NO_2 concentration.
DTC	11	0.6%	Average of value of initial HONO to initial NO2 which gave best fits to n-butane - NOx chamber experiments carried out in this chamber. The RN-I parameter was optimized at the same time.
	14	0.6%	
	15	0.7%	
CTC	All	0.8%	Same procedure as DTC
E-NO2/K1 (ppb)			Ratio of rate of NO_2 offgasing from the walls to the NO_2 photolysis rate.
All Teflon Bag Chambers		0	The NO_x offgasing caused by representing the radical source by HONO offgasing appears to be sufficient for accounting for NO_x offgasing effects in most cases. RN-I parameters adjusted to fit experiments sensitive to the radical source are consistent with NO_x offgasing rates adjusted to fit pure air or aldehyde - air runs, to within the uncertainty and variability.
k(NO2W) (min^{-1})			Rate of unimolecular loss (or hydrolysis) of NO_2 to the walls.
All Teflon Bag Chambers		1.6e-4	Based on dark NO_2 decay and HONO formation measured in the ETC by Pitts et al. (1984). Assumed to be the same in all Teflon bag chambers, regardless of volume.
YHONO			Yield of HONO in the unimolecular reaction (hydrolysis) of NO_2 on the walls.
All Teflon Bag Chambers		0.2	Based on dark NO_2 decay and HONO formation measured in the ETC by Pitts et al. (1984). Assumed to be the same in all Teflon bag chambers, regardless of volume.
k(O3W) (min^{-1})			Unimolecular loss rate of O_3 to the walls.

Table 2 (continued)

Cham.	Set(s)	Value	Discussion
DTC	All	1.5e-4	Based on results of O_3 decay in Teflon bag chambers experiments as discussed by Carter et al (1995b).
CTC	All	8.5e-5	Based on results of O_3 decay experiments in this chamber
k(N26I) (min^{-1})			Rate constant for N_2O_5 -> 2 Wall-NO_x. This represents the humidity-independent portion of the wall loss of N_2O_5, or the intercept of plots of rates of N_2O_5 loss against humidity.
All Teflon Bag Chambers		2.8e-3	Based on N_2O_5 decay rate measurements made by Tuazon et al (1983) for the ETC. Assumed to be independent of chamber size (Carter et al, 1995b).
k(N26S) (ppm^{-1} min^{-1})			Rate constant for N_2O_5 + H_2O -> 2 Wall-NO_x. This represents the humidity dependent portion of the wall loss of N_2O_5, or the slope of plots of rates of N_2O_5 loss against humidity.
All Teflon Bag Chambers		1.1e-6	Based on N_2O_5 decay rate measurements made by Tuazon et al (1983) for the ETC. Assumed to be independent of chamber size (Carter et al, 1995d).
k(XSHC) (min^{-1})			Rate constant for OH -> HO_2. This represents the effects of reaction of OH with reactive VOCs in the background air or offgased from the chamber walls. This parameter does not significantly affect model simulations of experiments other than pure air runs.
All Teflon Bag Chambers		250	Estimated from modeling several pure air in the ITC (Carter et al, 1996b), and also consistent with simulations of pure air runs in the ETC (Carter et al, 1997c).
H2O (ppm)			Default water vapor concentration for runs where no humidity data are available.
DTC and CTC		1.0e+3	Experiments in these chambers were carried out using dried purified air. The limited humidity data for such runs indicate that the humidity was less than 5%, probably no more than ~2.5%, and possibly much less than that. The default value corresponds to ~2.5 - 3% RH for the conditions of most experiments.

III. RESULTS AND DISCUSSION

A. Kinetic and Product Yield Studies

Although the major effort in this program consisted of environmental chamber experiments for mechanism evaluation, a limited number of kinetic and product experiments were conducted to reduce uncertainties in mechanisms for some of the VOCs that were studied. Because reaction with OH radicals is the major initial atmospheric reaction of all the VOCs studied, it is essential that this rate constant be known when developing reliable mechanisms for their atmospheric reactivity. Although the necessary OH rate constant data are available in the literature for most of the compounds studied, this was not the case for three of the four octanol isomers studied or for propylene glycol methyl ether acetate. Therefore, rate constants for the reaction of OH radicals were measured as part of this project. In addition, because results of the measurement of the OH + methyl isobutyrate rate constant by Wyatt et al (1999) were not available at the time this compound was studied for this program, an attempt was also made to measure this rate constant.

In addition, although in general basic mechanistic and product studies were beyond the scope of this project, a limited product study for the reaction of OH radicals with the octanol isomers was carried out. In particular, the yield of the oxygenated product predicted to be formed from the reaction of the OH radicals by abstraction either from the OH group or from the hydrogen bonded to the OH group was determined for each isomer, i.e., via:

$$OH + R_1R_2CHOH \rightarrow R_1R_2CHO\cdot + H_2O$$
$$R_1R_2CHO\cdot + O_2 \rightarrow R_1C(O)R_2 + HO_2$$

$$OH + R_1R_2CHOH \rightarrow R_1R_2C\,(\cdot)OH + H_2O$$
$$R_1R_2C\,(\cdot)OH + O_2 \rightarrow R_1C(O)R_2 + HO_2$$

(Note that for 1-octanol one of the R's is an H, and the product octanal, while for the other isomers the product is the corresponding ketone.) This information is important because it provides a direct indication of the role of peroxy radicals in the photooxidations of these compounds, since reactions at other positions all involve the formation of alkyl radicals that react with O_2 to form peroxy radicals. Alcohols are somewhat unusual among VOCs in that their OH reactions do not necessarily involve peroxy radical formation.

Peroxy radical formation in the octanols was of interest because one of the objectives of conducting reactivity experiments for the octanols was to obtain estimates of nitrate yields in the reaction of NO with OH-substituted peroxy radicals. This information is important because OH-substituted peroxy radicals are formed from a variety of compounds, including alkanes, and previous versions of the SAPRC mechanism had to make unreasonable assumptions about nitrate yields from their reactions in order to fit alkane reactivity data (Carter, 1990, 1995, Carter et al, 1997c). Although these yields currently cannot be determined directly by methods available in our laboratory, they can be derived by adjusting models to fit the chamber data because of the relatively large sensitivity of the predicted reactivities in the mini-surrogate experiments to the assumed nitrate yields (Carter et al, 1995a). For this purpose, it is important that the relative levels of peroxy radicals formed in the system be reasonably well established.

Note that determining yields of reactive organic products such as octanal or octanones requires a knowledge of their OH radical rate constants in order to correct the data for their secondary reactions with OH radicals in the product yield experiments. Therefore the rate constants for the reactions of OH with octanal and the octanones were also measured as part of this study.

1. Relative Rate Constant Measurements

The rate constants for the reactions of OH radicals with the four octanol and octanone isomers, propylene glycol methyl ether acetate, and (for control purposes) n-octane and o-xylene were measured using a relative rate method, with m-xylene used as a reference compound. Attempts were also made to measure the relative rate constant for methyl isobutyrate but the amount of methyl isobutyrate reacted in our experiments was too small to obtain useful data. The relative rate method employed has been used extensively in other laboratories for many years [see references cited by Atkinson (1989), e.g., Atkinson et al, 1981)], and involves measurements of the consumption of the various compounds in the presence of OH radicals generated by the photolysis of methyl nitrite

$$CH_3ONO + h\nu \rightarrow CH_3O\cdot + NO$$
$$CH_3O\cdot + O_2 \rightarrow HO_2 + HCHO$$
$$HO_2 + NO \rightarrow OH + NO_2$$

In the first experiment, the OH radicals were generated by the reaction of O_3 with trans-2-butene. However, the amount of test compounds and m-xylene reacted were relatively low, so methyl nitrite photolysis was used to generate OH radicals in all subsequent runs. Note that the method used to generate OH radicals should not affect the data analysis method, provided that the method employed not involve formation of other species that react with the organics besides OH radicals.

Assuming that the organics react only with OH radicals, the kinetic differential equations for the organics can be solved and rearranged to yield

$$\ln\left(\frac{[\text{Organic}]_{t0}}{[\text{Organic}]_t}\right) - D_t = \frac{k_{\text{Organic}}}{k_{\text{Reference}}} \ln\left[\left(\frac{[\text{Reference}]_{t0}}{[\text{Reference}]_t}\right) - D_t\right] \qquad \text{(IV)}$$

where $[\text{Organic}]_{t0}$ and $[\text{Organic}]_t$, $[\text{Reference}]_{t0}$, and $[\text{Reference}]_t$ are the initial and time=t concentrations of the test and reference compounds, respectively, k_{Organic} and $k_{\text{Reference}}$ are the test and reference compound's OH rate constant, and D_t is a factor added to account for dilution due to reactant injections, leaks, etc, from the beginning of the experiment up to time t. Since no reactant injections were made during the experiments and the leaks in this chamber are believed to be negligible during the time period of the experiments, D_t is assumed to be negligible in our analysis. Therefore plots of $\ln([\text{Organic}]_{t0}/[\text{Organic}]_t)$ against $\ln([\text{Reference}]_{t0}/[\text{Reference}]_t)$ should yield a straight line with intercept of approximately zero and a slope that is the ratio of rate constants. Given the known value of $k_{\text{Reference}}$, then k_{Organic} can then be derived. In principle all of the compounds could be present in the same experiment but because of GC interferences and other factors generally only 2-4 test compounds are present in any given experiment.

A total of 10 experiments were carried out in this study, and the data obtained are tabulated in Table A-2 in Appendix A. Plots of Equation (IV) are shown on Figure 1 for the octanol isomers, Figure 2 for the octanol products and on Figure 3 for propylene glycol methyl ether (PGME) acetate, methyl isobutyrate, n-octane, and o-xylene. Summaries of the rate constant ratios obtained, and the absolute rate constants derived from them using the Atkinson (1989)-recommended OH + m-xylene rate constant of

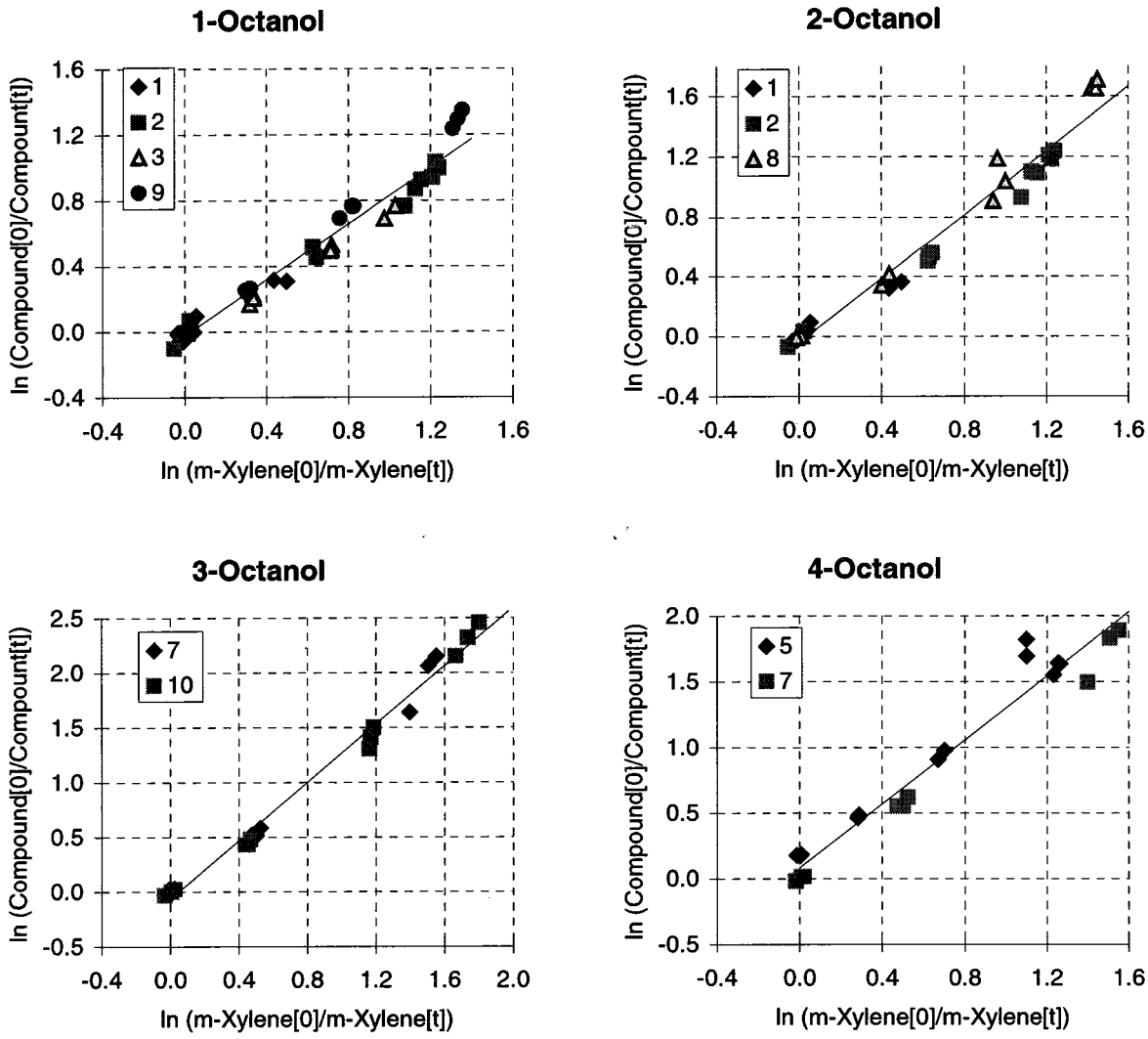

Figure 1. Plots of Equation (IV) for the relative rate constant measurements for the octanol isomers.

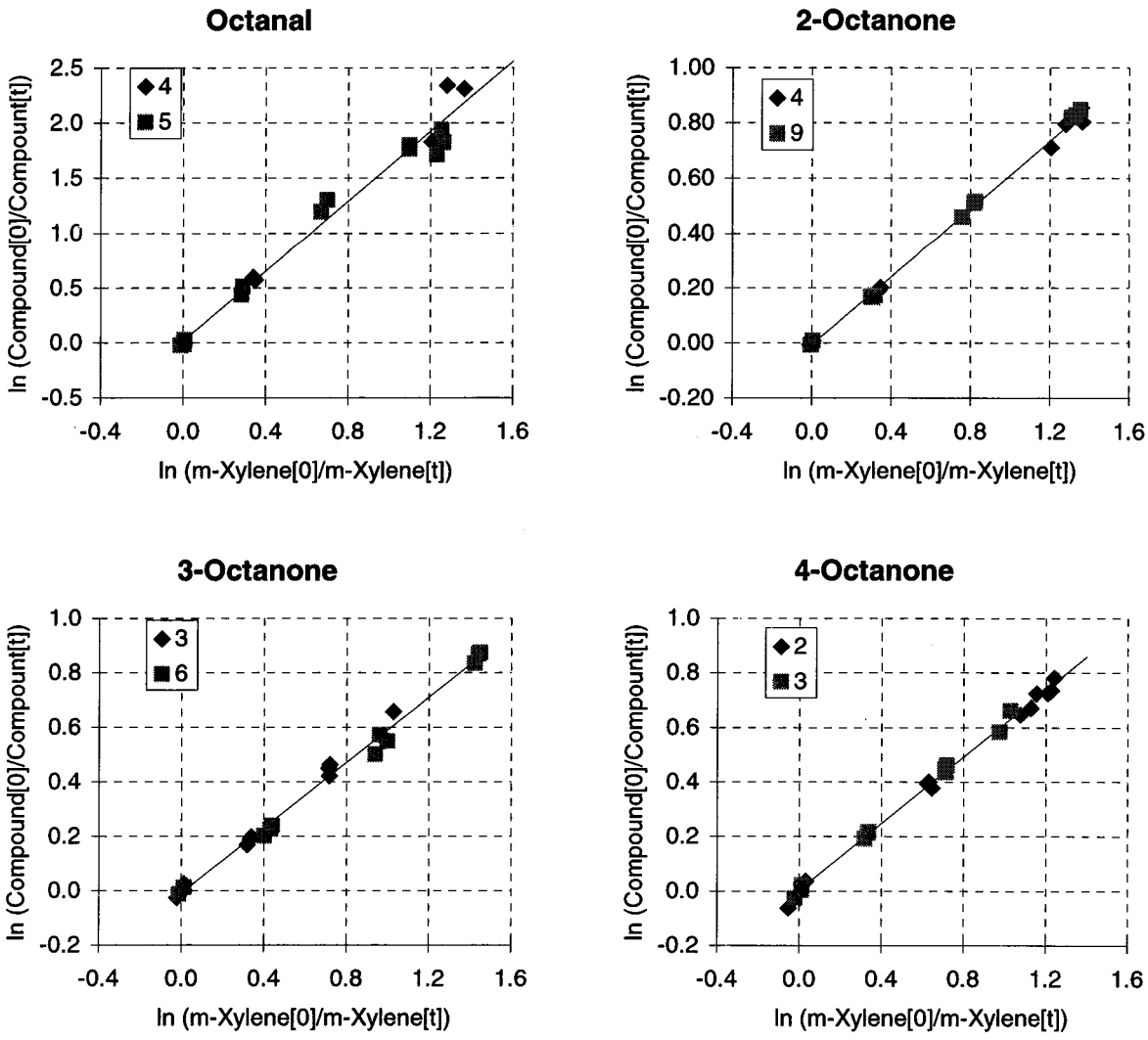

Figure 2. Plots of Equation (IV) for the relative rate constant measurements for the octanol products.

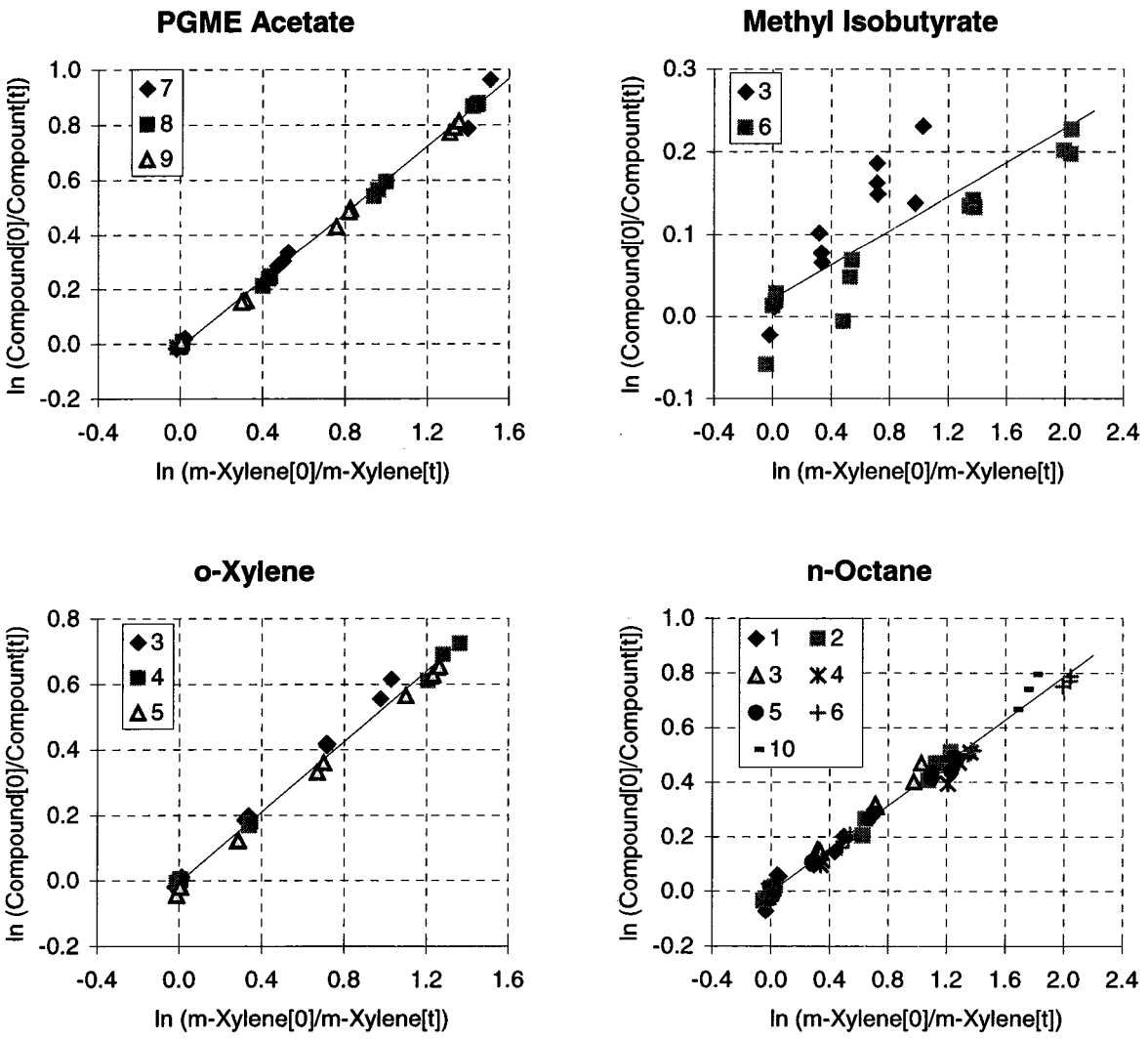

Figure 3. Plots of Equation (IV) for the relative rate constant measurements for propylene glycol methyl ether (PGME) acetate, methyl isobutyrate, n-octane, and o-xylene.

Table 3. Summary of results of the OH radical rate constant measurements, and comparison with literature and estimated rate constants.

Compound	kOH (Cmpd) / kOH (m-Xylene) [a]	kOH (Compound) (cm^3 $molec^{-1}$ s^{-1})				
		Previous	This Work	Diff.	Estimated	Est.Err
n-Octane	0.39 (±3%)	8.68e-12 [b]	9.29e-12	7%	8.29e-12	-11%
o-Xylene	0.54 (±3%)	1.37e-11 [c]	1.27e-11	-7%		
1-Octanol	0.85 (±6%)	1.44e-11 [d]	2.02e-11	40%	1.26e-11	-38%
2-Octanol	1.07 (±6%)		2.52e-11		1.57e-11	-38%
3-Octanol	1.33 (±5%)		3.14e-11		1.73e-11	-45%
4-Octanol	1.22 (±9%)		2.87e-11		1.73e-11	-40%
Octanal	1.59 (±6%)		3.75e-11		2.86e-11	-24%
2-Octanone	0.62 (±2%)	1.10e-11 [e]	1.45e-11	32%	9.59e-12	-34%
3-Octanone	0.60 (±4%)		1.41e-11		9.30e-12	-34%
4-Octanone	0.61 (±3%)		1.44e-11		1.13e-11	-22%
PGME Acetate	0.61 (±2%)		1.44e-11		2.33e-11	61%
Methyl Isobutyrate	0.104 (±27%)	1.73e-12 [f]	2.45e-12	42%	1.17e-12	-32% [g]
m-Xylene	1.00	2.36e-11 [c]	<- Reference			

[a] Indicated uncertainties in the rate constant ratios are one-σ standard deviations of the slopes of plots of Equation (IV).
[b] Rate constant recommended by Atkinson (1997).
[c] Rate constant recommended by Atkinson (1989) and not updated by Atkinson (1994).
[d] Rate constant from Nelson et al (1990).
[e] Rate constant measured by Wallington and Kurylo (1987).
[f] Rate constant from Wyatt et al (1999).
[g] Given relative to the rate constant of Wyatt et al (1999).

2.36×10^{-11} cm^3 $molec^{-1}$ s^{-1} are given on Table 3. Very low scatter and essentially zero intercepts are obtained for all the data except for methyl isobutyrate, where the data were scattered and the results of the two experiments were not in good agreement.

Table 3 also shows the rate constants from the literature, where available. The agreement with the literature is excellent for n-octane and o-xylene, but poor for 1-octanol, 2-octanone and methyl isobutyrate. Our methyl isobutyrate data are considered to be too scattered to be useful, so the rate constant of Wyatt et al (1999) is used in the current mechanism. The reason for the disagreement with the literature for 1-octanol and 2-octanone is more uncertain, though in each case there is only one other determination in the literature. We currently consider our values to be reliable because of the good precision of our data and the good agreement between our data and the data for n-octane and o-xylene, for which there are multiple measurements in the literature (Atkinson, 1989 and references therein). Therefore, for these compounds the rate constants determined in this study are used in the current mechanism, as is the case for the compounds where no kinetic data could be found in the literature.

Table 3 also shows the rate constants derived from the estimation method of Kwok and Atkinson (1995), which is used by the SAPRC-99 mechanism estimation system to estimate OH rate constants for

compounds where kinetic data are not available. The estimation method is considered to be reliable to within a factor of 1.5, and except for PGME acetate the agreement is within this factor. However, the rate constant estimates are consistently low for the octanols and octanol carbonyl products, suggesting the existence of biases in the method. On the other hand, the estimate for propylene glycol methyl ether acetate is high, and the disagreement is the greatest with this compound. Generally, the method does not seem to perform as well in estimating rate constants of compounds with multiple functional groups. This can be attributed to possible interactions between functional groups that are not taken into account with the estimation method.

2. Octanol Product Yield Measurements

The yields of the C_8 carbonyl products from the reaction of OH radicals with the octanone isomers were determined by measuring the consumption of the octanols and formation of their products when they reacted with OH radicals generated by the photolysis of methyl nitrite. A total of six experiments were carried out that obtained useful data, one each for octanal from 1-octanol and 2-octanone from 2-octanol and two each for 3-octanone from 3-octanol and 4-octanone from 4-octanol. The reactant and product data obtained prior to and after the intermittent irradiations are shown on Table A-3 through Table A-5 in Appendix A.

When analyzing the results of such experiments to obtain actual product yields, it is necessary to correct for consumption of the products by reactions with the OH radicals present in the system. This is particularly significant in the case of octanal from 1-octanol, where it can be seen from Table A-3 that the octanal concentration is actually decreasing at the end of the experiment, despite the fact that the octanol is continuing to react. As discussed by Atkinson et al (1982), a correction for secondary reactions of the product can be made by

$$[P]_t^{Corr} = [P]_t \left[\frac{\left(1 - \frac{k_P}{k_R}\right)\left(1 - \frac{[R]_0}{[R]_t}\right)}{\left(\frac{[R]_0}{[R]_t}\right)^{\frac{k_P}{k_R}} - \left(\frac{[R]_0}{[R]_t}\right)} \right] - [P]_0 \left(\frac{[R]_0}{[R]_t}\right)^{\frac{k_P}{k_R}} \qquad (V)$$

where $[P]_t^{Corr}$ is the corrected concentration of the product at time t, $[P]_0$, $[P]_t$, $[R]_0$, and $[R]_t$ are the initial and time t measured concentrations of the product[1] and reactant, respectively, and k_P and k_R are their respective OH radical rate constants. The product concentrations corrected according to Equation (V) are given in the tables, together with F, the ratio of the corrected to the measured product yields. The values of F indicate the magnitude of the correction that had to be made, which was relatively high (almost a factor of 4) in the case of octanal and non-negligible (up to a factor of 2) in the case of the octanones by the end of the experiments.

Plots of the corrected product yields against the amounts of octanol reacted are shown on Figure 4. Reasonably linear plots are observed, though some scatter is seen in the data, especially for octanal from 1-octanone, where the correction for secondary reaction is relatively large. The lines show fits to the data, forced through zero, whose slopes are taken as the product yields.

[1] A small but non-negligible amount of the product was observed prior to the irradiation in Run 7, but not in any of the other experiments.

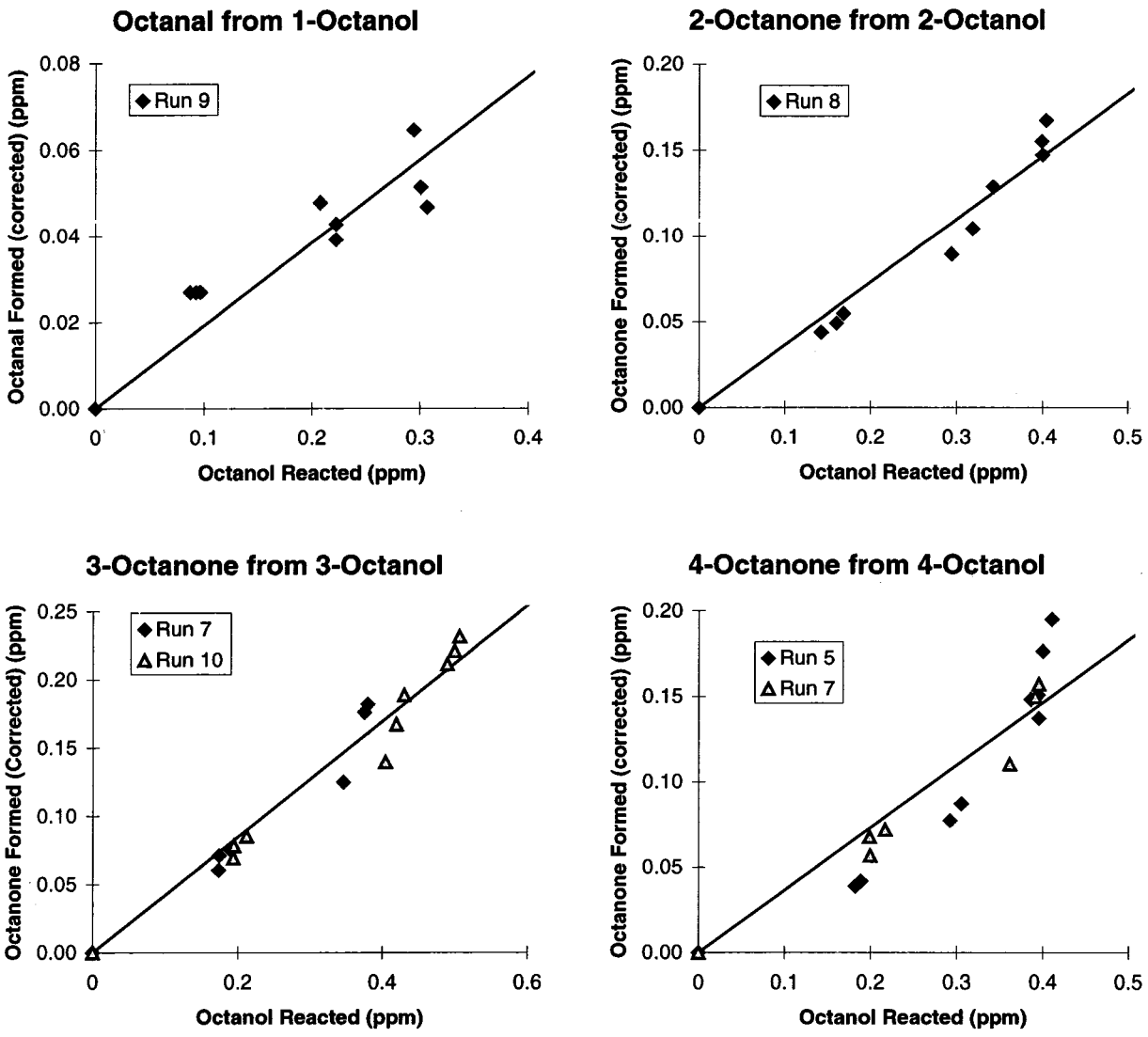

Figure 4. Plots of corrected product yields versus amounts of octanol reacted in the octanol product yield determination experiments.

Table 4. Summary of octanol product yields measured in this work, and comparison with the estimated product yields.

Product Yield	This Work [a]	Estimated
Octanal from 1-Octanal	0.19 ± 0.07 (±34%)	0.32
2-Octanone from 2-Octanol	0.37 ± 0.05 (±12%)	0.53
3-Octanone from 3-Octanol	0.42 ± 0.05 (±11%)	0.59
4-Octanone from 4-Octanol	0.37 ± 0.08 (±22%)	0.59

[a] Uncertainties are one-sigma standard deviations of slopes of lines forced through zero.

These product yields obtained are summarized on Table 4, where they can be compared with the yields estimated by the structure-reactivity method of Kwok and Atkinson (1995). The yields are consistently lower than those estimated by the group-additivity method. This suggests that either the method of Kwok and Atkinson (1995) overestimate the enhancement of the H abstraction rate caused by α-OH substitution, or underestimates the rates of abstraction from positions further away from the -OH group. Since our kinetic data for the octanols indicate that the Kwok and Atkinson (1995) method underestimates the total OH radical rate constant, our data indicates that the latter is more likely to be the case.

B. Environmental Chamber Results

Table A-6 and Table A-7 in Appendix A give chronological listings of all the environmental chamber experiments carried out for this project and indicates when changes were made to the reactors or lights, and Table A-8 gives the major conditions and selected $\Delta([O_3]-[NO])$ results for the experimental runs, sorted by type of experiments. The types of chamber experiments carried out for this program are summarized in Table 5, which also indicates the designation codes used in Table A-8. The results of the various types of experiments are discussed in more detail in the following sections.

1. Characterization Results

a. Light Characterization Results for the DTC

Light intensity measurements carried out during the course of this program included NO_2 actinometry runs using the quartz tube method of Zafonte et al (1977), and also using the Cl_2 - n-butane actinometry method as discussed by Carter et al (1995b,c). The results of those experiments carried out during the time period that is relevant to deriving the NO_2 photolysis rates during the period of this project are plotted against run number on Figure 5. Note that experiments carried out before and after this project are included, since they were used in deriving the NO_2 photolysis rates assigned for modeling purposes.

As noted in Table A-6, two different reaction bags were used during the course of the program, and Figure 5 indicates when the reaction bags where changed. More significantly, the light banks used during the irradiation were changed around the time of DTC471. Because the light intensity gradually

decreases with time as the lights age, one would expect the change in light banks to affect the light intensity, and indeed this was found to be the case.

Figure 5 shows that except for the quartz tube actinometry experiments carried out between DTC610 and DTC650, the quartz tube results are reasonably consistent. These data indicate a generally linear decrease in light intensity with run number, with a discontinuity at the time the lights were changed around DTC471 but not when the reaction bag was changed around DTC622. As discussed previously (Carter et al, 1999a), the quartz tube data taken between DTC610 and DTC650 are anomalously low, and their results are inconsistent with the apparent trend in light intensity indicated by the results of the replicate base case surrogate - NO_x experiments. This is attributed to probable incorrect positioning of the tube within the chamber, and the data from those actinometry experiments are therefore rejected (Carter et al, 1999a).

Figure 5 also shows the NO_2 photolysis rates derived from the results of the Cl_2 - n-butane actinometry experiments carried out during this period. The data tend to be highly scattered and in most, though not all, cases indicate light intensities that are lower than indicated by the quartz tube results. The reasons for this scatter are unclear, especially since more consistent and less scattered results were obtained in the Cl_2 - n-butane actinometry experiments carried out in the CTC.

The lines on Figure 5 show the assignments used for deriving NO_2 photolysis rates for modeling purposes. They were derived by fitting the non-rejected quartz tube data to lines for the periods where the light intensity trends appear to be linear. These lines are as follows, where k_1 is the NO_2 photolysis rate in min^{-1}:

Runs DTC225-429:	$k_1 = 0.288 - 0.000245$ x DTC Run No.
Runs DTC429-471:	$k_1 = 0.468 - 0.000664$ x DTC Run No.
Runs DTC472-703:	$k_1 = 0.358 - 0.000281$ x DTC Run No.

There appeared to be a slight acceleration in the rate of decrease in light intensity just before the light banks were changed around DTC471, so a separate line segment was used for that period.

Several measurements of the spectrum of the lights in the DTC were made during the course of this project using the LiCor-1800 spectroradiometer. The results were consistent with the blacklight spectrum recommended by Carter et al (1995b), so that spectrum, in conjunction with the NO_2 photolysis rates derived as indicated above, were used for calculating photolysis rates when modeling the DTC experiments for this project.

b. Light Characterization Results for the CTC

As discussed by Carter et al (1995b), the light intensity inside the CTC chamber is somewhat more complicated to characterize because of the non-uniform distribution of the intensity throughout the chamber enclosure. Several different methods are used to characterize the intensity, as follows:

- Relative trends in light intensity can be obtained using the quartz tube method of Zafonte et al (1977), modified as discussed by Carter et al (1995b, 1997c). The tube is located outside the reaction bags and between the bags and the lights. For this reason, it is expected that these measurements would be biased high, compared to the light intensity in the reactors. However, the position of the tube is always the same, so these data can be used to obtain relative trends.

Table 5. Codes used to designate types of experiments in tabulations of results.

Designation	Description
Types of Test VOC Runs	
CO	CO - NO_x runs carried out to determine the chamber radical source
N-C4	n-Butane - NO_x runs carried out to determine the chamber radical source.
PROPENE	Propene - NO_x control experiments.
FORMALD	Formaldehyde - NO_x control experiments.
CYCC6	Runs with cyclohexane as the test compound
I-C3-OH	Runs with isopropyl alcohol as the test compound
1-C8-OH	Runs with 1-octanol as the test compound
2-C8-OH	Runs with 2-octanol as the test compound
3-C8-OH	Runs with 3-octanol as the test compound
ET-O-ET	Runs with diethyl ether as the test compound
ET-ACET	Runs with ethyl acetate as the test compound
ME-IBUAT	Runs with methyl isobutyrate as the test compound
BU-ACET	Runs with n-butyl acetate as the test compound
PGME-ACT	Runs with 1-methoxy-2-propyl acetate as the test compound
MEK	Runs with methyl ethyl ketone as the test compound
CC6-KET	Runs with cyclohexanone as the test compound
MIBK	Runs with 4-methyl-2-pentanone as the test compound
DIACTALC	Runs with diacetone alcohol as the test compound
Types of Incremental Reactivity Experiments	
MR3	High NO_x mini-surrogate used as the base case. See Section II.A.1.a.
MRX	Same as MR3 except that n-octane replaced n-hexane in the base case mixture. See Section II.A.1.a.
MR8	High NO_x full surrogate used as the base case. See Section II.A.1.b.
R8	Low NO_x full surrogate used as the base case. See Section II.A.1.c.
Types of Surrogate - NOx (Base Case) Experiments.	
SURG-3M	Base case experiment using the high NO_x mini-surrogate.
SURG-m3M	Base case experiment using the high NO_x mini-surrogate with n-hexane replaced by n-octane.
SURG-8M	Base case experiment using the high NO_x full surrogate.
SURG-8	Base case experiment using the low NO_x full surrogate.

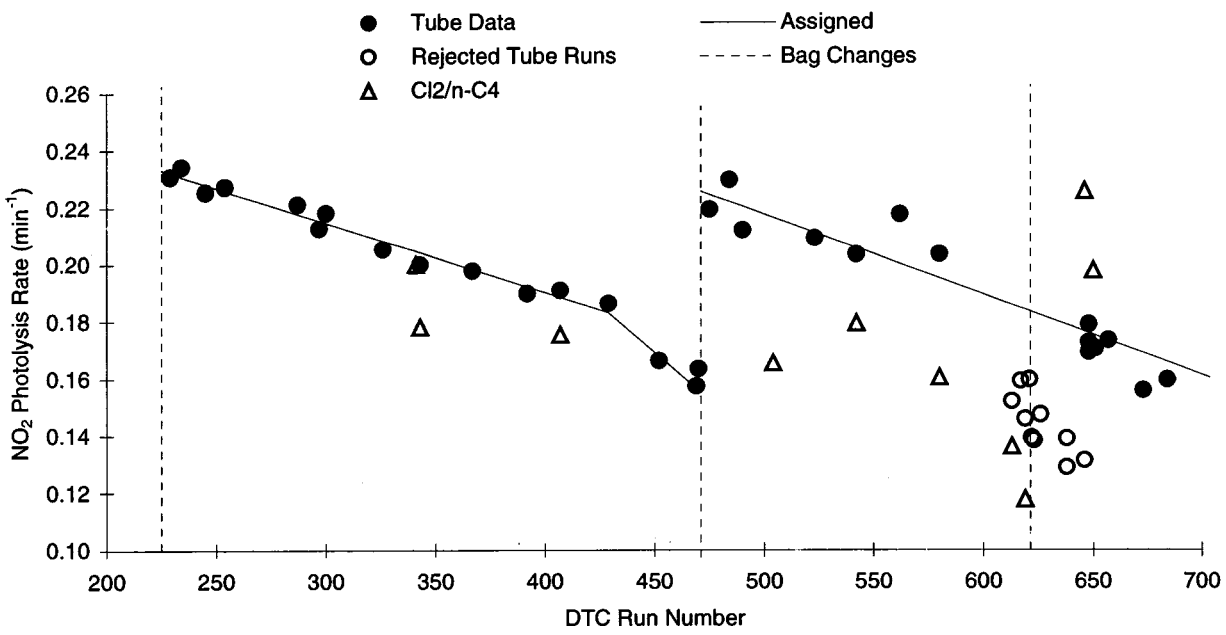

Figure 5. Plots of results of actinometry experiments against DTC run number, showing NO_2 photolysis rate assignments used for modeling purposes.

- Relative trends in light intensity can also be obtained using spectral data from the LiCor LI-1800 spectral radiometer, which is also located between the reactors and the lights, in the same position in each experiment. Relative NO_2 photolysis rates can be calculated using the measured spectrum and the NO_2 absorption cross sections and quantum yields used in the base mechanism.
- Absolute light intensities up to the time of around run CTC137 were measured using the steady-state method, involving monitoring NO, NO_2, and O_3 simultaneously when small amounts of NO_2 are injected (see Carter et al, 1997c for details). Routine use of this method was discontinued because the data tended to be scattered. However, it does obtain a measurement of the NO_2 photolysis rate inside the reactor, which is the quantity of interest.
- Absolute light intensities can also be measured using the Cl_2 actinometry method, which involves irradiation of Cl_2 and n-butane, and using the rate of consumption of n-butane as a measure of the formation rate of Cl atoms, with which it rapidly reacts (see Carter et al, 1997c for details). The NO_2 photolysis rate is calculated from the Cl_2 photolysis rate using the absorption cross sections for Cl_2 used by Carter et al (1997d,e) and those for NO_2 in the mechanism. For these xenon arc lights, the NO_2 photolysis rate is calculated to be 5.15 times the Cl_2 photolysis rate.

The results of these actinometry measurements in the CTC are given in Figure 6. The data from the quartz tube are corrected by being multiplied by a factor of 0.74, which was derived to minimize the least squares difference between the corrected quartz tube data and the trend derived from the in-chamber (Cl_2 and steady state) actinometry methods. The solid line is the least squares fit to the corrected quartz tube data, and is given by:

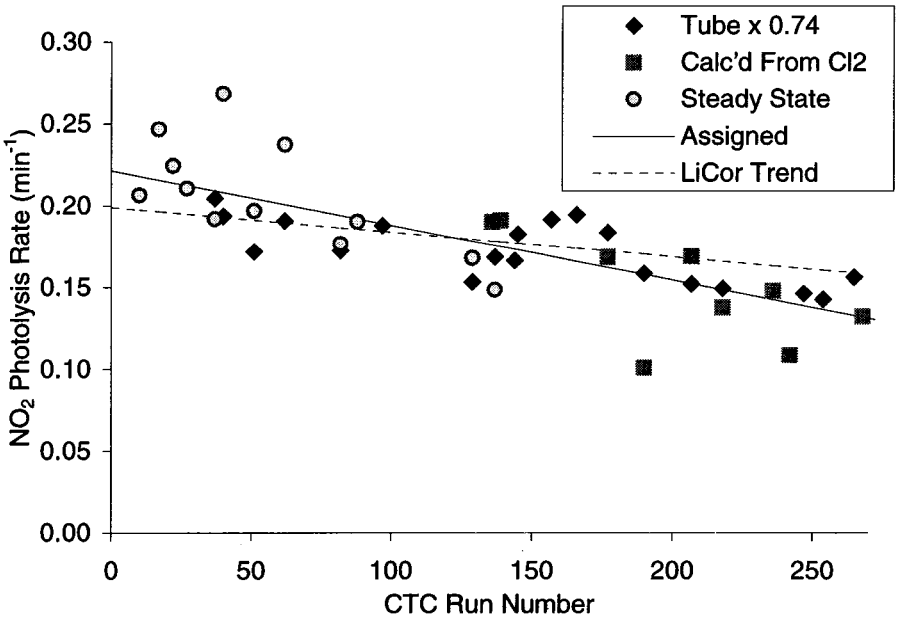

Figure 6. Plots of results of light intensity measurements against CTC run number for all experiments carried out to date in this chamber.

$$NO_2 \text{ photolysis rate } (min^{-1}) = 0.221 - 3.34 \times 10^{-4} \cdot \text{CTC Run Number} \quad \text{(VI)}$$

This was used for the purpose of assigning light intensities for the purpose of model simulations of the CTC experiments. Note that the in-chamber and quartz tube actinometry measurements give a consistent declining trend of light intensity with time, after the quartz tube data are corrected by the factor that makes them consistent with the in-chamber data.

Figure 6 shows that the LiCor data indicate a somewhat slower decline in light intensity with time than determined by the other methods. Although the LiCor data were used previously as the primary means to determine the trend in light intensity in this chamber (Carter et al, 1997b), it was found that using the LiCor-derived trend gives an incorrect simulation of how the results of the replicate base case surrogate experiments vary with time (Carter et al, 1999b). On the other hand, model simulations using light intensities derived using Equation (VI) gives a reasonably good simulation of these data (Carter et al, 1999b).

Unlike the blacklights in the DTC, the spectrum of the xenon arc light source varies slowly with time. The spectrum of the light source was measured several (usually five) times during each CTC experiment using a LiCor LI-1800 spectroradiometer. The relative spectra used for modeling purposes were obtained by averaging the results of these measurements for experiments carried out around the same time. The groups of experiments that are assumed to have the same spectral distribution are indicted by the "characterization set" number, which is given in the summary of run conditions and results on Table A-8. These average relative intensities changed approximately linearly with run number.

Figure 7 shows representative averaged CTC spectra that were used for calculation of photolysis rates, and how the relative intensities at various wavelength changed during the period in which the CTC was used. Note that the change during the course of this program was less than shown on Figure 7. It can be seen that the intensity changes relatively little for wavelengths greater than ~350 nm, but tends to decrease more rapidly with time at lower wavelengths. This is probably due to aging of the Pyrex filter used in the lamps; changes of lamps themselves were found to have an insignificant effect on the relative spectra.

c. Radical Source Characterization Results

Among the important parameters that must be specified when modeling chamber experiments are those related to the chamber radical source, which is manifested by higher radical levels in chamber experiments than can be accounted for by known homogeneous gas-phase chemistry (Carter et al, 1982, 1995b). In the current chamber model (Carter et al, 1995b, 1997c; Carter, 2000), the chamber

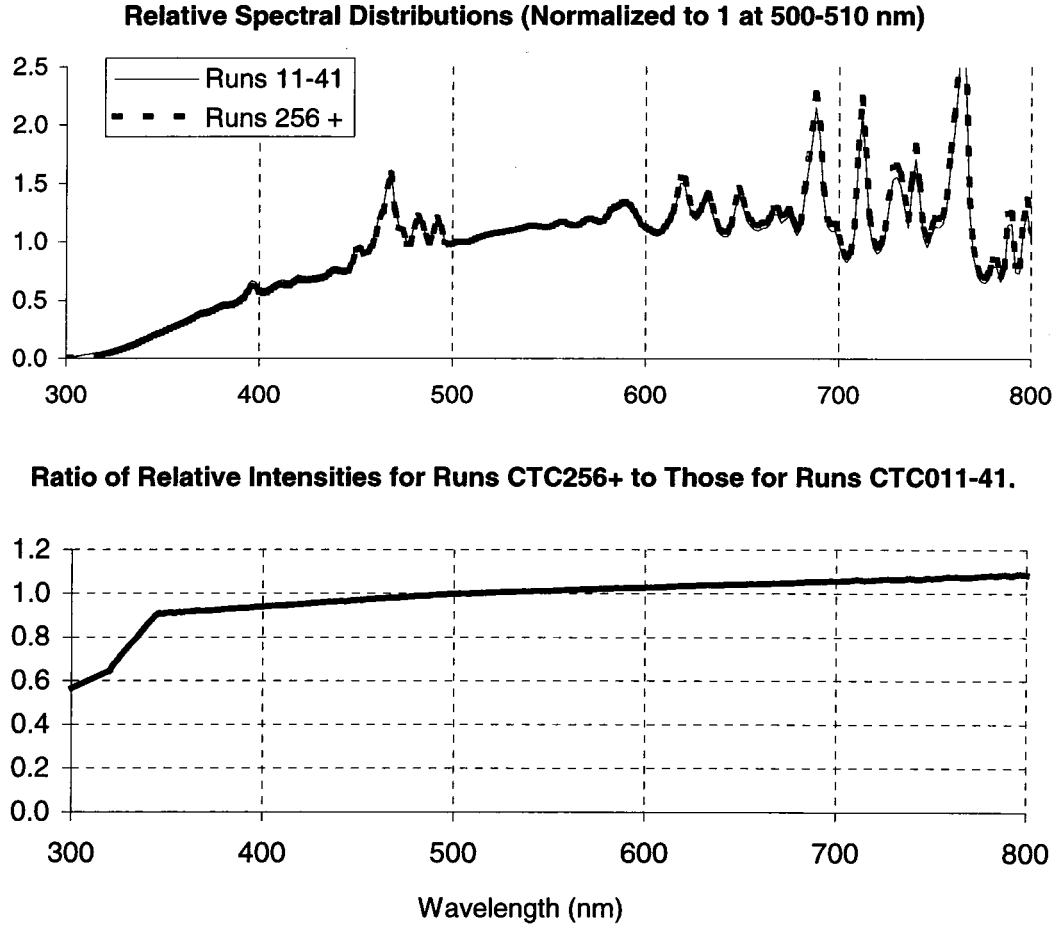

Figure 7. Plots of Representative average spectral distributions for the CTC chamber, and ratios of the relative intensities for the latest CTC runs relative to those for the initial experiments, against wavelength.

radical source is represented by a light-dependent offgasing of HONO, whose subsequent rapid photolysis provides a source of OH radicals. This parameterization also accounts for the NO_x offgasing effect observed in chambers, since generally the rate of this reaction that gives best fits of model simulations to radical source characterization runs also gives reasonably good simulations of pure air and aldehyde - air experiments. The magnitude of this parameter is measured by the ratio of the HONO offgasing rate to the NO_2 photolysis rate, and it is referred to as "RN-I" (Carter et al, 1997b, 2000).

The radical source input rate is determined by modeling n-butane - NO_x - air and CO - NO_x - air experiments to determine the value of RN-I that minimizes the sum of squares error in the model calculations of the NO concentrations. The predicted NO consumption rates in these experiments are highly sensitive to RN-I. However, they are also sensitive to the initial HONO concentrations in the experiments, so the best fit values of the initial HONO are also determined during this optimization.

The best fit values of the RN-I parameters and the initial HONO concentrations in the radical source characterization runs that incorporate the period of the experiments shown in this report are shown on Figure 8 for the DTC and on Figure 9 for the CTC. Some run-to-run variability is observed, particularly in the initial HONO in the DTC experiments. However, the variability in initial HONO is not an important concern, since the levels tend to be sufficiently low so that they are not particularly important in affecting results of model simulations of mechanism evaluation experiments. The values of the RN-I parameter used for modeling the experiments for this program are determined by averaging the optimized values for runs carried out using the same reactor or reactors that are believed to have similar background effects. The values of initial HONO used are determined by averaging the ratio of the best fit initial HONO levels in the radical source characterization runs to the initial NO_2 concentrations, and then using this ratio when modeling the experiments (Carter et al, 1995b). The assignments used for these experiments are given in Table 2, above (see also Carter, 2000).

d. Results of Other Characterization and Control Runs

Most of the other characterization and control experiments consisted of replicate propene - NO_x control runs carried out to assure reproducibility of conditions with respect to O_3 formation from high reactivity systems. Plots of the results for these replicate propene - NO_x experiments are shown on Figure 10 for the runs in the DTC and on Figure 11 for those in the CTC. Results of model simulations for all experiments for DTC471, where the measured initial propene disagreed with the amount injected, are also shown. As shown on the figures, these experiments indicated excellent side equivalency and good run-to-run reproducibility (see also Table A-7). The model gave reasonably good and consistent fits to the DTC runs, though it tended to somewhat underpredict O_3 formation and propene consumption rates during the middle period of some, though not all, of the CTC runs.

The results of the formaldehyde - NO_x control experiment carried out in the CTC are also shown on Figure 11. Good side equivalency was observed, and the model gave reasonably good fits to the $\Delta([O_3]-[NO])$ and formaldehyde data.

A few surrogate - NO_x irradiations were carried out with the same mixture irradiated on both sides to evaluate side equivalency for reactivity experiments. The results of such experiments carried out during the course of this program are shown on Figure 12. As with the propene runs, good side equivalency was observed in both cases, not only for $\Delta([O_3]-[NO])$, but also for the m-xylene data that are used to measure reactivity with respect to integrated OH radical levels.

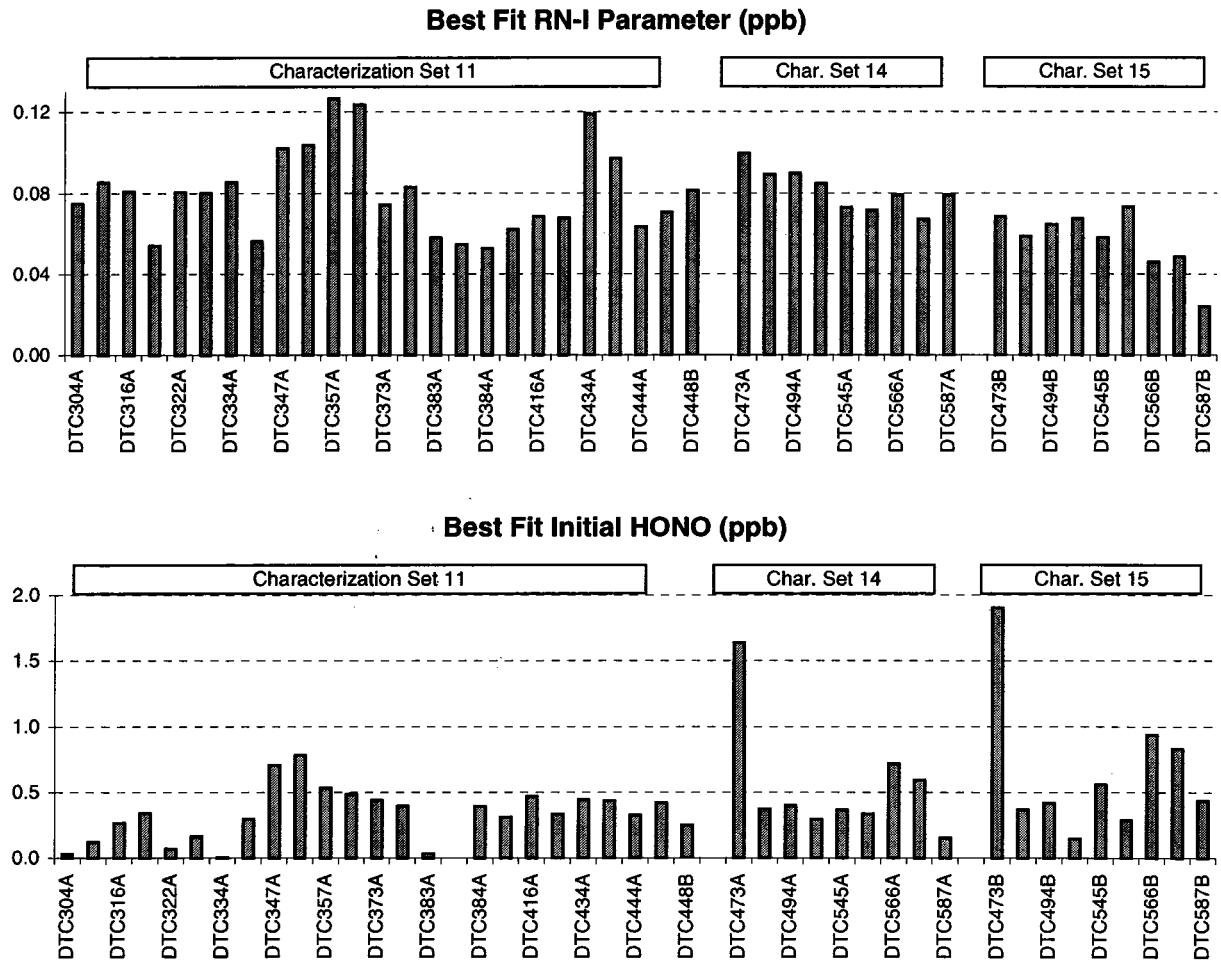

Figure 8. Radical source parameters that gave the best fits to the results of the n-butane - NO_x and CO - NO_x experiments used to characterize the conditions of the DTC during the period of this project.

The experimental and calculated ozone data from the pure air and the acetaldehyde - air characterization experiments carried out during this program are shown on Figure 13. The model using the assigned characterization parameters in Table 2 tended to overpredict O_3 in most, though not all, the pure air experiments, but gave good fits to the O_3 in the one acetaldehyde - air run. The discrepancy in the O_3 simulations in the pure air runs is not considered to be significant, and could be due to a number of factors, such as assuming too high NO_x offgasing rates or too high levels of background reactive species. However, the results of the acetaldehyde - air run suggests that the chamber effects model is probably not significantly overestimating the NO_x offgasing effects. Several O_3 dark decay experiments were carried out during this project, and the results are shown on Table 6. Except for run DTC499, which appeared to have an unusually low O_3 decay rate, the results were within the expected range of variability, and did not indicate a need to change the representation of this process in the standard wall model used when modeling these runs.

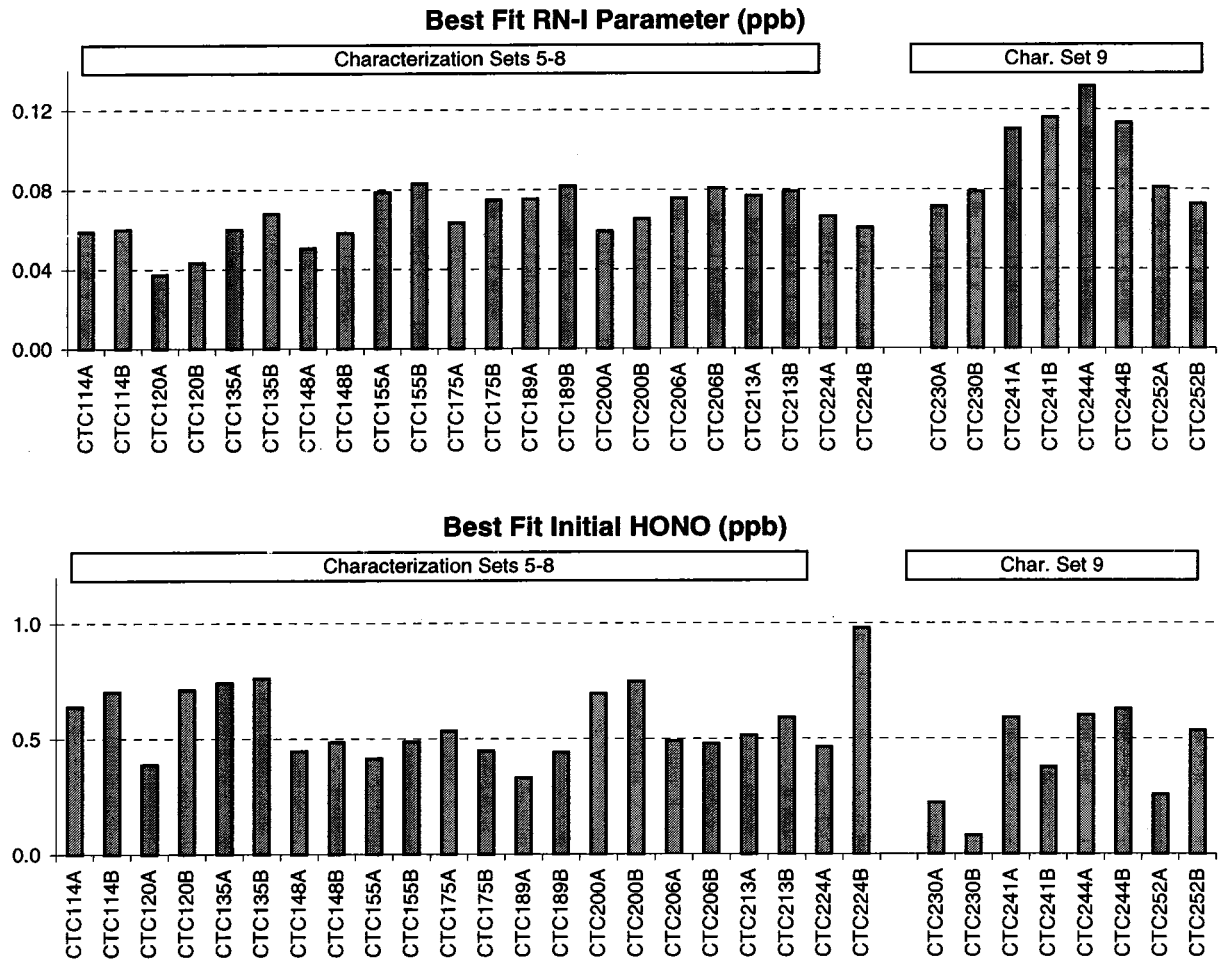

Figure 9. Radical source parameters that gave the best fits to the results of the n-butane - NO_x and CO - NO_x experiments used to characterize the conditions of the CTC during the period of this project.

2. Mechanism Evaluation Results

The major portion of this program consisted of conducting experiments to evaluate mechanisms for the set of compounds selected for study in this program. The conditions and $\Delta([O_3]-[NO])$ results of these experiments are summarized on Table A-8 in Appendix A. Most of these consisted of incremental reactivity experiments where the effect of adding the three compounds to one of the three types of standard surrogate - NO_x mixtures was determined. As discussed above in Section II.F, the reactivity results were analyzed to determine the effect of the VOC on $\Delta([O_3]-[NO])$ and integrated OH radical levels (IntOH). These incremental reactivity results are summarized in Table A-9 in Appendix A, and are also discussed for the various types of VOCs in the following sections.

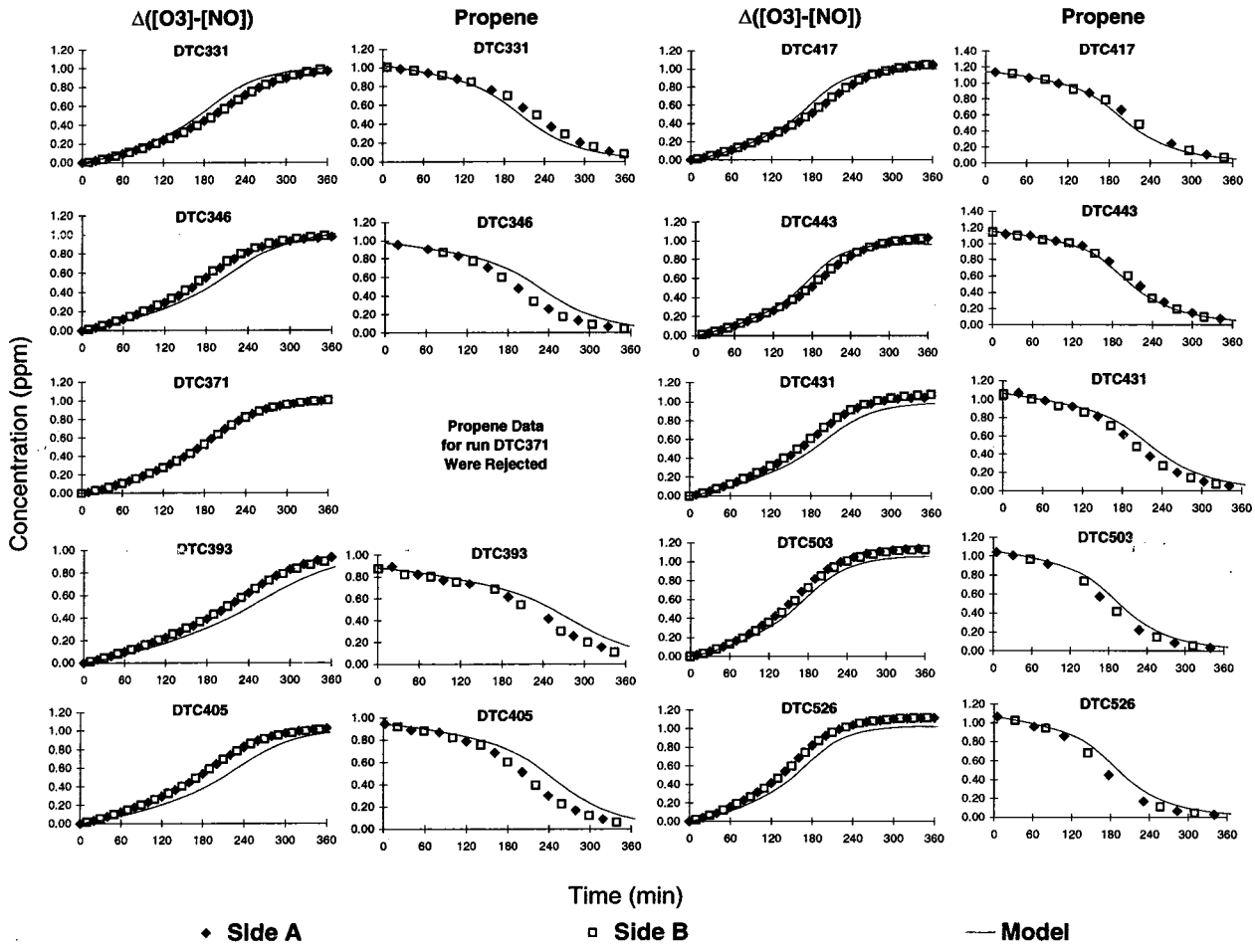

Figure 10. Experimental and calculated concentration-time plots for the $\Delta([O_3]-[NO])$ and propene data in the propene - NO_x control experiments in the DTC.

The results of these experiments were used in the development and evaluation of the SAPRC-99 mechanism as discussed by Carter (2000). The results of these experiments and their implications in terms of the mechanism are summarized in the following sections. However, since other data were also used in the development and evaluation of this mechanism, the full mechanism documentation given by Carter (2000) should be consulted for details.

a. Cyclohexane

Cyclohexane was studied in this program because it is the simplest representative of cycloalkanes, and well characterized mechanism evaluation data for such compounds were limited prior to this project. Six incremental reactivity experiments (two for each of the three types) were carried out in the DTC, and the results are shown on Figure 14. Results of model simulations using the SAPRC-99

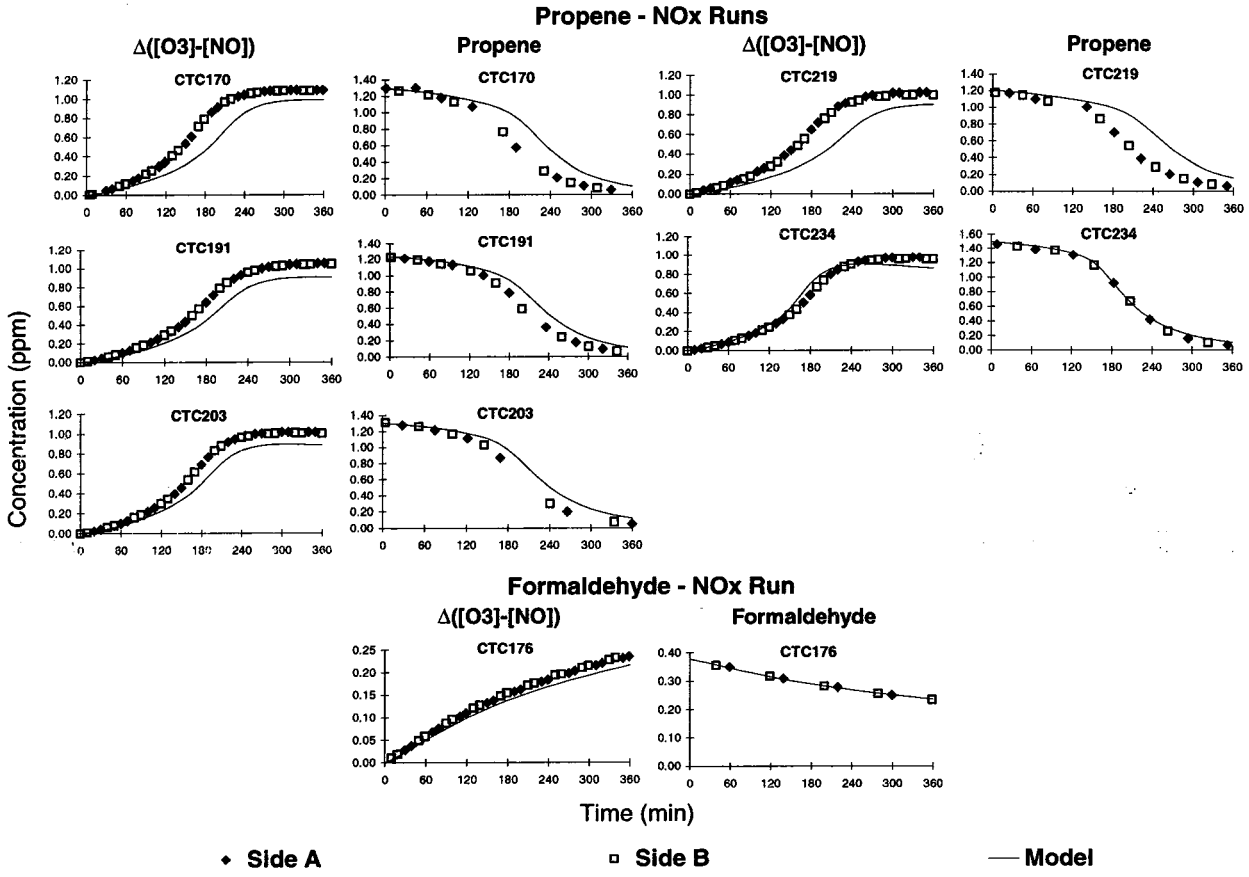

Figure 11. Experimental and calculated concentration-time plots for the $\Delta([O_3]-[NO])$ and propene or formaldehyde data for the propene - NO_x and formaldehyde - NO_x control experiments in the CTC.

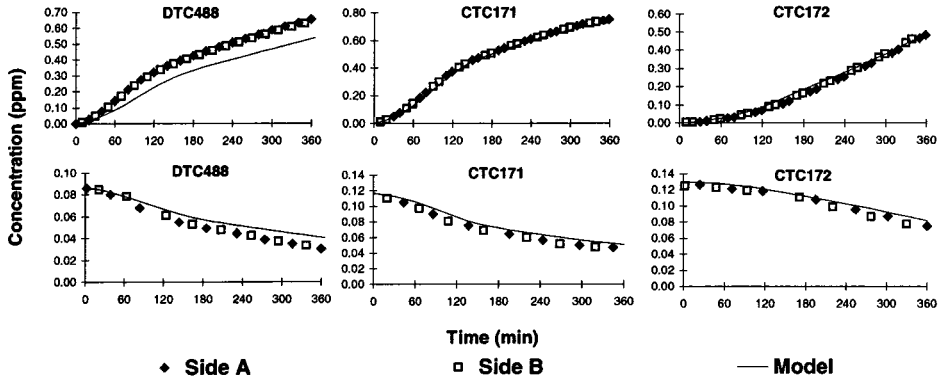

Figure 12. Experimental and calculated concentration-time plots for the $\Delta([O_3]-[NO])$ and m-xylene data in the surrogate - NO_x side equivalency test experiments.

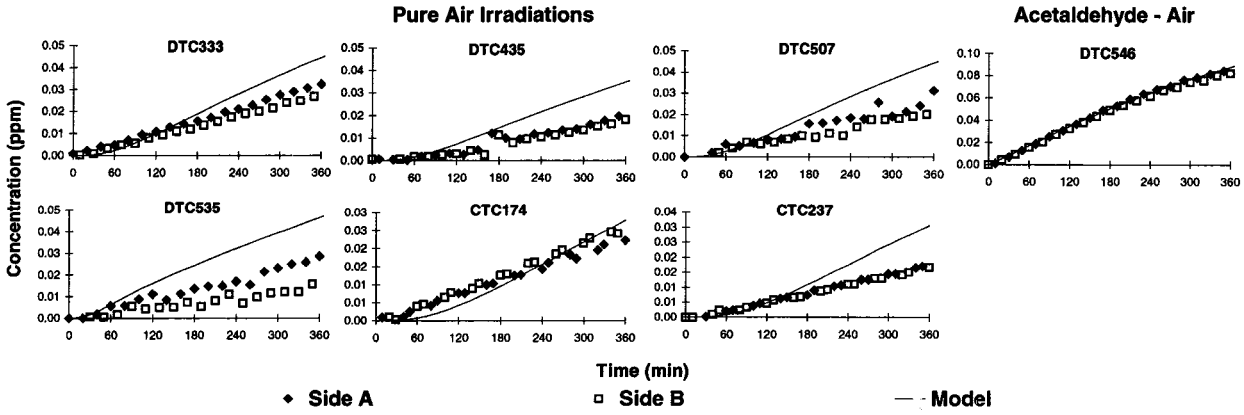

Figure 13. Experimental and calculated concentration-time plots for the O_3 data for the pure air and the acetaldehyde - air irradiations carried out during this program.

Table 6. Results of ozone dark decay experiments.

Run	O_3 Dark Decay Rate (min^{-1})	
	Side A	Side B
DTC436	1.76e-4	1.76e-4
DTC445	1.16e-4	1.14e-4
DTC499	4.33e-5	4.03e-5
CTC173	6.01e-5	7.19e-5

mechanism of Carter (2000) are also shown. No adjustments were made to the mechanism were made to obtain the fits shown.

The figure shows that the model gives excellent fits to the incremental reactivities with respect to $\Delta([O_3]-[NO])$, though there may be a slight bias towards underpredicting IntOH incremental reactivities in the high NO_x full surrogate experiments. There is also a definite bias towards underpredicting IntOH reactivity in the low NO_x full surrogate runs. However, this IntOH underprediction bias for the low NO_x full surrogate runs is observed for almost all VOCs, and is believed to represent a problem with the mechanism for the base case experiment rather than with the mechanism for the VOC (Carter et al, 1995a, 1997c). Therefore, the model performance for cyclohexane is considered to be generally satisfactory.

The good model performance for this compound tends to support the predictive capabilities of the mechanism generation and estimation system for the cycloalkanes. Its performance is generally satisfactory for other types of alkanes, as indicated by the full evaluation data given by Carter (2000).

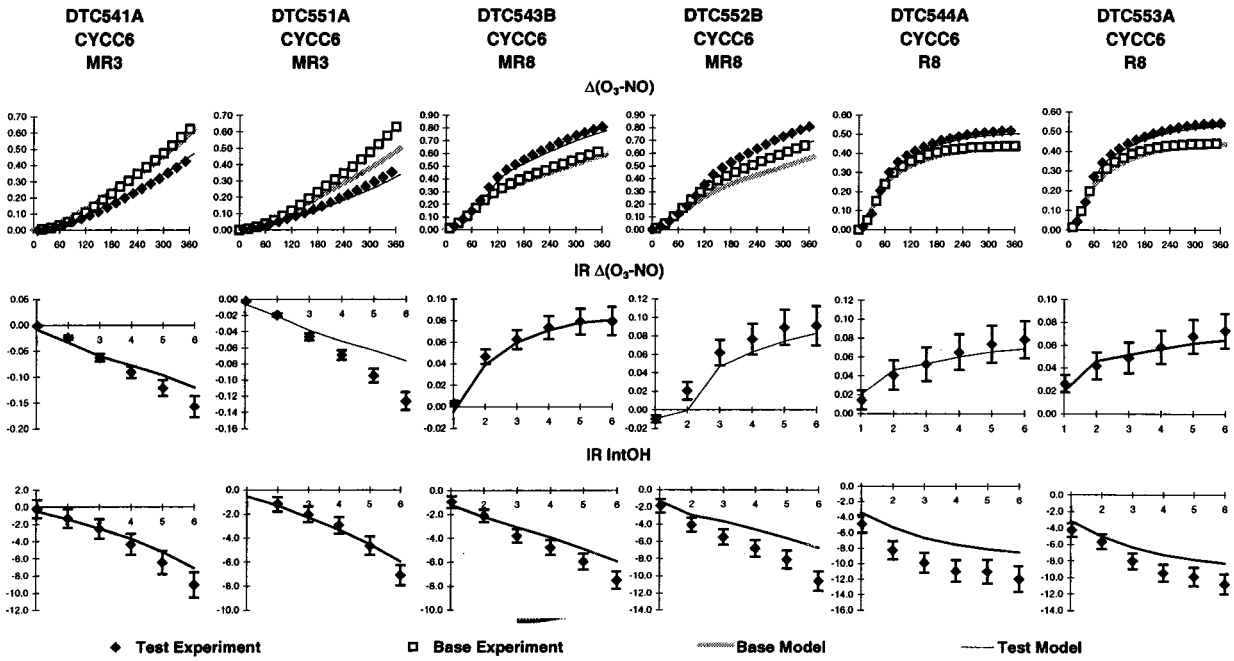

Figure 14. Plots of experimental and calculated results of the incremental reactivity experiments with cyclohexane.

b. Methyl Ethyl Ketone

Methyl ethyl ketone (MEK) is an important solvent species and prior to this program mechanism evaluation data have been limited to a small number of relatively poorly characterized outdoor chamber runs (Carter and Lurmann, 1990, 1991). Because MEK is a photoreactive compound, it is useful that data be obtained using differing light sources to evaluate whether the mechanism correctly predicts how varying lighting conditions affect its reactivity. In addition, because MEK has internal radical sources, single compound - NO_x irradiations can be used to obtain mechanism evaluation data without the complications caused by the presence of other reacting VOCs. However, incremental reactivity experiments are also needed to evaluate mechanisms under conditions more representative of ambient atmospheres. Therefore, single MEK - NO_x experiments and selected types of MEK incremental reactivity experiments[2] were carried out in both the DTC and CTC.

The results of the MEK - NO_x experiments are shown on Figure 15, and the incremental reactivity experiments are shown on Figure 16. Model simulations using the SAPRC-99 mechanism (Carter, 2000) are also shown. Excellent fits to the results of the single compound and reactivity experiments are obtained.

[2] Because MEK and n-hexane have the same retention time on the GC column normally used in our laboratory to monitor these compounds, the mini-surrogate experiments used n-octane rather than n-hexane. The results of the base case experiments were comparable to those using n-hexane, and the model predicts that this substitution should not significantly affect reactivity characteristics of test compounds in these experiments.

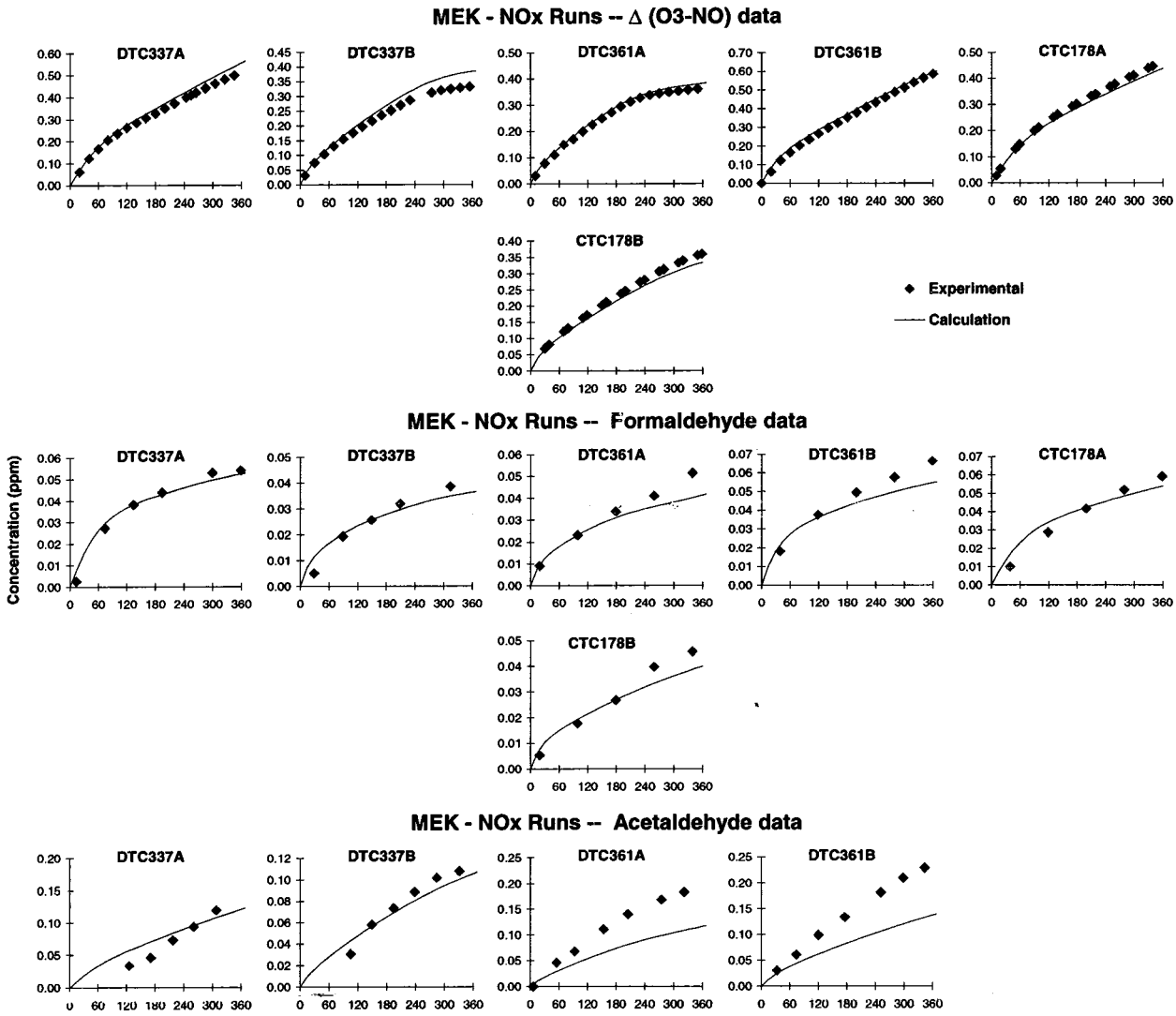

Figure 15. Plots of experimental and calculated $\Delta([O_3]-[NO])$, formaldehyde, and acetaldehyde data for the methyl ethyl ketone (MEK) - NO_x experiments.

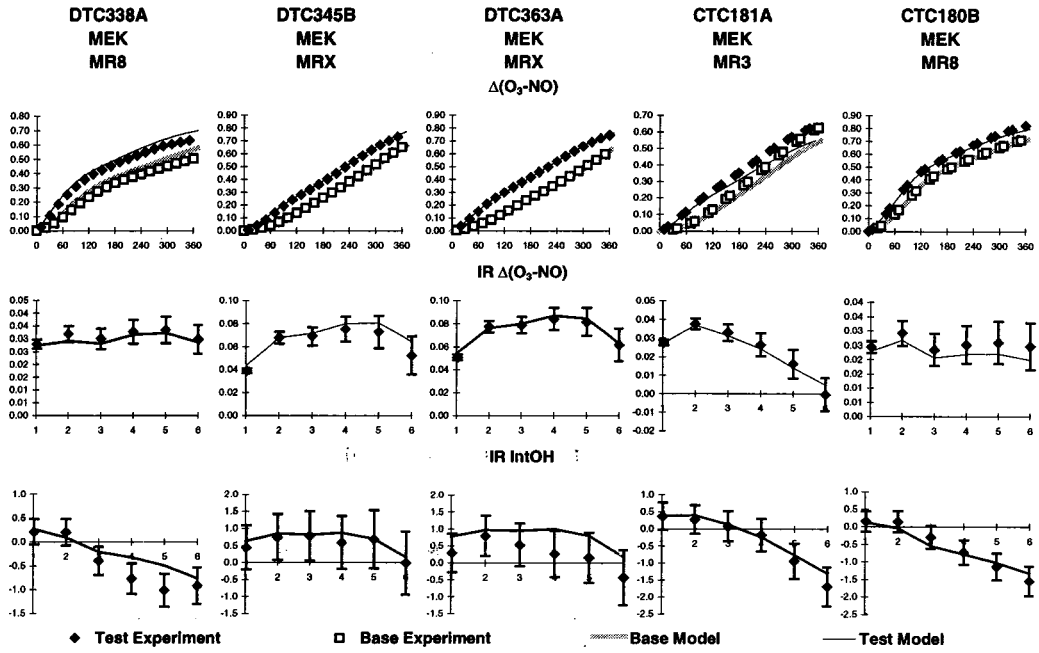

Figure 16. Plots of experimental and calculated results of the incremental reactivity experiments with methyl ethyl ketone.

To obtain the fits shown, it was necessary to increase the overall quantum yield for the photodecomposition of MEK from the value of 0.1 assumed in the SAPRC-90 mechanism (Carter, 1990) to the value of 0.15 used in SAPRC-99. Known available laboratory data are insufficient to determine the MEK quantum yield under atmospheric conditions and to determine how it varies with wavelength, so the value used for modeling has to be derived by adjusting to fit chamber data. Since there is no information concerning the wavelength dependence, an overall wavelength-dependence quantum yield is assumed. The previous value of 0.1 was based on modeling two outdoor chamber experiments (Carter, 1990, Carter and Lurmann, 1991), and because of uncertainties in conditions and light characterization this value was considered to be uncertain. Because of the relatively large number and types of MEK experiments in this study and the fact that consistent results are obtained using different light sources, the value obtained in this study is considered to be much less uncertain. As discussed by Carter (2000), this result, in conjunction with quantum yields obtained in model simulations of chamber data for other ketones (including the methyl isobutyl ketone studied in this program), is used as a basis for the estimation of overall quantum yields for ketones for which such data are not available.

The model also gives reasonably good simulations of the formaldehyde and acetaldehyde yields in the MEK - NO_x experiments, though there is an underprediction of acetaldehyde in one of the dual sided experiments. This indicates that the model is probably not significantly in error in its assumed branching ratios for reaction of OH at differing positions in the molecule, which is based on the estimation method of Kwok and Atkinson (1995).

c. Cyclohexanone

Cyclohexanone is a representative of cyclic ketone species that are also used as solvents, and for which mechanism evaluation and reactivity data were not available prior to this study. As with MEK (and for the same reasons), evaluation data were obtained using cyclohexanone - NO_x and cyclohexanone incremental reactivity experiments in both the DTC and the CTC. The results of the cyclohexanone - NO_x experiments are shown on Figure 17, and the cyclohexanone reactivity experiments are shown on Figure 18.

Results of model simulations using the SAPRC-99 mechanism are also shown on the figures. The initially estimated mechanism derived by the mechanism generation system gave poor fits to the data, and several adjustments had to be made to obtain the fits shown. These were as follows:

- The estimation method of Kwok and Atkinson (1995) predicts that most (~74%) of the initial OH reaction occurs at the 2- position, with reaction at the 1- and 3- positions predicted to occur 14%, and 12% of the time, respectively. This is based on data for other compounds that indicate that the carbonyl group inhibits reaction at the immediate neighbor but enhances it one group away. However, satisfactory model simulations can only be obtained if it is assumed that reaction at the 1-position, i.e., immediately next to the carbonyl group, is relatively more important in the case of cyclohexanone. To fit the data, it is assumed that reaction at the 1- and 2- positions occur at approximately equal rates, i.e., 44% each, with reaction at the 3-position still being assumed to occur 12% of the time, as initially estimated. However, it is uncertain whether this can be generalized to other compounds, so the overall estimation method for ketones for which data are unavailable was not modified
- The nitrate yield in the reactions of NO with the peroxy radicals formed from in the cyclohexanone + OH reaction was increased from the initial estimate of ~10% to 15%. This is well within the range of variability of the predictive capabilities of the nitrate yield estimation method for substituted peroxy radicals (Carter, 2000). These data were used in part to determine the optimum parameters for estimating these yields.

The mechanism assumes that there is no significant radical production in the photolysis of cyclohexanone. This is because it is expected that if the photolysis proceeds via C(O)..C cleavage (as is assumed for other ketones), the biradical should primarily recombine before reacting with O_2. In addition,

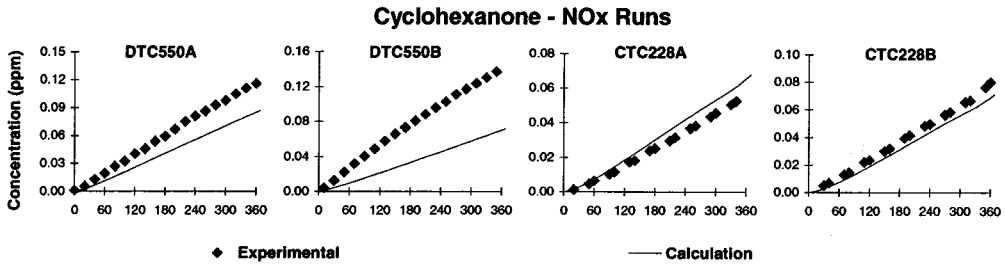

Figure 17. Plots of experimental and calculated $\Delta([O_3]-[NO])$ results for the cyclohexanone - NO_x experiments.

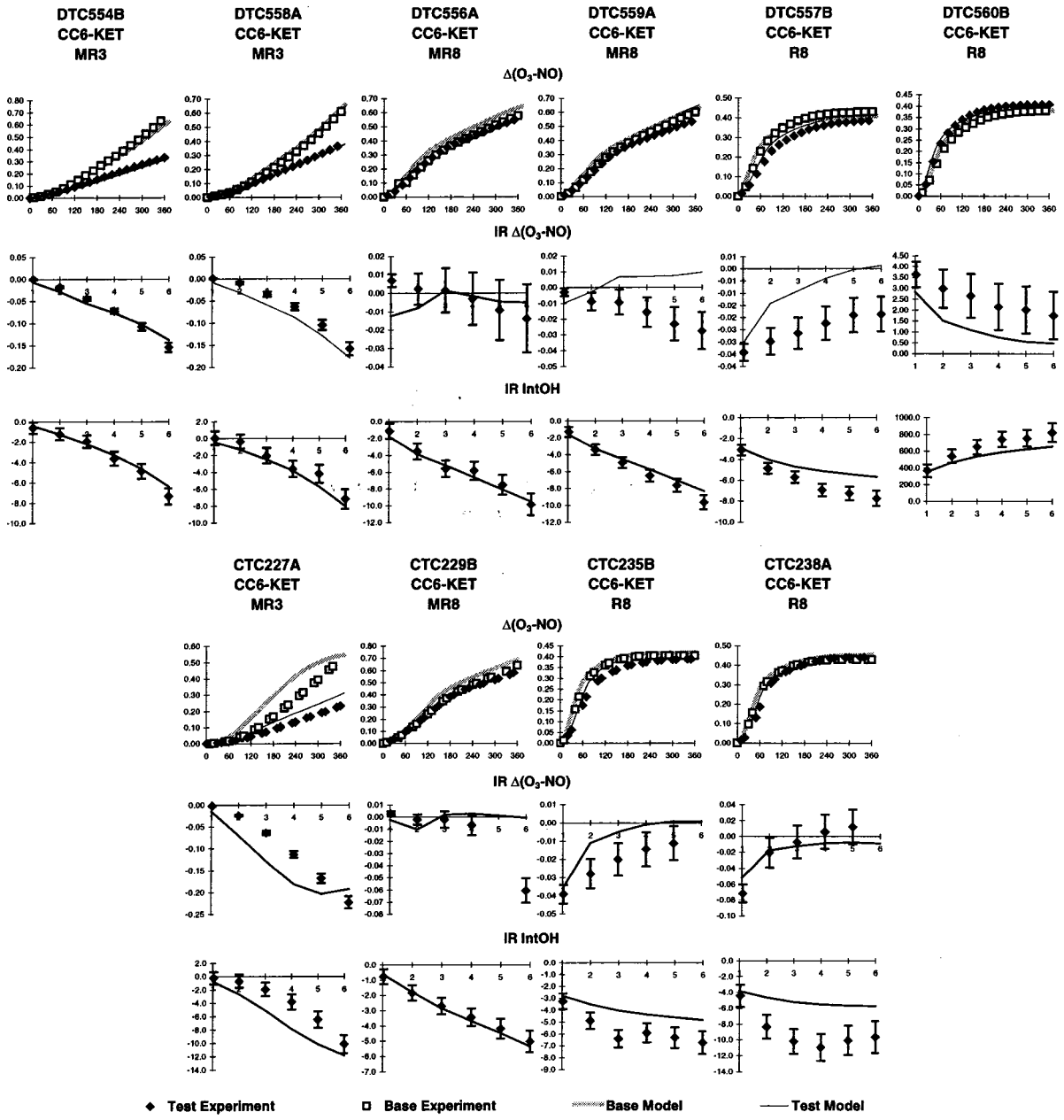

Figure 18. Plots of experimental and calculated results of the incremental reactivity experiments with cyclohexanone.

chamber data with other higher ketones are best fit if radical production from their photolysis is minor (Carter, 2000). The simulations of the chamber results for cyclohexanone tend to support this assumption.

The adjusted mechanism gives fair fits to most of the data obtained in this program. The main exception is the underprediction of $\Delta([O_3]-[NO])$ in the dual cyclohexanone - NO_x experiment DTC550A and B. However, because cyclohexanone has no significant internal radical sources, simulations of these experiments are sensitive to the assumed chamber radical source, and better fits of model calculation can be obtained if the radical source is increased within approximately its range of variability. Therefore, these runs (and also the CTC runs, which turn out to be reasonably well fit by the model) are not good tests of the mechanism.

Potentially more significant is the small but reasonably consistent bias towards underpredicting $\Delta([O_3]-[NO])$ incremental reactivities in the low NO_x full surrogate experiments. Adjustments to the mechanism that improve the fits in this regard were not found, but given the fact that it was necessary to adjust the initial branching ratio in the OH reaction it is likely that further adjustments to reduce this relatively small discrepancy may not necessarily give a mechanism of greater predictive capability. Mechanistic studies are needed to reduce the uncertainties in the current mechanism. However, the performance of the current mechanism in simulating the data for this program is reasonably good given the uncertainties involved.

d. Methyl Isobutyl Ketone

Methyl isobutyl ketone (MIBK) is another example of a ketone solvent species that can occur in consumer product inventories, for which no mechanism evaluation data were available prior to this program. The mechanism evaluation experiments consisted of MIBK - NO_x and the three types of incremental reactivity experiments, though in this case experiments were carried out only in the DTC. Although experiments with differing light sources would be desirable, the fact that the mechanisms for MEK and cyclohexanone perform reasonably consistently in simulating runs in both the DTC and CTC suggests that this probably would be the case for MIBK as well. The results of the MIBK - NO_x experiments are shown on Figure 19, and the reactivity experiments are shown on Figure 20.

The results of model calculations using the SAPRC-99 mechanism are also shown on these figures. Reasonably good fits to most of the data are obtained, including the formaldehyde yields in the MIBK - NO_x experiments. The only adjustment made to obtain these fits was the overall quantum yield for the photolysis reaction.

MIBK chamber data are best fit using an overall quantum yield of 0.04, which is lower than the 0.15 overall quantum yield that best fit the MEK data, and also lower than the 0.10 overall quantum yield that best fit the methyl propyl ketone data (Carter, 2000). These results, and the fact that the 2-heptanone data are best fit assuming no photodecomposition (i.e., an overall quantum yield of zero) (Carter, 2000) suggest that the overall quantum yields for ketone photolysis decrease monotonically with the size of the molecule. The SAPRC-99 mechanism generation system uses these results as a basis for estimating overall quantum yields in photolyses of ketones for which no data are available.

e. Isopropyl Alcohol

Isopropyl alcohol is an important component of the stationary source inventory, and although reactivity experiments with this compound were carried out previously (Carter et al, 1993b), the

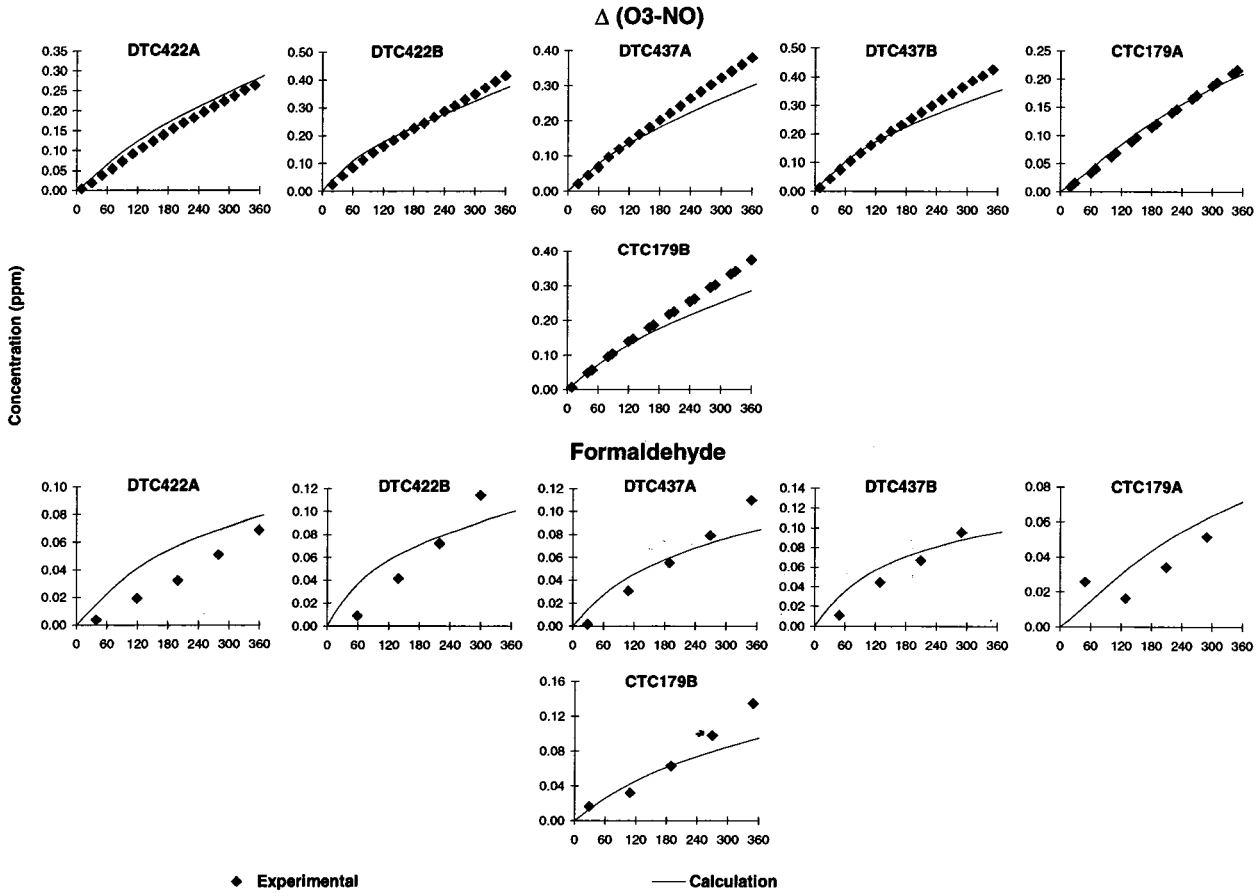

Figure 19. Plots of experimental and calculated $\Delta([O_3]-[NO])$ and formaldehyde data for the methyl isobutyl ketone - NO_x experiments

data were of relatively low precision and the results not totally conclusive. Therefore, additional reactivity experiments with isopropyl alcohol were carried out as part of this project. These consisted of two reactivity experiments of each type in the DTC. The results are shown on Figure 21.

The results of model simulations using the SAPRC-99 mechanism are also shown on this figure. The model performance was variable, but the discrepancies observed were relatively minor and no consistent biases were observed. Given the relative simplicity of isopropyl alcohol photooxidation mechanisms it is probable that the variability is more due to experimental factors than indicative of mechanism problems. Overall, the model performance is considered to be satisfactory.

f. Octanol Isomers

Three of the four octanol isomers were studied in this program because "octanol" is present in stationary source inventories, and because studies of such compounds provide useful

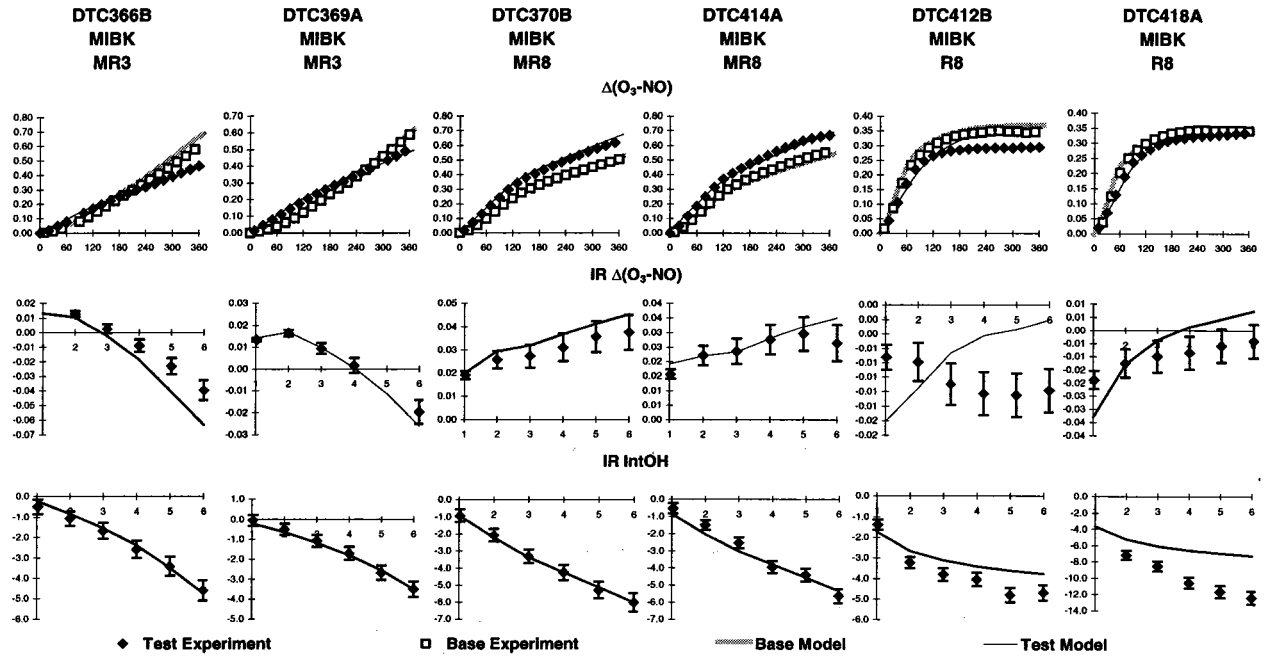

Figure 20. Plots of experimental and calculated results of the incremental reactivity experiments with methyl isobutyl ketone.

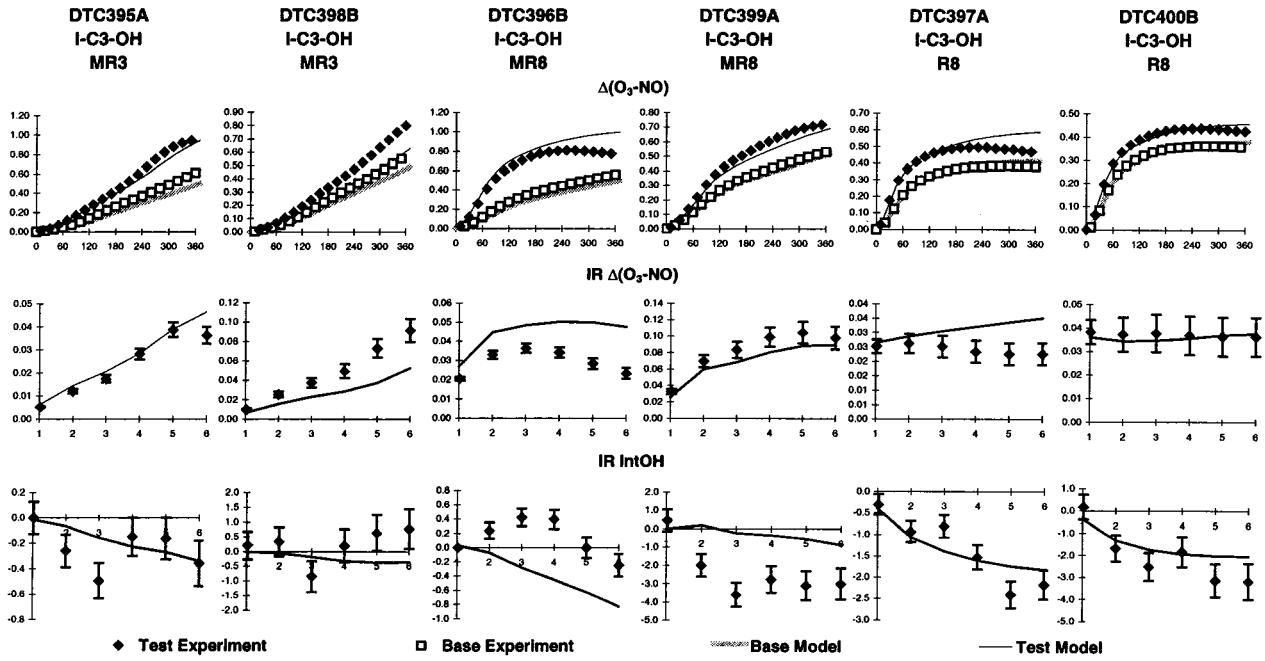

Figure 21. Plots of experimental and calculated results of the incremental reactivity experiments with isopropyl alcohol.

mechanism evaluation data for high molecular weight alcohols in general, which is applicable to estimation of mechanisms for a variety of compounds. Selected types of reactivity experiments were carried out for all three isomers in the DTC. In addition, as discussed above in Section III.A, separate kinetic and mechanistic experiments were carried out as part of this project to obtain additional information about their mechanisms. The results of these experiments are given in Figure 22.

The results of the model simulations using the SAPRC-99 mechanism are also shown on this figure. Other than incorporating the results of the kinetic and mechanistic study discussed above in Section III.A, no adjustment to the mechanisms were made to achieve these fits. Some variability is observed but because the discrepancies were relatively small and not confirmed by replicate runs, adjustments to the mechanisms were not considered to be appropriate.

The fact that it was not necessary to adjust the nitrate yields in the reaction of NO with the OH-substituted peroxy radicals formed in these reactions is of particular interest because evaluating the estimation method for predicting nitrate yields for such radicals was one of the objectives of studying these compounds. This is of interest because OH-substituted peroxy radicals are believed to be important intermediates in the photooxidation mechanisms of the alkanes. In previous versions of the SAPRC mechanism it had to be assumed that nitrate formation in the reaction of NO with these radicals was much less than is the case for unsubstituted peroxy radicals. However, because of new nitrate yield data it is no longer necessary to make this assumption for model calculations to fit alkane reactivity data (Carter, 2000 and references therein). The results of these experiments are consistent with the present estimate that OH substitution on peroxy radicals only slightly reduces the nitrate yields.

g. Diethyl Ether

Diethyl ether was studied not only because it is present in stationary source inventories but also because it provides a means to evaluate general estimation methods for the effects of ether groups on the mechanisms and reactivities of relatively high molecular weight compounds. Two each of the three types of incremental reactivity experiments were carried out in the DTC. The results are shown on Figure 23.

The results of the model simulations using the SAPRC-99 mechanism are also shown on that figure. No adjustments were made to achieve these fits, including the nitrate yields in the substituted peroxy + NO reactions. Generally the fits were good, though there may be a slight bias towards $\Delta([O_3]-[NO])$ reactivities. However, the bias was too small to merit adjustment to the mechanism.

h. Ethyl Acetate

Esters are important components of stationary source inventories, and until this project the only reactivity data available concerning atmospheric reactivities of esters concerned methyl (Carter et al, 1996) and t-butyl (Carter et al, 1997a) acetates, and dimethyl succinate (Carter et al, 1997f). Because of the wide variety of esters that are emitted, it is important that data be obtained on additional examples of such compounds. Ethyl acetate was studied because it is the simplest ester for which reactivity data were not previously available, and also because it is present in stationary source inventories. Two or more of each of the three types of incremental reactivity experiments with ethyl acetate were carried out in the DTC, and, to evaluate possible light source effects, two low NO_x full surrogate experiments were also carried out in the CTC. The results are shown on Figure 24.

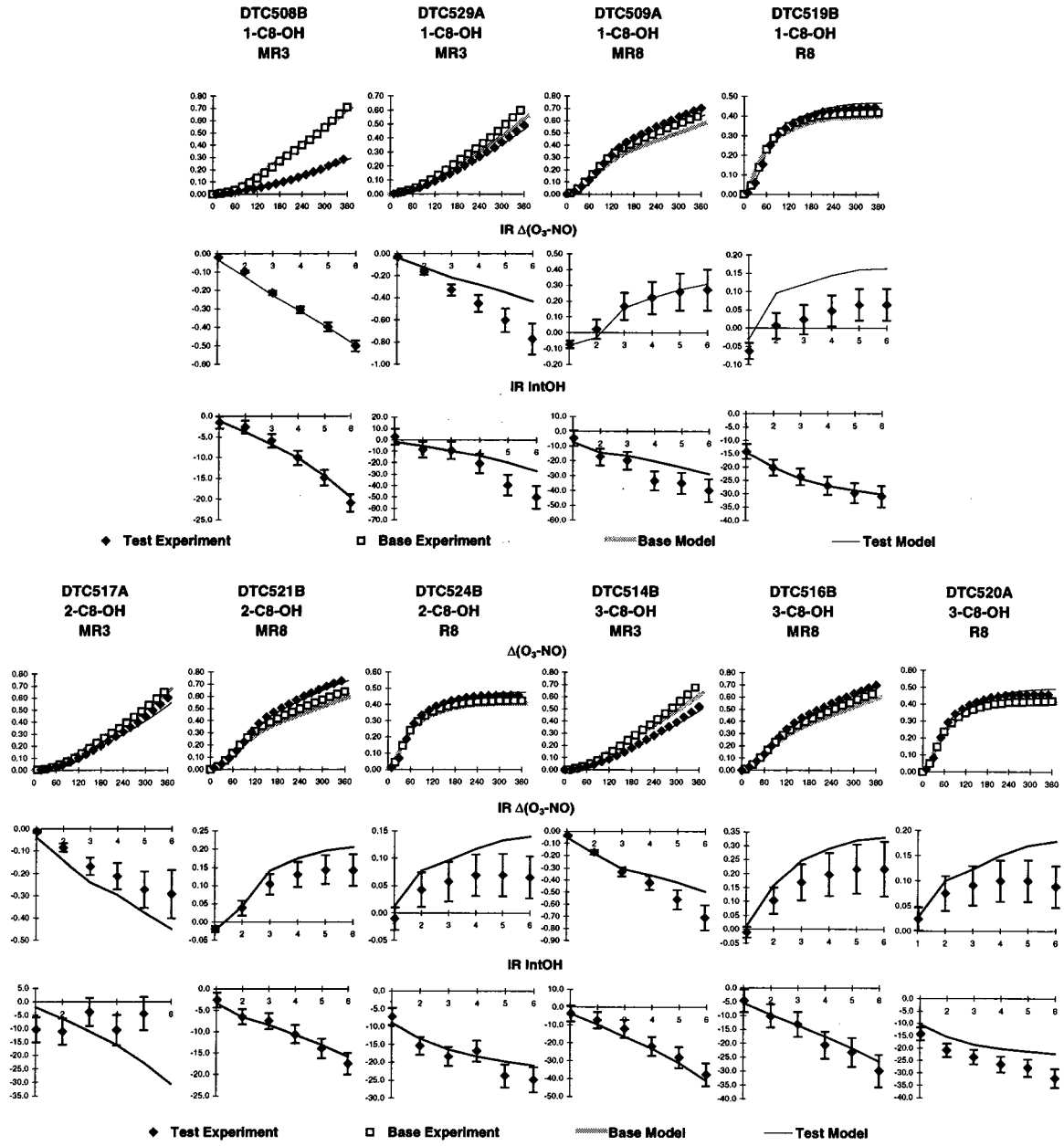

Figure 22. Plots of experimental and calculated results of the incremental reactivity experiments with 1-, 2-, and 3-octanols.

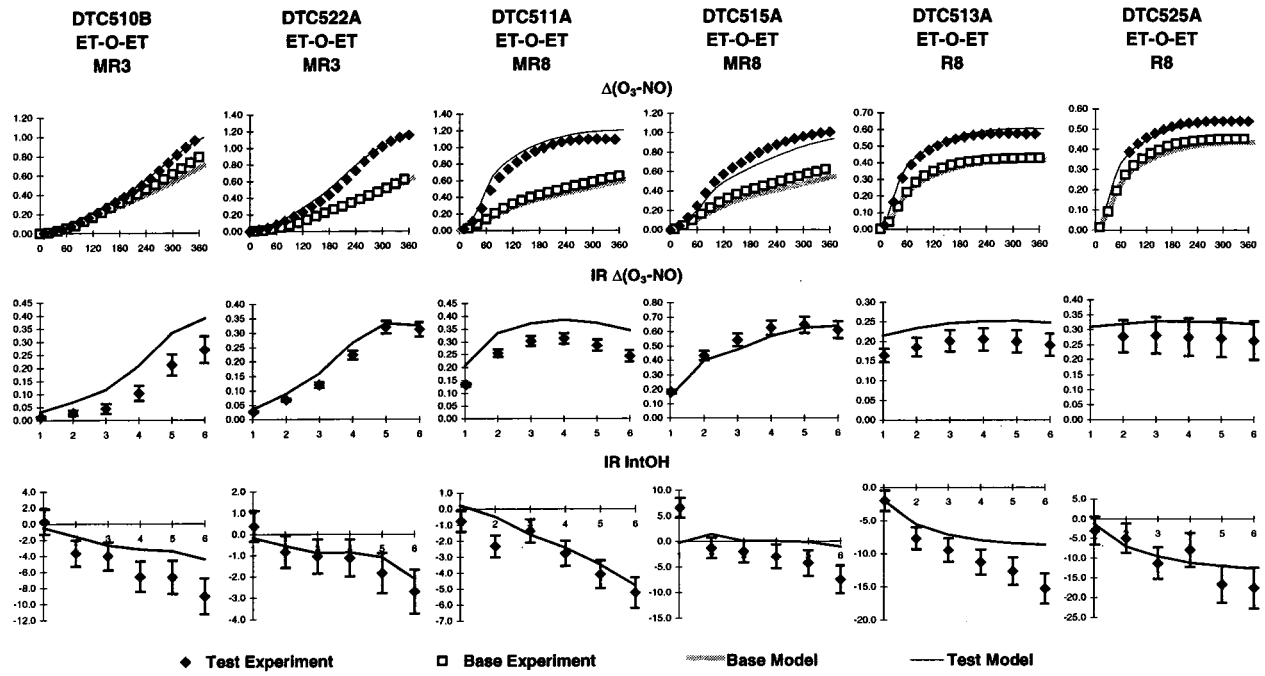

Figure 23. Plots of experimental and calculated results of the incremental reactivity experiments with diethyl ether.

The initial model simulations of the ethyl acetate experiments gave very poor fits to the data, and no adjustments of nitrate yields or other uncertain parameters in *known* reactions would yield satisfactory simulations. Satisfactory fits could only be obtained if it was assumed that the OH reaction formed a PAN precursor radical ($CH_3C(O)OO\cdot$) in high yields, whose subsequent reaction with NO_2 to form relatively stable PAN has significant effects on predictions of reactivity and how they vary with conditions. The only chemically reasonable way to rationalize this is to postulate a reaction of the type

$$RCH(O\cdot)\text{-}O\text{-}C(O)\text{-}R' \rightarrow RC(O)\cdot + R\text{-}C(O)OH,$$

which could occur via 5-member ring transition state with the hydrogen α to the alkoxy center migrating to the carbonyl oxygen, which becomes the OH group in the acid product. This postulated "ester rearrangement" reaction was subsequently confirmed in laboratory studies carried out by Tuazon et al (1998), which was carried out as a direct result of the modeling of these experiments. This reaction is now incorporated into the SAPRC-99 mechanism generation system (Carter, 2000), and is predicted to be important in the photooxidations of all esters where this might occur.

The results of the model simulations of the ethyl acetate experiments using the SAPRC-99 mechanism, which incorporates the now-confirmed ester rearrangement, are shown on Figure 24. Once the ester rearrangement is assumed, essentially no adjustments to the mechanism are necessary to obtain the fits shown[3]. The apparent discrepancy in simulations of Δ([O_3]-[NO]) reactivity in the low

[3] The estimated nitrate yield in the reaction of NO with the peroxy radical formed in the reaction of OH with ethyl acetate is 3.9%, but an adjustment to 4% is used in the standard SAPRC-99 mechanisms for

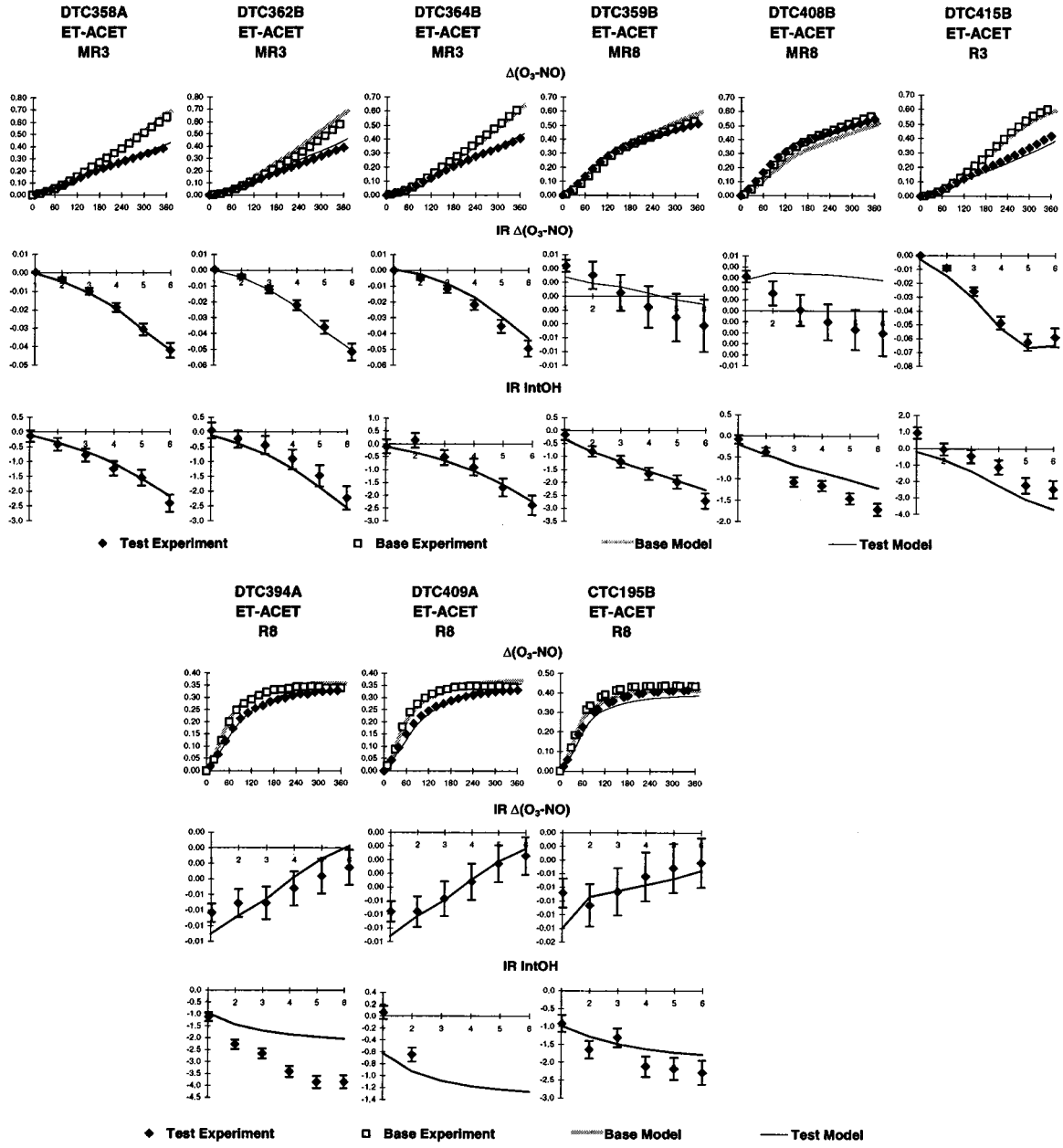

Figure 24. Plots of experimental and calculated results of the incremental reactivity experiments with ethyl acetate.

this compound, which is an insignificant difference. This adjustment was made when an earlier version of the mechanism estimation system predicted a somewhat different nitrate yield for this reaction, and was not removed after the prediction method was modified.

NO_x full surrogate run DTC408 is not significant because of the low magnitude in the change of $\Delta([O_3]-[NO])$ caused by ethyl acetate addition.

i. Methyl Isobutyrate

Although not important in emissions inventories, methyl isobutyrate was studied in this program to provide evaluation data for other types of esters besides acetates. This is necessary because while reaction at the group next to the carbonyl is not important in acetates, it may be non-negligible for other esters such as isobutyrates, and evaluation data for such compounds are not available. At least two of each of the three types of reactivity experiments were carried out with this compound, and the results of most of these experiments[4] are shown on Figure 25. In addition, Figure 26 shows the formaldehyde and acetone data obtained during these experiments.

It should be noted that the model simulations do not fit the data satisfactorily unless it is assumed that radicals of the type $CH_3OC(O)\cdot$ react primarily with O_2 to form the PAN analogue precursor $CH_3OC(O)OO\cdot$, rather than decompose to $CH_3\cdot + CO_2$. These radicals are predicted to be formed following OH reaction at the tertiary hydrogen of the isobutyrate molecule and decomposition of the

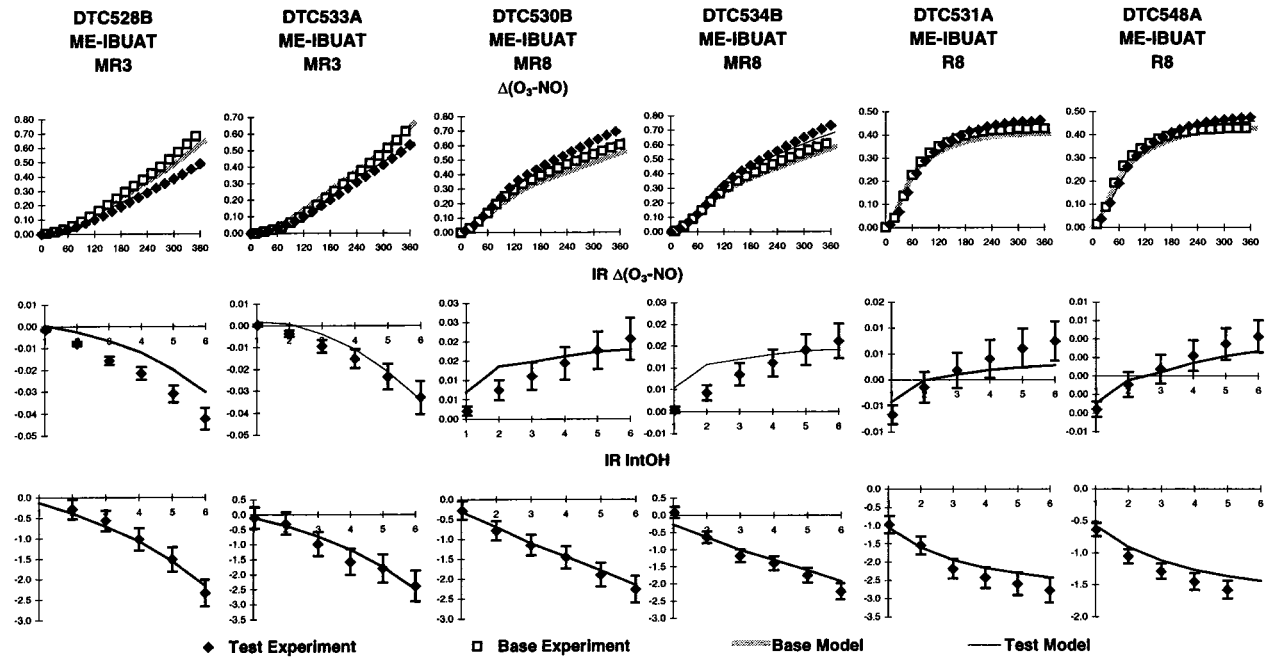

Figure 25. Plots of experimental and calculated results of the incremental reactivity experiments with methyl isobutyrate.

[4] The results and model performance for the low NO_x full surrogate run DTC539 were essentially the same as for the other two low NO_x full surrogate runs for methyl isobutyrate, and are not shown.

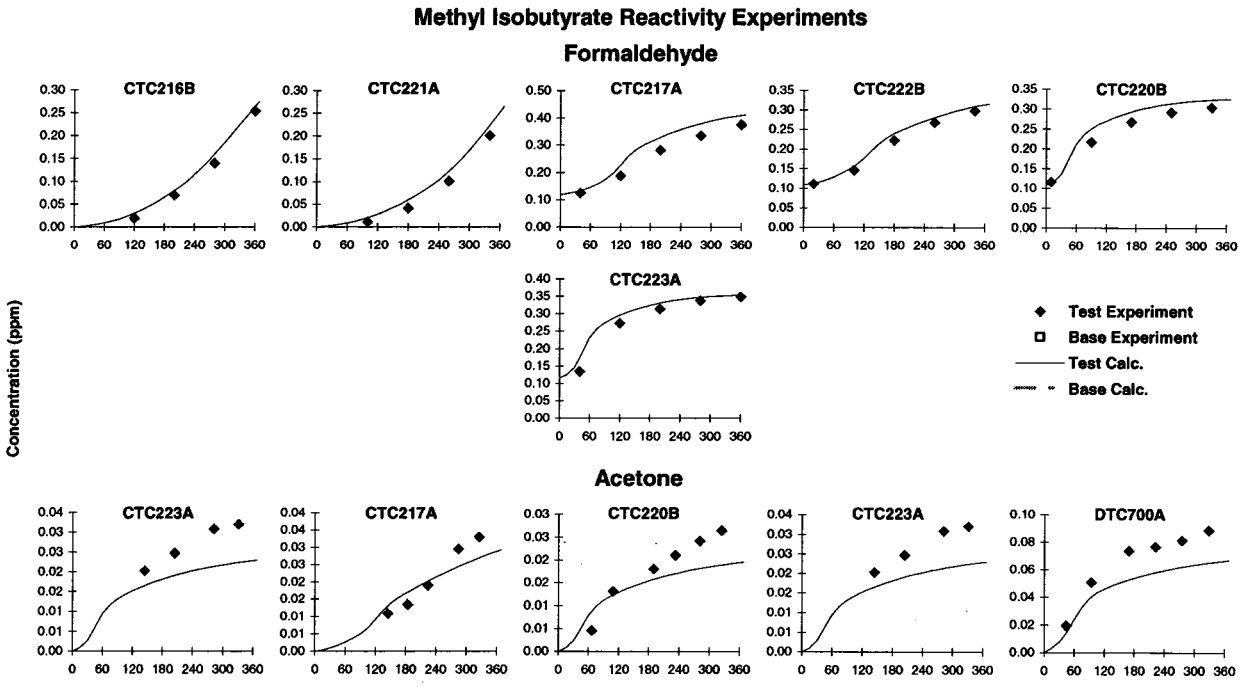

Figure 26. Plots of experimental and calculated formaldehyde and acetone data for the incremental reactivity experiments with methyl isobutyrate.

alkoxy radical subsequently formed. An earlier version of the mechanism generation system assumed that the decomposition to CO_2 dominated for such radicals, but this was modified as a result of experiments with this compound. No reasonable adjustment of the other uncertainties in the mechanism yielded acceptable fits unless this decomposition was assumed to be unimportant.

The results of model simulations using the SAPRC-99 mechanism are also shown on the figures. To obtain these fits, and in particular to correctly predict the acetone yields observed in these experiments, it was necessary to adjust the branching ratios assumed for the initial reaction of OH with methyl isobutyrate. On the other hand, essentially no adjustment was necessary to the nitrate yields assumed in the peroxy radical reactions with NO.[5]

The estimation method of Kwok and Atkinson (1995) predicts that ~30% of the reaction occurs at the tertiary carbon on the isobutyrate group, with the remainder of the reaction at the various methyl groups in the molecule. This results in significant underprediction of the acetone yields, which are predicted to be formed primarily following reaction of OH with the tertiary hydrocarbon on the isobutyrate. It also results in underprediction of the total OH radical rate constant. If it is assumed that the Kwok and Atkinson (1995) method underestimates the rate of the rate of reaction at the tertiary hydrogen but correctly predicts the reaction rates at the methyl groups, then the total rate constant can be used to

[5] The estimated nitrate yield in the reaction of NO with the peroxy radical formed in the reaction of OH with methyl isobutyrate is 6.5%, but an adjustment to 6.4% is used in the standard mechanism for this compound, which is an insignificant difference.

derive an estimate that reaction at the tertiary hydrogen occurs approximately 67% of the time. This gives significantly better fits to the acetone data, and is therefore used in the mechanism.

j. Butyl Acetate

N-butyl acetate was studied in this program to provide additional data concerning effects of structure on reactivities and mechanisms for esters, and because it is also present in stationary source emissions inventories. Two or more of each of the three types of incremental reactivity experiments were carried out with this compound in the DTC, and the results are shown on Figure 27. Results of model calculations using the SAPRC-99 mechanism are also shown on the figure. Reasonably satisfactory fits to most of the data were obtained.

The butyl acetate mechanism is relatively complex and has a number of uncertain branching ratios. One of these concerned a competition between the ester rearrangement and a 1,4-H shift isomerization reaction of the alkoxy radical formed following reaction of OH at the 1-position on the butyl group:

$$CH_3CH_2CH_2CH(O\cdot)OC(O)CH_3 \rightarrow CH_3CH_2CH_2C(O)\cdot + CH_3C(O)OH$$
$$CH_3CH_2CH_2CH(O\cdot)OC(O)CH_3 \rightarrow \cdot CH_2CH_2CH_2CH(OH)OC(O)CH_3$$

The chamber data could only be satisfactorily fit if it was assumed that these occurred at competitive rates, and in particular that the ester rearrangement did not dominate over the 1,5-H shift isomerization. This happened to be consistent with the branching ratio predicted by current estimation system, though the uncertainties of these estimates are high. The other potentially uncertainties concern the branching ratios for the initial reaction of OH at various position in the molecule and the competition between reaction with O_2 and decomposition for the alkoxy radical formed after reaction at the 3-position on the butyl group. Despite these uncertainties, essentially no adjustments[6] to the mechanism had to be made to obtain the fits shown on Figure 27.

Because this compound provides a good example of a compound with an uncertain mechanisms that still fits environmental chamber data, a comprehensive uncertainty analysis of atmospheric reactivity predictions for this compound was carried out by Wang et al (2000). This involved systematically varying these and other uncertain parameters to within their range of uncertainties, while still constraining the model predictions to fit the environmental chamber data obtained in this study. The results indicate that the parameters contributing most to the uncertainty in relative atmospheric reactivity of this compound are uncertainties in the base mechanism, with uncertainties in the total rate constant being the next most important (Wang et al, 2000). Because of the constraints to the mechanism provided by these chamber data, the other mechanistic uncertainties had relatively low impacts on the predicted overall atmospheric reactivities.

[6] The estimated nitrate yield in the reaction of NO with the peroxy radical formed in the reaction of OH with n-butyl acetate is 9.8%, but an adjustment to 10% is used in the standard SAPRC-99 mechanisms for this compound, which is an insignificant difference.

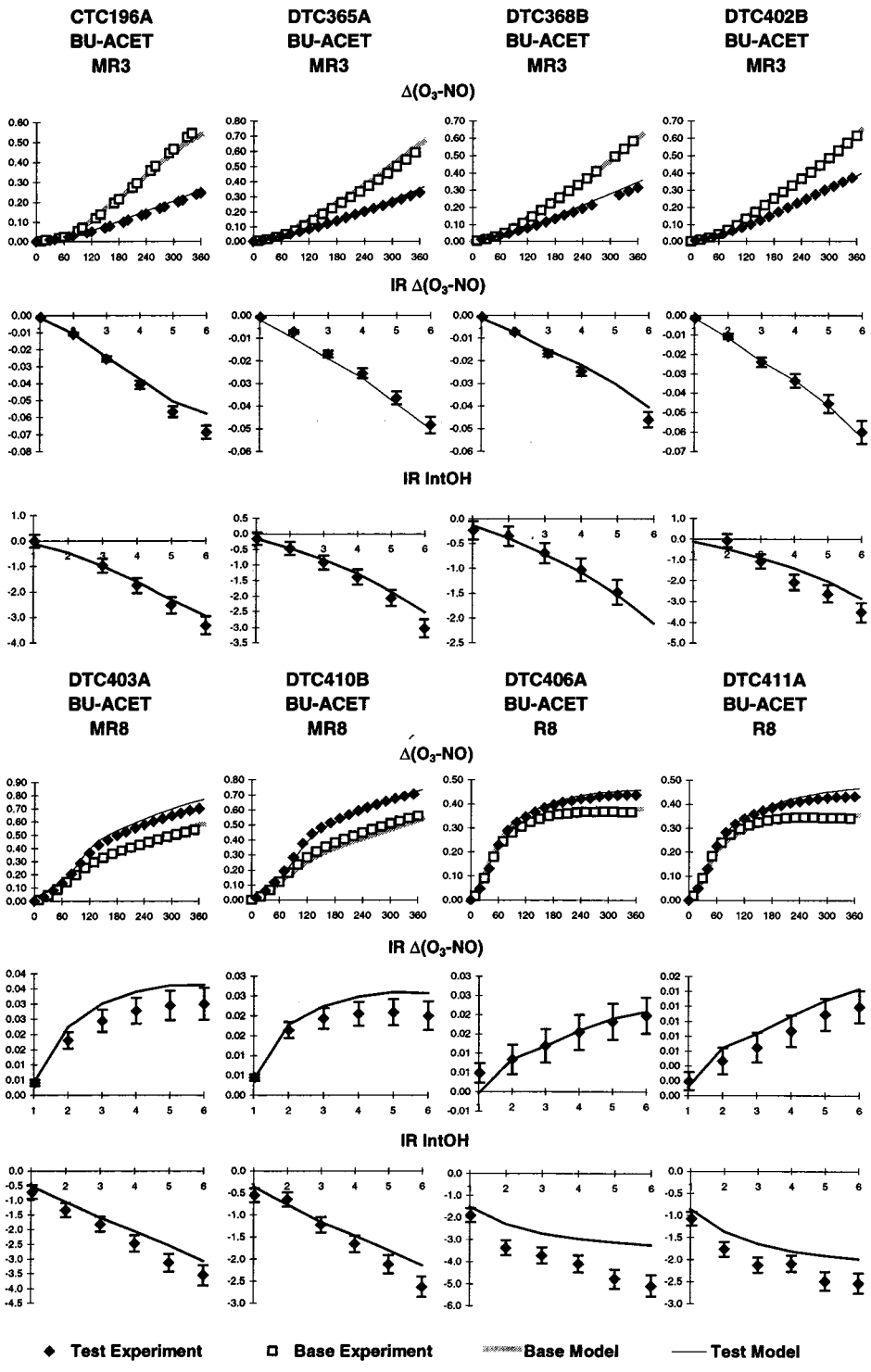

Figure 27. Plots of experimental and calculated results of the incremental reactivity experiments with butyl acetate.

k. Propylene Glycol Methyl Ether Acetate

Propylene glycol methyl ether acetate (PGME acetate or 1-Methoxy-2-Propyl Acetate) was studied for this program because it is present in emissions inventories and provides an example of a compound with both an ether and an acetate group, for which mechanism evaluation data were not available prior to this project. Two of each of the three types of incremental reactivity experiments were carried out in the DTC, and the results are shown on Figure 28.

Results of model calculations using the SAPRC-99 mechanism are also shown on the figure. This incorporates the OH radical rate constant that was measured as part of this study (see Section III.A.1), but no other adjustments were made to attain the fits that are shown. The model has a very slight bias towards overpredicting the inhibition of $\Delta([O_3]-[NO])$ in the mini-surrogate experiments and overpredicting the $\Delta([O_3]-[NO])$ in the full surrogate runs, but the discrepancies are relatively minor and overall the model performance is considered to be satisfactory. The results tend to validate the performance of the SAPRC-99 estimation system for at least one multifunctional compound.

l. Diacetone Alcohol

Diacetone alcohol (4-methyl, 4-hydroxy-2-pentanone) was chosen for study because it is present in the stationary source inventory and it provides a representation of another type of compound with more than one functional group, for which mechanism evaluation data would be useful. However, although DTC reactivity experiment with this compound was attempted, the experiment turned out not to

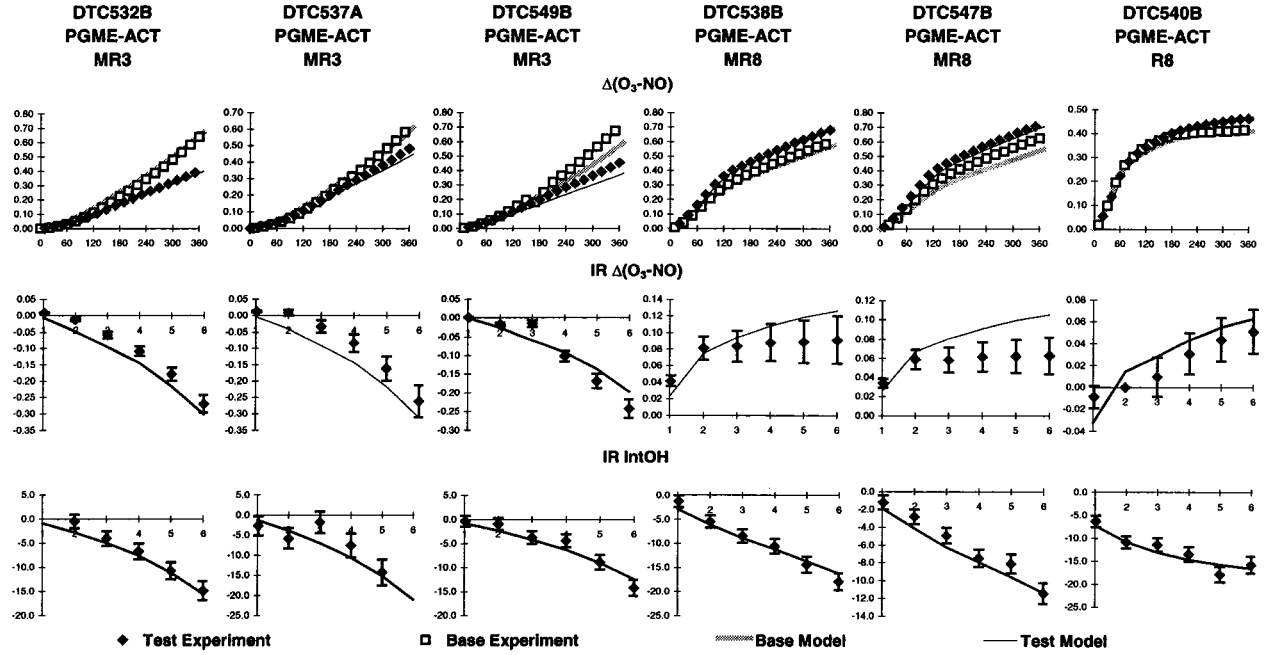

Figure 28. Plots of experimental and calculated results of the incremental reactivity experiments with propylene glycol methyl ether acetate.

be successful. It was found that this compound was too nonvolatile at room temperature to be injected into the gas phase at the necessary concentrations for our chamber experiments in a reasonable amount of time, but that it underwent decomposition when heated to the temperature deemed necessary for this purpose. It was determined that the priority to study this compound was not sufficiently high to merit the effort required to develop the alternative injection methods that would be necessary to obtain sufficiently well characterized data for mechanism evaluation.

IV. CONCLUSIONS

This project has been successful in achieving its objective of generating useful data for reducing uncertainties in ozone reactivity impacts for major classes of stationary source VOCs. Its particular utility has been to provide data needed to develop and evaluate mechanisms for higher molecular weight oxygenated compounds such as esters, ketones, alcohols, ethers, and multifunctional oxygenates for which inadequate data had been available in the past. This information has permitted the development and evaluation of estimation and mechanism generation methods that now can be used to estimate atmospheric ozone impacts for a wide variety of such compounds for which no data are available (Carter, 2000). In general, these data tended to verify that the estimation and mechanism generally performs surprisingly well considering all the uncertainties involved. This has resulted in much lower uncertainty assignments for estimates of ozone reactivities for such compounds where no data are available than otherwise would have been the case.

The data from this project were certainly not the only data that were used to reduce the reactivity uncertainties for these classes of oxygenated compounds. In recent years there have been a number of useful studies of ozone reactivities of individual VOCs, primarily under funding from private sector groups desiring reactivity information on chemicals they manufacture or use, usually with the hope of obtaining a VOC exemption for a compound. Although the data obtained were valuable, from a mechanistic perspective the choices of compounds to study were haphazard, and information on groups of related compounds that is needed to evaluate trends or estimation methods was extremely limited. In addition, because reactivity considerations in current national regulations tend to focus on exemptions rather than total ozone impacts, the focus has been mainly on low reactivity compounds. The great value of this program is that the compounds chosen for study were based on a much broader analysis and perspective, with input not only from the investigators and the CARB staff, but also from the industry groups that produce and use these chemicals. The result has been to provide data most useful to complement and fill in the gaps left by other studies, resulting in a reasonably comprehensive data base that proved to be of great value to reducing chemical uncertainties in reactivity predictions. We believe this project has been extremely successful in this regard, and should serve as a model for future studies.

One important area of uncertainty in estimating ozone impacts for high molecular weight oxygenated compounds concerns estimates of nitrate yields from reactions of NO with substituted peroxy radicals. This is a potentially important radical and NO_x termination process and assumptions made in the model concerning these nitrate yields are important in affecting reactivity predictions, and until recently there has been essentially no information on nitrate yields from substituted peroxy radicals. Although this study did not provide direct measurement data for these yields, it, in conjunction with the private-sector funded studies referenced above, provided data that could be used to develop and evaluate methods for estimating these yields for modeling purposes (Carter, 2000). These data suggest that oxygen substitution tends to reduce overall nitrate yields by about a factor of 1.5, and that these can probably usually be estimated to within about this same factor (Carter, 2000). The data with the octanols confirm our conclusion that, contrary to what was assumed in previous versions of our mechanism (Carter, 1990, 1997c), nitrate formation from the hydroxy-substituted peroxy radicals formed in the oxidations of alkanes as well as oxygenated VOCs is non-negligible.

An important and unexpected result of this study is that it led to the discovery of the previously unsuspected "ester rearrangement" reaction that significantly affect the reactivities and products formed in the atmospheric oxidations of many types of esters. The particular esters studied for the private sector

groups all were unusual in that this reaction could not occur (or, in the case of methyl acetate, had no net effect on the predicted reactivity), but this is expected to be a dominant reaction for many other compounds. The discovery of the need to postulate this reaction to explain the environmental chamber data for ethyl acetate lead directly to the laboratory experiments of Tuazon et al (1998) that confirmed its existence. Without this project that reaction would probably had not been discovered, and the estimated mechanisms for most esters would have been incorrect in major respects.

This study, in conjunction with studies of higher ketones funded by Eastman Chemical provided data that indicated that the overall quantum yields for photodecomposition of ketones to form radicals decreases monotonically with the size of the molecule (Carter, 2000). This has significant impacts on reactivity estimates for ketones, which are important solvent species.

Although the data from this project has reduced uncertainties in overall reactivity predictions, significant uncertainties remain. Results of our kinetic and product studies on the octanols and the fact that it was necessary to adjust initial reaction branching ratios in the reactions of OH with cyclohexanone and methyl isobutyrate suggest that refinements are needed to the structure-reactivity estimation methods of Kwok and Atkinson (1997). Recent data where ketone photolysis rates were measured directly indicate that the present model used for ketone photolysis is almost certainly an oversimplification (Wirtz, 1999). The nitrate yield estimates that are important in affecting reactivity predictions for many compounds are based primarily on adjustments to fit chamber data, and compensating errors due to other mechanistic uncertainties are likely in some if not most cases. Many of the branching ratio estimates for the many competing alkoxy radical reactions are uncertain and probably only good to within a factor of ~5, and satisfactory simulations of O_3 reactivity in chamber experiments may only be because the O_3 predictions are not sensitive to these estimates. However, these mechanistic details may significantly affect what products are formed, and this, in at least some cases, may affect predictions of the VOC's reactions impact the environment in other ways, such as, for example, effects on formation of secondary particulate matter. Therefore, further research to refine current estimation methods is clearly needed.

This study has also not eliminated the need for studies of additional classes of compounds for which reactivity data are unavailable or inadequate. Although the types of oxygenated species that were studied represent the major previously inadequately studied component of the stationary source inventory, they are not the only component of the inventory for which reactivity data were needed. Amines and halogenated organics are also emitted, and the current mechanism either does not represent them at all, or represents them in such an approximate manner that reactivity estimates for them should be considered likely to be significantly in error. In terms of emissions and reactivity, and likelihood of obtaining data of near-term utility to reducing uncertainties in reactivity estimates, studies of amines probably should be given the highest priority. Halogenated organics tend to have very low reactivities and many are being regulated anyway because of toxicity concerns, so studies of ozone reactivities of such compounds may have lower priorities from a regulatory perspective. However, because of their low reaction rates they may persist in the atmosphere longer, and thus impact the regional environment in ways that are not adequately understood. The limited data on reactivities of halogenated organics (e.g., Carter et al, 1996b, 1997g) indicate that current mechanisms cannot successfully predict the impacts of emissions of such compounds in the atmosphere, even if the chemistry of the predicted halogen species are added to the mechanism. This is an area where considerable long-term research will eventually be needed.

V. REFERENCES

Atkinson, R. (1989): "Kinetics and Mechanisms of the Gas-Phase Reactions of the Hydroxyl Radical with Organic Compounds," J. Phys. Chem. Ref. Data, Monograph no 1.

Atkinson, R. (1994): "Gas-Phase Tropospheric Chemistry of Organic Compounds," J. Phys. Chem. Ref. Data, Monograph No. 2.

Atkinson, R. (1997): "Gas Phase Tropospheric Chemistry of Volatile Organic Compounds: 1. Alkanes and Alkenes," J. Phys. Chem. Ref. Data, 26, 215-290.

Atkinson, R., W. P. L. Carter, A. M. Winer and J. N. Pitts, Jr. (1981): "An Experimental Protocol for the Determination of OH Radical Rate Constants with Organics Using Methyl Nitrite as an OH Radical Source," J. Air Pollut. Control Assoc., 31, 1090-1092.

Atkinson, R., S. M. Aschmann, W. P. L. Carter, A. M. Winer and J. N. Pitts, Jr. (1982): "Alkyl Nitrate Formation from the NO_x-Air Photooxidations of C_2-C_8 n-Alkanes," J. Phys. Chem. 86, 4562-4569.

CARB (1993): "Proposed Regulations for Low-Emission Vehicles and Clean Fuels -- Staff Report and Technical Support Document," California Air Resources Board, Sacramento, CA, August 13, 1990. See also Appendix VIII of "California Exhaust Emission Standards and Test Procedures for 1988 and Subsequent Model Passenger Cars, Light Duty Trucks and Medium Duty Vehicles," as last amended September 22, 1993. Incorporated by reference in Section 1960.

CARB (1999) California Air Resources Board, Proposed Regulation for Title 17, California Code of Regulations, Division 3, Chapter 1, Subchapter 8.5, Article 3.1, sections 94560- 94539.

Carter, W. P. L. (1990): "A Detailed Mechanism for the Gas-Phase Atmospheric Reactions of Organic Compounds," Atmos. Environ., 24A, 481-518.

Carter, W. P. L. (1994): "Development of Ozone Reactivity Scales for Volatile Organic Compounds," J. Air & Waste Manage. Assoc., 44, 881-899.

Carter, W. P. L. (1995): "Computer Modeling of Environmental Chamber Measurements of Maximum Incremental Reactivities of Volatile Organic Compounds," Atmos. Environ., 29, 2513-2527.

Carter, W. P. L. (2000): "Documentation of the SAPRC-99 Chemical Mechanism for VOC Reactivity Assessment," Draft report to the California Air Resources Board, Contracts 92-329 and 95-308, April 11.

Carter, W. P. L., R. Atkinson, A. M. Winer, and J. N. Pitts, Jr. (1982): "Experimental Investigation of Chamber-Dependent Radical Sources," Int. J. Chem. Kinet., 14, 1071.

Carter, W. P. L. and R. Atkinson (1987): "An Experimental Study of Incremental Hydrocarbon Reactivity," Environ. Sci. Technol., 21, 670-679

Carter, W. P. L., and F. W. Lurmann (1990): "Evaluation of the RADM Gas-Phase Chemical Mechanism," Final Report, EPA-600/3-90-001.

Carter, W. P. L. and F. W. Lurmann (1991): "Evaluation of a Detailed Gas-Phase Atmospheric Reaction Mechanism using Environmental Chamber Data," Atm. Environ. 25A, 2771-2806.

Carter, W. P. L, D. Luo, I. L. Malkina, and J. A. Pierce (1993a): "An Experimental and Modeling Study of the Photochemical Ozone Reactivity of Acetone," Final Report to Chemical Manufacturers Association Contract No. KET-ACE-CRC-2.0. December 10.

Carter, W. P. L., J. A. Pierce, I. L. Malkina, D. Luo and W. D. Long (1993b): "Environmental Chamber Studies of Maximum Incremental Reactivities of Volatile Organic Compounds," Report to Coordinating Research Council, Project No. ME-9, California Air Resources Board Contract No. A032-0692; South Coast Air Quality Management District Contract No. C91323, United States Environmental Protection Agency Cooperative Agreement No. CR-814396-01-0, University Corporation for Atmospheric Research Contract No. 59166, and Dow Corning Corporation. April 1.

Carter, W. P. L., D. Luo, I. L. Malkina, and J. A. Pierce (1995a): "Environmental Chamber Studies of Atmospheric Reactivities of Volatile Organic Compounds. Effects of Varying ROG Surrogate and NO_x," Final Report to Coordinating Research Council, Inc., Project ME-9, California Air Resources Board, Contract A032-0692, and South Coast Air Quality Management District, Contract C91323. March 24.

Carter, W. P. L., D. Luo, I. L. Malkina, and D. Fitz (1995b): "The University of California, Riverside Environmental Chamber Data Base for Evaluating Oxidant Mechanism. Indoor Chamber Experiments through 1993," Report submitted to the U. S. Environmental Protection Agency, EPA/AREAL, Research Triangle Park, NC., March 20..

Carter, W. P. L., D. Luo, I. L. Malkina, and J. A. Pierce (1995c): "Environmental Chamber Studies of Atmospheric Reactivities of Volatile Organic Compounds. Effects of Varying Chamber and Light Source," Final Report to National Renewable Energy Laboratory, Contract XZ-2-12075, Coordinating Research Council, Inc., Project M-9, California Air Resources Board, Contract A032-0692, and South Coast Air Quality Management District, Contract C91323, March 26.

Carter, W. P. L., D. Luo, and I. L. Malkina (1996): "Investigation of the Atmospheric Ozone Impact of Methyl Acetate," Report to Eastman Chemical Company, July.

Carter, W. P. L., D. Luo, and I. L. Malkina (1996b): "Investigation of the Atmospheric Ozone Formation Potential of Trichloroethylene," Report to the Halogenated Solvents Industry Alliance, August.

Carter, W. P. L., D. Luo, and I. L. Malkina (1997a): "Investigation of the Atmospheric Ozone Formation Potential of t-Butyl Acetate," Report to ARCO Chemical Corporation, July 2.

Carter, W. P. L., D. Luo, and I. L. Malkina (1997b): "Investigation of the Atmospheric Ozone Formation Potential of Propylene Glycol," Report to Philip Morris, USA, May 2.

Carter, W. P. L., D. Luo, and I. L. Malkina (1997c): "Environmental Chamber Studies for Development of an Updated Photochemical Mechanism for VOC Reactivity Assessment," Final Report to the California Air Resources Board, the Coordinating Research Council, and the National Renewable Energy Laboratory, November 26.

Carter, W. P. L., D. Luo and I. L. Malkina (1997d): "Investigation of that Atmospheric Reactions of Chloropicrin," Atmos. Environ. 31, 1425-1439.; Report to the Chloropicrin Manufacturers Task Group, May 19.

Carter, W. P. L., D. Luo and I. L. Malkina (1997e): "Investigation of that Atmospheric Reactions of Chloropicrin," Atmos. Environ. 31, 1425-1439.

Carter, W. P. L., D. Luo, and I. L. Malkina (1997f): "Investigation of the Atmospheric Ozone Formation Potentials of Selected Dibasic Esters," Draft Report to the Dibasic Esters Group, SOCMA, May 15.

Carter, W. P. L., D. Luo, and I. L. Malkina (1997g): "Investigation of the Atmospheric Ozone Formation Potential of Selected Alkyl Bromides," Report to Albemarle Corporation, November 10.

Carter, W. P. L., M. Smith, D. Luo, I. L. Malkina, T. J. Truex, and J. M. Norbeck (1999a): "Experimental Evaluation of Ozone Forming Potentials of Motor Vehicle Emissions", Final Report to California Air Resources Board Contract No. 95-903, and South Coast Air Quality Management District Contract No 95073/Project 4, Phase 2, May 14.

Carter, W. P. L., D. Luo, and I. L. Malkina (1999b): 'Investigation of the Atmospheric Impacts and Ozone Formation Potential of Styrene," Report to the Styrene Information and Research Center. March 10.

Carter, W. P. L., D. Luo, I. L. Malkina, and J. A. Pierce (1995a): "Environmental Chamber Studies of Atmospheric Reactivities of Volatile Organic Compounds. Effects of Varying ROG Surrogate and NO_x," Final Report to Coordinating Research Council, Inc., Project ME-9, California Air Resources Board, Contract A032-0692, and South Coast Air Quality Management District, Contract C91323. March 24.

Carter, W. P. L., D. Luo, I. L. Malkina, and D. Fitz (1995b): "The University of California, Riverside Environmental Chamber Data Base for Evaluating Oxidant Mechanism. Indoor Chamber Experiments through 1993," Report submitted to the U. S. Environmental Protection Agency, EPA/AREAL, Research Triangle Park, NC., March 20..

Carter, W. P. L., D. Luo, I. L. Malkina, and J. A. Pierce (1995c): "Environmental Chamber Studies of Atmospheric Reactivities of Volatile Organic Compounds. Effects of Varying Chamber and Light Source," Final Report to National Renewable Energy Laboratory, Contract XZ-2-12075, Coordinating Research Council, Inc., Project M-9, California Air Resources Board, Contract A032-0692, and South Coast Air Quality Management District, Contract C91323, March 26.

Carter, W. P. L., D. Luo, and I. L. Malkina (1997a): "Environmental Chamber Studies for Development of an Updated Photochemical Mechanism for VOC Reactivity Assessment," Final Report to the California Air Resources Board, the Coordinating Research Council, and the National Renewable Energy Laboratory, November 26.

Gery, M. W. (1991): "Review of the SAPRC-90 Chemical Mechanism," Report to the California Air Resources Board, Contract No. A132-055, Sacramento, CA.

Jeffries, H. E., K. G. Sexton, J. R. Arnold, and T. L. Kale (1989): "Validation Testing of New Mechanisms with Outdoor Chamber Data. Volume 2: Analysis of VOC Data for the CB4 and CAL Photochemical Mechanisms," Final Report, EPA-600/3-89-010b.

Johnson, G. M. (1983): "Factors Affecting Oxidant Formation in Sydney Air," in "The Urban Atmosphere -- Sydney, a Case Study." Eds. J. N. Carras and G. M. Johnson (CSIRO, Melbourne), pp. 393-408.

Kwok, E. S. C., and R. Atkinson (1995): "Estimation of Hydroxyl Radical Reaction Rate Constants for Gas-Phase Organic Compounds Using a Structure-Reactivity Relationship: An Update," Atmos. Environ 29, 1685-1695.

McNair, L. A., A. G. Russell, M. T. Odman, B. E. Croes, and L. Kao (1994): "Airshed Model Evaluation of Reactivity Adjustment Factors Calculated with the Maximum Incremental Reactivity Scale for Transitional Low-Emissions Vehicles," J. Air Waste Manage. Assoc., 44, 900-907.

Nelson, L., O. Rattigan, R. Neavyn, H. Sidebottom, J. Treacy and O. J. Nielson (1990): Int. J. Chem. Kinet. 22, 1111.

Pitts, J. N., Jr., E. Sanhueza, R. Atkinson, W. P. L. Carter, A. M. Winer, G. W. Harris, and C. N. Plum (1984): "An Investigation of the Dark Formation of Nitrous Acid in Environmental Chambers," Int. J. Chem. Kinet., 16, 919-939.

Tuazon, E. C., R. Atkinson, C. N. Plum, A. M. Winer, and J. N. Pitts, Jr. (1983): "The Reaction of Gas-Phase N_2O_5 with Water Vapor," Geophys. Res. Lett. 10, 953-956.

Tuazon, E. C., S. M. Aschmann, R. Atkinson, and W. P. L. Carter (1998): "The reactions of Selected Acetates with the OH radical in the Presence of NO: Novel Rearrangement of Alkoxy Radicals of Structure RC(O)OCH(O.)R'", J. Phys. Chem A 102, 2316-2321.

Wallington, T. J. and M. J. Kurylo (1987): "Flash Photolysis Resonance Fluorescence Investigation of the Gas-Phase Reactions of OH Radicals with a Series of Aliphatic Ketones over the Temperature Range 240-440 K," J. Phys. Chem 91, 5050.

Wang, L, J. B. Milford and W. P. L. Carter (2000): "Uncertainty in Reactivity Estimates for n-Butyl Acetate and 2-Butoxy Ethanol," Final Report to the California Air Resources Board Contract No. 95-331, April 10.

Wirtz, K. (1999): "Determination of Photolysis Frequencies and Quantum Yields for Small Carbonyl Compounds using the EUPHORE Chamber," Presented at the US/German - Environmental Chamber Workshop, Riverside, California, October 4-6.

Wyatt, S. E., J. S. Baxley and J. R. Wells (1999), "The Hydroxyl Radical Reaction Rate Constant and Products of Methyl Isobutyrate," Int. J. Chem. Kinet. 31, 551-557.

Zafonte, L., P. L. Rieger, and J. R. Holmes (1977): "Nitrogen Dioxide Photolysis in the Los Angeles Atmosphere," Environ. Sci. Technol. 11, 483-487.

APPENDIX A. MECHANISM AND DATA TABULATIONS

Table A-1. Listing of the mechanisms used to represent the test VOCs when modeling the experiments carried out for this project. See Carter (2000) for a full listing of the base mechanism and the mechanisms used to represent the VOCs in the base case and control and characterization experiments.

Compound	Rate Parameters [a] k(298)	A	Ea	B	Reactions and Products [b]
Cyclohexane	7.21e-12	2.59e-12	-0.61	2.0	CYCC6 + HO. = #.799 RO2-R. + #.201 RO2-N. + #.473 R2O2. + #.608 XC + #.597 PRD1 + #.203 PRD2
	6.39e-12	6.39e-12			PRD1 + HO. = #.386 RO2-R. + #.178 RO2-N. + #.722 R2O2. + #.436 RCO-O2. + #.059 HCHO + #.194 RCHO + #.197 PROD2 + #1.802 XC
	PF=KETONE QY = 5.0e-2				PRD1 + HV = #6 XC
	5.19e-11	5.19e-11			PRD2 + HO. = #.18 HO2. + #.07 RO2-R. + #.008 RO2-N. + #.743 RCO-O2. + #.01 CO + #.26 RCHO + #.004 GLY + #.014 MGLY + #-0.116 XC
	7.60e-15	7.60e-15 PF=C2CHO			PRD2 + NO3 = RCO-O2. + XN
					PRD2 + HV = #.437 HO2. + #1.462 RO2-R. + #.101 RO2-N. + #1.021 CO + #.365 HCHO + #.899 RCHO + #-1.691 XC
Isopropyl Alcohol	5.39e-12	6.49e-13	-1.25		I-C3-OH + HO. = #.953 HO2. + #.046 RO2-R. + #.001 RO2-N. + #.046 HCHO + #.046 CCHO + #.953 ACET + #-0.003 XC
1-Octanol	2.02e-11	2.02e-11			1-C8-OH + HO. = #.771 RO2-R. + #.229 RO2-N. + #.32 R2O2. + #.054 HCHO + #3.108 XC + #.387 PRD1 + #.384 PRD2
	2.97e-11	2.97e-11			PRD1 + HO. = #.068 HO2. + #.171 RO2-R. + #.075 RO2-N. + #.147 R2O2. + #.686 RCO-O2. + #.007 CO + #.248 RCHO + #.014 MGLY + #-0.303 XC
	3.80e-15	3.80e-15 PF=C2CHO			PRD1 + NO3 = RCO-O2. + #-0 XC + XN
					PRD1 + HV = #.13 HO2. + #1.627 RO2-R. + #.243 RO2-N. + CO + #.777 RCHO + #-1.786 XC
	2.49e-11	2.49e-11			PRD2 + HO. = #.545 HO2. + #.319 RO2-R. + #.066 RO2-N. + #.004 CCO-O2. + #.065 RCO-O2. + #.011 HCHO + #.071 CCHO + #.544 RCHO + #.45 PROD2 + #.016 MGLY + #.86 XC
2-Octanol	2.52e-11	2.52e-11			2-C8-OH + HO. = #.062 HO2. + #.775 RO2-R. + #.163 RO2-N. + #.008 HCHO + #.183 CCHO + #2.219 XC + #.64 PRD1 + #.198 PRD2
	1.79e-11	1.79e-11			PRD1 + HO. = #.256 HO2. + #.418 RO2-R. + #.197 RO2-N. + #.532 R2O2. + #.119 CCO-O2. + #.01 RCO-O2. + #.008 HCHO + #.017 CCHO + #.3 RCHO + #.574 PROD2 + #.164 XC
	PF=KETONE QY = 5.8e-3				PRD1 + HV = #.814 RO2-R. + #.186 RO2-N. + #.902 R2O2. + CCO-O2. + #.814 RCHO + #.443 XC
	2.82e-11	2.82e-11			PRD2 + HO. = #.123 HO2. + #.117 RO2-R. + #.028 RO2-N. + #.086 R2O2. + #.731 RCO-O2. + #.012 CO + #.001 HCHO + #.007 CCHO + #.247 RCHO + #.016 MGLY + #-0.181 XC
	3.80e-15	3.80e-15 PF=C2CHO			PRD2 + NO3 = RCO-O2. + XN
					PRD2 + HV = #.065 HO2. + #1.809 RO2-R. + #.126 RO2-N. + CO + #.034 CCHO + #.874 RCHO + #-1.445 XC
3-Octanol	3.14e-11	3.14e-11			3-C8-OH + HO. = #.225 HO2. + #.641 RO2-R. + #.134 RO2-N. + #.142 CCHO + #.098 RCHO + #2.19 XC + #.609 PRD1 + #.257 PRD2
	1.28e-11	1.28e-11			PRD1 + HO. = #.164 HO2. + #.443 RO2-R. + #.193 RO2-N. + #.57 R2O2. + #.003 CCO-O2. + #.196 RCO-O2. + #.013 HCHO + #.079 CCHO + #.487 RCHO + #.405 PROD2 + #.181 XC

Table A-1 (continued)

Compound	Rate Parameters [a] k(298)	A	Ea	B	Reactions and Products [b]
	PF=KETONE QY = 7.2e-3				PRD1 + HV = #.874 RO2-R. + #.126 RO2-N. + #.935 R2O2. + RCO-O2. + #.874 RCHO + #-0.377 XC
	2.83e-11	2.83e-11			PRD2 + HO. = #.068 HO2. + #.11 RO2-R. + #.024 RO2-N. + #.082 R2O2. + #.798 RCO-O2. + #.023 CO + #.005 HCHO + #.008 CCHO + #.177 RCHO + #.002 GLY + #.011 MGLY + #-0.152 XC
	3.80e-15	3.80e-15			PRD2 + NO3 = RCO-O2. + XN
		PF=C2CHO			PRD2 + HV = #.316 HO2. + #1.592 RO2-R. + #.091 RO2-N. + CO + #.179 HCHO + #.909 RCHO + #-1.452 XC
4-Octanol	2.87e-11	2.87e-11			4-C8-OH + HO. = #.161 HO2. + #.693 RO2-R. + #.145 RO2-N. + #.18 RCHO + #2.002 XC + #.497 PRD1 + #.535 PRD2
	1.29e-11	1.29e-11			PRD1 + HO. = #.053 HO2. + #.487 RO2-R. + #.181 RO2-N. + #.535 R2O2. + #.279 RCO-O2. + #.102 HCHO + #.22 CCHO + #.389 RCHO + #.377 PROD2 + #.104 XC
	PF=KETONE QY = 7.9e-3				PRD1 + HV = #.98 RO2-R. + #.02 RO2-N. + RCO-O2. + #.98 RCHO + #-0.06 XC
	2.61e-11	2.61e-11			PRD2 + HO. = #.079 HO2. + #.077 RO2-R. + #.008 RO2-N. + #.024 R2O2. + #.835 RCO-O2. + #.038 CO + #.01 HCHO + #.018 CCHO + #.145 RCHO + #.006 GLY + #.001 MGLY + #-0.088 XC
	3.80e-15	3.80e-15			PRD2 + NO3 = RCO-O2. + XN
		PF=C2CHO			PRD2 + HV = #.848 HO2. + #1.121 RO2-R. + #.031 RO2-N. + CO + #.255 HCHO + #.117 CCHO + #.852 RCHO + #-1.232 XC
Diethyl Ether	1.33e-11	8.02e-13	-1.66		ET-O-ET + HO. = #.131 RO2-R. + #.04 RO2-N. + #.848 R2O2. + #.829 C-O2. + #.006 HCHO + #.168 CCHO + #.006 RCHO + #.858 MEK + #.01 PROD2 + #-0.924 XC
Ethyl Acetate	1.60e-12	1.60e-12			ET-ACET + HO. = #.148 RO2-R. + #.04 RO2-N. + #.818 R2O2. + #.812 CCO-O2. + #.018 MGLY + #.807 CCO-OH + #.005 RCO-OH + #.033 INERT + #.128 XC + #.096 PRD1
	2.04e-11	2.04e-11			PRD1 + HO. = #.053 RO2-R. + #.002 RO2-N. + #.945 RCO-O2. + #.053 CO + #.047 XC
	3.80e-15	3.80e-15			PRD1 + NO3 = RCO-O2. + XN
		PF=C2CHO			PRD1 + HV = HO2. + #.985 RO2-R. + #.015 RO2-N. + #1.368 CO + #.368 CCO-OH + #.188 XC
Methyl Isobutyrate	1.73e-12	1.73e-12			ME-IBUAT + HO. = #.378 RO2-R. + #.075 RO2-N. + #.771 R2O2. + #.547 RCO-O2. + #.082 CO + #.106 HCHO + #.008 CCHO + #.539 ACET + #.135 MEK + #.005 PROD2 + #.077 RCO-OH + #-0.276 XC + #.081 PRD1 + #.081 PRD2
	2.01e-11	2.01e-11			PRD1 + HO. = #.032 RO2-R. + #.002 RO2-N. + #.002 R2O2. + #.966 RCO-O2. + #.024 CO + #.012 RCHO + #.02 BACL + #-0.052 XC
	3.80e-15	3.80e-15			PRD1 + NO3 = RCO-O2. + XN
		PF=C2CHO			PRD1 + HV = #.737 HO2. + #1.142 RO2-R. + #.047 RO2-N. + #.074 RCO-O2. + #1.046 CO + #.074 CCHO + #.071 MEK + #.046 PROD2 + #.761 BACL + #-2.307 XC
	3.26e-13	3.26e-13			PRD2 + HO. = #.784 RO2-R. + #.039 RO2-N. + #.176 R2O2. + #.176 RCO-O2. + #.257 CO + #.176 HCHO + #.131 MGLY + #.653 BACL + #-0.205 XC
		PF=BACL_ADJ			PRD2 + HV = CCO-O2. + RCO-O2. + #-1 XC
n-Butyl Acetate	4.20e-12	4.20e-12			BU-ACET + HO. = #.675 RO2-R. + #.12 RO2-N. + #.516 R2O2. + #.205 RCO-O2. + #.006 CO + #.116 CCHO + #.03 RCHO + #.252 MEK + #.211 CCO-OH + #.024 INERT + #.95 XC + #.142 PRD1 + #.251 PRD2
	2.35e-11	2.35e-11			PRD1 + HO. = #.081 HO2. + #.055 RO2-R. + #.003 RO2-N. + #.862 RCO-O2. + #.047 CO + #.093 RCHO + #.02 XC
	3.80e-15	3.80e-15			PRD1 + NO3 = RCO-O2. + XN

Table A-1 (continued)

Compound	Rate Parameters [a] k(298)	A	Ea	B	Reactions and Products [b]
		PF=C2CHO			PRD1 + HV = #.996 HO2. + #.978 RO2-R. + #.026 RO2-N. + #1.29 CO + #.007 HCHO + #.195 RCHO + #.29 CCO-OH + #-0.107 XC
	6.44e-12	6.44e-12			PRD2 + HO. = #.33 HO2. + #.14 RO2-R. + #.065 RO2-N. + #.508 R2O2. + #.106 CCO-O2. + #.36 RCO-O2. + #.154 HCHO + #.497 RCHO + #.024 BACL + #.351 CCO-OH + #1.821 XC
		PF=KETONE QY = 1.1e-2			PRD2 + HV = #.96 RO2-R. + #.04 RO2-N. + CCO-O2. + #.96 RCHO + #.88 XC
1-Methoxy-2-Propyl (Propylene glycol methyl ether) Acetate	1.44e-11	1.44e-11			PGME-ACT + HO. = #.324 RO2-R. + #.127 RO2-N. + #1.4 R2O2. + #.542 CCO-O2. + #.006 RCO-O2. + #.031 HCHO + #.003 RCHO + #.049 MEK + #.549 CCO-OH + INERT + #1.499 XC + #.05 PRD1
	5.06e-12	5.06e-12			PRD1 + HO. = #.051 RO2-R. + #.099 RO2-N. + #.902 R2O2. + #.016 CCO-O2. + #.834 RCO-O2. + #.007 CO + #.012 CO2 + #.018 HCHO + #.025 RCHO + #.007 MEK + #.159 HCOOH + #.02 CCO-OH + #2.485 XC
Cyclohexanone	6.39e-12	6.39e-12			CC6-KET + HO. = #.386 RO2-R. + #.178 RO2-N. + #.722 R2O2. + #.436 RCO-O2. + #.059 HCHO + #1.802 XC + #.197 PRD1 + #.194 PRD2
		PF=KETONE QY = 5.0e-2			CC6-KET + HV = #6 XC
	1.52e-11	1.52e-11			PRD1 + HO. = #.124 RO2-R. + #.145 RO2-N. + #1.218 R2O2. + #.731 RCO-O2. + #.44 HCHO + #.124 MEK + #2 XC
		PF=KETONE QY = 5.0e-2			PRD1 + HV = #5.212 XC
	8.38e-11	8.38e-11			PRD2 + HO. = #.03 RO2-R. + #.004 RO2-N. + #.009 R2O2. + #.966 RCO-O2. + #.03 CO + #.039 RCHO + #-0.071 XC
	7.60e-15	7.60e-15			PRD2 + NO3 = RCO-O2. + XN
		PF=C2CHO			PRD2 + HV = #.489 HO2. + #.956 RO2-R. + #.066 RO2-N. + #.488 RCO-O2. + CO + #.468 HCHO + #.446 RCHO + #.02 GLY + #-1.708 XC
4-Methyl-2-Pentanone (Methyl Isobutyl Ketone)	1.41e-11	1.41e-11			MIBK + HO. = #.012 RO2-R. + #.099 RO2-N. + #1.706 R2O2. + #.878 CCO-O2. + #.011 RCO-O2. + #.827 HCHO + #.021 CCHO + #.768 ACET + #.004 MEK + #.135 XC + #.096 PRD1
		PF=KETONE QY = 5.0e-2			MIBK + HV = #.947 RO2-R. + #.053 RO2-N. + #.348 R2O2. + CCO-O2. + #.348 HCHO + #.334 ACET + #.492 XC + #.613 PRD2
	2.60e-11	2.60e-11			PRD1 + HO. = #.082 RO2-R. + #.004 RO2-N. + #.011 R2O2. + #.914 RCO-O2. + #.078 CO + #.011 HCHO + #.011 CCHO + #.004 RCHO + #.067 ACET + #-0.09 XC
	3.80e-15	3.80e-15			PRD1 + NO3 = RCO-O2. + XN
		PF=C2CHO			PRD1 + HV = HO2. + #.96 RO2-R. + #.04 RO2-N. + CO + #.96 ACET + #-1.12 XC
	2.60e-11	2.60e-11			PRD2 + HO. = #.082 RO2-R. + #.004 RO2-N. + #.011 R2O2. + #.914 RCO-O2. + #.078 CO + #.011 HCHO + #.011 CCHO + #.004 RCHO + #.067 ACET + #-0.09 XC
	3.80e-15	3.80e-15			PRD2 + NO3 = RCO-O2. + XN
		PF=C2CHO			PRD2 + HV = HO2. + #.96 RO2-R. + #.04 RO2-N. + CO + #.96 ACET + #-1.12 XC

[a] Thermal rate constants are given by $k(T) = A \cdot (T/300)^B \cdot e^{-Ea/RT}$, where the units of k and A are $cm^3\ molec^{-1}\ s^{-1}$, Ea are kcal mol^{-1}, T is °K, and R=0.0019872 kcal $mol^{-1}\ deg^{-1}$. Rate expressions for photolysis reactions are given by Phot Set = *name*, where *name* designates a set of set of absorption coefficients and quantum yields as given by Carter (2000). If a "qy = *number*" notation is given, the number given is the overall quantum yield, which is assumed to be wavelength independent.

[b] Format of reaction listing: "=" separates reactants from products; "*#number*" indicates stoichiometric coefficient

Table A-2. Tabulation of data obtained in the relative rate constant determination experiments.

Run	Compounds and Concentrations (ppm)				
Run 1	m-Xylene	n-Octane	1-Octanol	2-Octanol	2-Octanone
Init.	0.304	0.357	0.230	0.310	0.253
Init.	0.315	0.383	0.234	0.324	0.262
Init.	0.314	0.366	0.231	0.320	0.261
Init.	0.291	0.336	0.230	0.297	0.248
Init.	0.287	0.338	0.209	0.282	0.238
Init.	0.312	0.362	0.233	0.321	0.256
	0.306	0.358	0.244	0.317	0.256
	0.185	0.291	0.169	0.215	0.212
Run 2	m-Xylene	n-Octane	1-Octanol	2-Octanol	4-Octanone
Init.	0.435	0.466	0.332	0.439	0.398
Init.	0.425	0.460	0.309	0.425	0.386
Init.	0.422	0.457	0.319	0.423	0.383
	0.459	0.481	0.367	0.469	0.423
	0.233	0.380	0.197	0.265	0.268
	0.232	0.379	0.199	0.257	0.266
	0.228	0.357	0.211	0.250	0.273
	0.148	0.310	0.153	0.173	0.208
	0.137	0.291	0.131	0.147	0.193
	0.141	0.291	0.139	0.146	0.203
	0.128	0.279	0.118	0.134	0.191
	0.126	0.286	0.122	0.127	0.182
Run 3	m-Xylene	n-Octane	o-Xylene	1-Octanol	3-Octanone
Init.	0.402	0.433	0.412	0.337	0.410
Init.	0.398	0.429	0.409	0.339	0.409
Init.	0.410	0.441	0.420	0.341	0.420
	0.397	0.429	0.407	0.332	0.400
	0.292	0.372	0.342	0.285	0.346
	0.288	0.373	0.339	0.269	0.339
	0.287	0.375	0.338	0.275	0.336
	0.196	0.314	0.273	0.204	0.269
	0.196	0.317	0.271	0.199	0.258
	0.197	0.315	0.271	0.206	0.261
	0.151	0.289	0.236	0.169	0.234
Run 4	m-Xylene	n-Octane	o-Xylene	Octanal	2-Octanone
Init.	0.447	0.457	0.453	0.590	0.371
Init.	0.444	0.458	0.452	0.592	0.368
Init.	0.452	0.456	0.456	0.593	0.372
Init.	0.445	0.452	0.451	0.590	0.371
Init.	0.448	0.462	0.454	0.590	0.372
	0.448	0.459	0.454	0.587	0.371
	0.316	0.408	0.379	0.333	0.303

Table A-2 (continued)

Run	Compounds and Concentrations (ppm)				
	0.319	0.415	0.383	0.325	0.306
	0.134	0.308	0.246	0.095	0.182
	0.124	0.285	0.227	0.057	0.168
Run 5	m-Xylene	n-Octane	o-Xylene	4-Octanol	Octanal
Init.	0.440	0.441	0.427	0.489	0.609
Init.	0.437	0.436	0.436	0.405	0.591
Init.	0.445	0.451	0.446	0.408	0.620
	0.438	0.437	0.436	0.410	0.615
	0.331	0.396	0.378	0.307	0.392
	0.330	0.399	0.378	0.300	0.363
	0.225	0.338	0.306	0.197	0.185
	0.218	0.331	0.298	0.184	0.166
	0.147	0.287	0.243	0.079	0.104
	0.147	0.291	0.243	0.090	0.101
	0.126	0.270	0.223	0.095	0.087
	0.128	0.284	0.227	0.103	0.110
Run 6	m-Xylene	n-Octane	Methyl Isobutyrate		
Init.	0.554	0.518	0.531		
Init.	0.579	0.534	0.563		
Init.	0.553	0.515	0.524		
Init.	0.541	0.510	0.517		
	0.543	0.513	0.521		
	0.322	0.421	0.496		
	0.342	0.441	0.534		
	0.326	0.428	0.507		
	0.144	0.313	0.464		
	0.141	0.308	0.461		
	0.139	0.309	0.465		
	0.075	0.244	0.434		
	0.072	0.235	0.423		
Run 7	m-Xylene	3-Octanol	4-Octanol	PGME Acetate	
Init.	0.482	0.427	0.462	0.456	
Init.	0.472	0.414	0.454	0.446	
Init.	0.491	0.431	0.468	0.462	
Init.	0.490	0.435	0.470	0.464	
	0.477	0.429	0.454	0.450	
	0.292	0.255	0.265	0.336	
	0.300	0.254	0.266	0.343	
	0.286	0.238	0.247	0.326	
	0.119	0.083	0.103	0.207	
	0.107	0.054	0.074	0.174	

Table A-2 (continued)

Run	Compounds and Concentrations (ppm)			
Run 8	m-Xylene	2-Octanol	3-Octanone	PGME Acetate
Init.	0.325	0.497	0.441	0.444
Init.	0.000	0.000	0.000	0.000
Init.	0.321	0.495	0.436	0.439
	0.329	0.500	0.447	0.449
	0.218	0.354	0.361	0.359
	0.211	0.336	0.352	0.350
	0.210	0.327	0.347	0.346
	0.127	0.201	0.267	0.258
	0.120	0.176	0.255	0.245
	0.124	0.152	0.249	0.253
	0.078	0.094	0.192	0.186
	0.077	0.095	0.185	0.185
Run 9	m-Xylene	1-Octanol	2-Octanone	PGME Acetate
Init.	0.459	0.402	0.418	0.462
Init.	0.000	0.000	0.000	0.000
Init.	0.460	0.404	0.420	0.462
Init.	0.461	0.405	0.420	0.465
	0.456	0.399	0.414	0.459
	0.337	0.317	0.354	0.395
	0.333	0.308	0.351	0.394
	0.340	0.312	0.353	0.396
	0.215	0.201	0.264	0.300
	0.201	0.187	0.250	0.281
	0.202	0.187	0.251	0.284
	0.124	0.117	0.184	0.213
	0.121	0.110	0.183	0.209
Run 10	m-Xylene	n-Octane	3-Octanol	
Init.	0.552	0.596	0.550	
Init.	0.000	0.000	0.000	
Init.	0.570	0.621	0.565	
Init.	0.539	0.567	0.537	
	0.548	0.600	0.549	
	0.351	0.499	0.358	
	0.356	0.509	0.357	
	0.345	0.495	0.340	
	0.172	0.367	0.148	
	0.171	0.366	0.134	
	0.168	0.367	0.123	
	0.104	0.305	0.064	
	0.097	0.284	0.054	

Table A-3. Measured reactant and measured and corrected product data obtained during the experiments to determine the octanal yields from 1-octanol and the 2-octanone yields from 2-octanol.

Run 9 - Octanal from 1-Octanol

Reactant (ppm)	Product (ppm)	Corrected	F
	Initial		
0.416	0.000		
0.417	0.000		
0.411	0.000		
	Reacted		
0.327	0.022	0.027	1.2
0.318	0.021	0.027	1.3
0.322	0.021	0.027	1.3
0.207	0.025	0.048	1.9
0.192	0.021	0.043	2.1
0.192	0.019	0.039	2.1
0.120	0.020	0.065	3.2
0.114	0.015	0.051	3.4
0.108	0.013	0.047	3.6

Run 8 - 2-Octanone from 2-Octanol

Reactant (ppm)	Product (ppm)	Corrected	F
	Initial		
0.491	0.007		
0.496	0.007		
	Reacted		
0.351	0.045	0.044	1.0
0.333	0.049	0.049	1.0
0.325	0.053	0.055	1.0
0.199	0.070	0.089	1.3
0.175	0.077	0.104	1.3
0.151	0.090	0.129	1.4
0.093	0.085	0.147	1.7
0.094	0.089	0.155	1.7
0.089	0.094	0.167	1.8

Table A-4. Measured reactant and measured and corrected product data obtained during the experiments to determine the 3-octanone yields from 3-octanol.

Run 7

Reactant (ppm)	Product (ppm)	Corrected	F
	Initial		
0.417	0.000		
0.434	0.000		
0.437	0.000		
	Reacted		
0.256	0.054	0.061	1.1
0.255	0.063	0.071	1.1
0.239	0.065	0.075	1.2
0.084	0.080	0.125	1.6
0.055	0.098	0.176	1.8
0.050	0.099	0.182	1.8

Run 10

Reactant (ppm)	Product (ppm)	Corrected	F
	Initial		
0.569	0.000		
0.540	0.000		
0.552	0.000		
	Reacted		
0.360	0.063	0.069	1.1
0.359	0.071	0.078	1.1
0.342	0.076	0.085	1.1
0.149	0.099	0.140	1.4
0.135	0.115	0.167	1.5
0.123	0.126	0.189	1.5
0.064	0.114	0.211	1.8
0.054	0.113	0.221	2.0
0.047	0.113	0.231	2.1

Table A-5. Measured reactant and measured and corrected product data obtained during the experiments to determine the 4-octanone yields from 4-octanol.

Run 5				Run 7			
Reactant (ppm)	Product (ppm)	Corrected	F	Reactant (ppm)	Product (ppm)	Corrected	F
	Initial				Initial		
0.406	0.000			0.454	0.000		
0.409	0.000			0.469	0.000		
0.411	0.000			0.471	0.000		
	Reacted				Reacted		
0.307	0.034	0.039	1.1	0.265	0.049	0.057	1.2
0.301	0.037	0.042	1.1	0.266	0.058	0.068	1.2
0.197	0.060	0.077	1.3	0.248	0.061	0.072	1.2
0.184	0.066	0.087	1.3	0.104	0.071	0.110	1.6
0.079	0.112	0.195	1.7	0.074	0.085	0.150	1.8
0.090	0.106	0.176	1.7	0.070	0.088	0.157	1.8
0.095	0.084	0.137	1.6				
0.104	0.093	0.148	1.6				
0.095	0.092	0.151	1.6				

Table A-6. Chronological listing of the DTC experiments carried out for this program.

Run ID	Date	Run Title
DTC322	3/4/96	CO + NOx
DTC326	3/11/96	NO2 Actinometry
DTC331	4/3/96	Propene + NOx
DTC333	4/11/96	Pure Air Irradiation
DTC334	4/12/96	CO + NOx
DTC337	4/18/96	MEK + NOx
DTC338	4/19/96	Full Surrogate + MEK (A)
DTC343	4/29/96	NO2 Actinometry
DTC345	5/1/96	Mini-Surrogate + MEK (B)
DTC346	5/2/96	Propene + NOx
DTC356	5/20/96	n-Butane + Chlorine Actinometry
DTC358	5/22/96	Mini-Surrogate + Ethyl Acetate (A)
DTC359	5/23/96	Full Surrogate + Ethyl Acetate (B)
DTC360	5/24/96	Mini-Surrogate (Side Eq. Test)
DTC361	5/30/96	MEK + NOx
DTC362	5/31/96	Mini-Surrogate + Ethyl Acetate (B)
DTC363	6/4/96	Modefied Mini-Surrogate + MEK (A)
DTC364	6/5/96	Mini-Surrogate + Ethyl Acetate (B)
DTC365	6/6/96	Mini-Surrogate + Butyl Acetate (A)
DTC366	6/7/96	Mini-Surrogate + MIBK (B)
DTC367	6/8/96	NO2 Actinometry
DTC368	6/11/96	Mini-Surrogate + Butyl Acetate (B)
DTC369	6/12/96	Mini-Surrogate + MIBK (A)
DTC370	6/13/96	Full Surrogate + MIBK (B)
DTC371	6/17/96	Propene + NOx
DTC373	6/21/96	n-Butane + NOx
DTC383	7/16/96	CO + NOx
DTC384	7/19/96	n-Butane + NOx
		Runs for other programs
DTC392	8/5/96	NO2 Actinometry
DTC393	8/6/96	Propene + NOx
DTC394	8/7/96	Low NOx Full Surrogate + Ethyl Acetate (A)
DTC395	8/13/96	Mini-Surrogate + Isopropyl Alcohol (A)
DTC396	8/14/96	Full Surrogate + Isopropyl Alcohol (B)
DTC397	8/15/96	Low NOx Surrogate + Isopropyl Alcohol (B)
DTC398	8/16/96	Mini-Surrogate + Isopropyl Alcohol (B)
DTC399	8/20/96	Full Surrogate + Isopropyl Alcohol (A)
DTC400	8/21/96	Mini-Surrogate + Isopropyl Alcohol (B)
DTC402	8/23/96	Mini-Surrogate + Butyl Acetate (B)
DTC403	8/27/96	Full Surrogate + Butyl Acetate (4 ppm)
DTC405	8/29/96	Propene + NOx
DTC406	8/30/96	Low NOx Full Surrogate + Butyl Acetate (A)
DTC407	9/4/96	NO2 Actinometry
DTC407	9/4/96	n-Butane + Chlorine Actinometry
DTC408	9/5/96	Full Surrogate + Ethyl Acetate (B)

Table A-6 (continued)

Run ID	Date	Run Title
DTC409	9/6/96	Low NOx Full Surrogate + ethy acetate (A)
DTC410	9/10/96	Full Surrogate + Butyl Acetate (B)
DTC411	9/11/96	Low NOx Full Surrogate + Butyl Acetate (A)
DTC412	9/12/96	Low NOx Full Surrogate + MIBK (B)
DTC414	9/17/96	Full Surrogate + MIBK (A)
DTC415	9/18/96	Low NOx Mini-Surrogate + Ethyl Acetate (B)
DTC416	9/19/96	n-Butane + NOx
DTC417	9/20/96	Propene + NOx
DTC418	9/24/96	Low NOx Full Surrogate + MIBK (A)
DTC422	10/1/96	MIBK + NOx
DTC425	10/4/96	CO + NOx
DTC429	10/14/96	NO2 actinometry
DTC431	10/16/96	Propene + NOx
DTC434	10/21/96	n-Butane + NOx
DTC435	10/22/96	Pure Air irradiation
DTC436	10/23/96	Ozone decay
DTC437	10/29/96	MIBK + NOx
DTC443	11/12/96	Propene + NOx
DTC444	11/13/96	n-Butane + NOx
	4/1/97	Reaction bags and lights changed.
DTC488	5/15/97	Full Surrogate + NOx
DTC490	5/19/97	NO2 Actinometry
DTC494	5/23/97	n-Butane - NOx
DTC499	6/2/97	Ozone Dark Decay
DTC503	6/6/97	Propene - NOx
DTC504	6/9/97	Chlorine Actinometry
DTC507	6/13/97	Pure Air Irriadiation
DTC508	6/17/97	Mini-Surrogate + 1-Octanol
DTC509	6/18/97	Full Surrogate + 1-Octanol
DTC510	6/19/97	Mini Surrogate + Diethyl Ether
DTC511	6/20/97	Full Surrogate + Diethyl Ether
DTC512	6/24/97	Mini-Surrogate + Diacetone Alcohol
DTC513	6/25/97	Low NOx Full Surrogate + Diethyl Ether
DTC514	6/26/97	Mini-Surrogate + 3-Octanol
DTC515	6/27/97	Full Surrogate + Diethyl Ether
DTC516	6/30/97	Full Surrogate + 3-Octanol
DTC517	7/1/97	Mini Surrogate + 2-Octanol
DTC518	7/2/97	n-Butane + NOx
DTC519	7/8/97	Low NOx Full Surrogate + 1-Octanol
DTC520	7/9/97	Low NOx Full Surrogate + 3-Octanol
DTC521	7/10/97	Full Surrogate + 2-Octanol
DTC522	7/11/97	Mini Surrogate + Diethyl Ether
DTC523	7/14/97	NO2 Actinometry
DTC524	7/15/97	Low NOx Full Surrogate + 2-Octanol
DTC525	7/16/97	Low NOx Full Surrogate + Diethyl Ether(A)
DTC526	7/17/97	Propene + NOx

Table A-6 (continued)

Run ID	Date	Run Title
DTC527	7/18/97	CO + NOx
DTC528	7/22/97	Mini Surrogate + Methyl Isobutyrate
DTC529	7/23/97	Mini Surrogate + 1-Octanol
DTC530	7/24/97	Full Surrogate + Methyl Isobutyrate
DTC531	7/29/97	Low NOx Full Surrogate + Methyl Isobutyrate
DTC532	7/30/97	Mini Surrogate + PGME Acetate
DTC533	7/31/97	Mini Surrogate + Methyl Isobutyrate
DTC534	8/1/97	Full Surrogate + Methyl Isobutyrate (B)
DTC535	8/6/97	Pure Air Irradiation
DTC536	8/7/97	Aborted run
DTC537	8/12/97	Mini-Surrogate + PGME Acetate
DTC538	8/13/97	Full Surrogate + PGME Acetate
DTC539	8/14/97	Low NOx Full Surrogate + Methyl Isobutyrate
DTC540	8/15/97	Low NOx Full Surrogate + PGME Acetate
DTC541	8/19/97	Mini Surrogate + Cyclohexane
DTC542	8/20/97	Cl2 - n-Butane Actinometry
DTC543	8/21/97	Full Surrogate + Cyclohexane
DTC544	8/22/97	Low NOx Full Surrogate + Cyclohexane
DTC545	8/26/97	n-Butane + NOx
DTC546	8/27/97	Acetaldehyde + Air
DTC547	8/28/97	Full Surrogate + PGME Acetate
DTC548	8/29/97	Low NOx Full Surrogate + Methyl Isobutyrate
DTC549	9/3/97	Mini Surrogate + PGME Acetate
DTC550	9/4/97	Cyclohexanone - NOx
DTC551	9/8/97	Mini Surrogate + Cyclohexane
DTC552	9/9/97	Full Surrogate + Cyclohexane
DTC553	9/10/97	Low NOx Full Surrogate + Cyclohexane
DTC554	9/12/97	Mini Surrogate + Cyclohexanone
DTC555	9/16/97	N-Butane + NOx
DTC556	9/17/97	Full Surrogate + Cyclohexanone
DTC557	9/18/97	Low NOx Full Surrogate + Cyclohexanone
DTC558	9/22/97	Mini Surrogate + Cyclohexanone (A)
DTC559	9/24/97	Full Surrogate + Cyclohexanone
DTC560	9/25/97	Low NOx Full Surrogate + Cyclohexanone (A)
DTC561	9/26/97	(Run for vehicle exhaust reactivity program)
DTC562	9/29/97	NO2 Actinometry

Table A-7. Chronological listing of the CTC experiments carried out for this program.

Run ID	Date	Run Title
CTC170	11/15/96	Propene + NOx
CTC171	11/19/96	Full Surrogate + NOx
CTC172	11/20/96	Mini Surrogate + NOx
CTC173	11/21/96	Ozone Dark Decay
CTC174	11/22/96	Pure Air irradiation
CTC175	11/25/96	n-Butane + NOx
CTC176	11/26/96	Formaldehyde + NOx
CTC177	11/27/96	NO_2 and n-Butane + Chlorine Actinometry
CTC178	12/3/96	MEK + NOx
CTC179	12/4/96	MIBK + NOx
CTC180	12/5/96	Full Surrogate + MEK (B)
CTC181	12/6/96	Mini Surrogate + MEK (A)
CTC182	12/10/96	Full Surrogate + MIBK (B)
CTC183	12/11/96	Mini Surrogate + MIBK (A)
CTC189	12/23/96	n-Butane + NOx
CTC190	1/3/97	n-Butane + Chlorine Actinometry
CTC191	1/7/97	Propene + NOx
CTC195	1/15/97	Low NOx Full Surrogate + Ethyl Acetate (B)
CTC196	1/16/97	Mini Surrogate + Butyl Acetate
CTC200	1/24/97	CO + NOx
CTC203	1/31/97	Propene + NOx
CTC206	2/6/97	n-Butane + NOx
CTC207	2/7/97	n-Butane + Chlorine Actinometry
CTC213	3/28/97	n-Butane - NOx
CTC218	4/10/97	n-Butane + Chlorine Actinometry
CTC219	4/11/97	Propene + NOx
CTC224	4/21/97	CO + NOx
		Chamber inactive for a period
CTC225	10/8/97	n-Butane + Chlorine Actinometry
CTC226	10/9/97	Propene + NOx
CTC227	10/10/97	Mini surrogate + Cyclohexanone (A)
CTC228	10/14/97	Cyclohexanone + NOx
CTC229	10/15/97	Full surrogate + Cyclohexanone (B)
CTC230	12/12/97	n-Butane - NOx
CTC234	12/19/97	Propene - NOx
CTC235	12/22/97	Low NOx Full Surrogate + Cyclohxanone
CTC236	12/23/97	n-Butane + Chlorine Actinometry
CTC237	1/6/98	Pure air irradiation
CTC238	1/7/98	Low NOx Full Surrogate + Cyclohexanone (A)
CTC241	1/16/98	N-Butane + NOx
CTC242	1/21/98	n-Butane + chlorine

Table A-8. Summary of the conditions and results of the environmental chamber experiments carried out for this program.

Run	Run Type or VOC [a]	Rct'y Type [a]	Chr Set [b]	NOx (ppm)	VOC (ppm) [c]	Surg (ppmC) [d]	k_1 (min^{-1}) [e]	T (K) [f]	Δ (O_3-NO) Results (pphm) 2 Hour Expt	2 Hour Calc	2 Hour Δ%	4 Hour Expt	4 Hour Calc	4 Hour Δ%	6 Hour Expt	6 Hour Calc	6 Hour Δ%
Background Characterization Runs																	
CTC174A	Pure Air		7	-	-	-	0.16	298	1	0	-88	1	2	11	2	3	21
CTC174B	Pure Air		7	-	-	-	0.16	298	1	0	-87	2	2	-8	3	3	10
CTC237A	Pure Air		9	-	-	-	0.14	300	1	0	-3	1	2	38	2	3	44
CTC237B	Pure Air		9	-	-	-	0.14	300	1	0	-4	1	2	36	2	3	43
DTC333A	Pure Air		11	-	-	-	0.21	297	1	1	-12	2	3	25	3	4	28
DTC333B	Pure Air		11	-	-	-	0.21	297	1	1	9	2	3	36	3	4	40
DTC435A	Pure Air		11	-	-	-	0.18	293	0	1	59	1	2	45	2	3	43
DTC435B	Pure Air		11	-	-	-	0.18	293	0	1	59	1	2	49	2	4	49
DTC507A	Pure Air		14	-	-	-	0.22	298	1	1	24	2	3	37	3	4	30
DTC507B	Pure Air		15	-	-	-	0.22	298	1	1	5	1	2	45	2	3	40
DTC535A	Pure Air		14	-	-	-	0.21	301	1	2	32	2	3	47	3	5	37
DTC535B	Pure Air		15	-	-	-	0.21	301	1	1	37	1	2	46	2	2	39
DTC546A	Acetald. Air		14	-	0.24	-	0.21	300	3	3	4	7	6	-2	9	9	1
DTC546B	Acetald. Air		15	-	0.25	-	0.21	300	3	3	1	6	6	-2	8	8	0
Radical Source Characterization Runs																	
DTC322A	CO		11	0.16	44.0	-	0.21	298	3	3	9	6	6	-7	8	8	-2
DTC322B	CO		11	0.16	44.0	-	0.21	298	3	3	2	6	6	3	8	8	0
DTC334A	CO		11	0.17	43.7	-	0.21	297	3	3	9	5	6	6	8	8	-5
DTC334B	CO		11	0.17	43.7	-	0.21	297	3	3	16	5	6	18	7	8	15
DTC347A	N-C4		11	0.29	4.5	-	0.20	298	5	4	-27	9	8	-20	14	12	-20
DTC347B	N-C4		11	0.30	4.5	-	0.20	298	5	4	-29	10	8	-23	14	12	-22
DTC357A	N-C4		11	0.24	3.9	-	0.20	298	5	4	-46	11	8	-39	15	12	-34
DTC357B	N-C4		11	0.24	4.0	-	0.20	298	5	4	-39	10	8	-31	15	11	-32
DTC373A	N-C4		11	0.25	2.9	-	0.20	298	3	3	3	-	6		9	10	2
DTC373B	N-C4		11	0.24	2.8	-	0.20	298	3	3	-2	-	6		10	9	-1
DTC383A	CO		11	0.06	45.9	-	0.19	298	4	5	21	8	9	17	11	12	14
DTC383B	CO		11	0.06	45.9	-	0.19	298	4	5	31	7	9	24	10	12	16
DTC384A	N-C4		11	0.25	3.6	-	0.19	298	3	3	20	6	7	20	9	11	19
DTC384B	N-C4		11	0.25	3.7	-	0.19	298	3	3	12	6	7	18	10	11	10
DTC416A	N-C4		11	0.25	4.6	-	0.19	297	4	4	4	7	8	6	11	12	7
DTC416B	N-C4		11	0.25	4.7	-	0.19	297	3	4	12	7	8	11	11	12	8
DTC434A	N-C4		11	0.25	4.1	-	0.18	295	4	3	-32	8	6	-24	13	10	-35
DTC434B	N-C4		11	0.25	4.1	-	0.18	295	4	3	-14	7	6	-8	11	10	-19
DTC444A	N-C4		11	0.27	4.8	-	0.17	297	3	3	17	6	7	16	10	11	13
DTC444B	N-C4		11	0.27	4.5	-	0.17	297	3	3	8	6	7	9	10	11	7
DTC448B	N-C4		11	0.26	4.4	-	0.17	297	3	3	6	7	7	4	11	11	-1
DTC473A	N-C4		14	0.29	4.2	-	0.23	297	5	4	-26	9	7	-23	13	11	-19
DTC482A	N-C4		14	0.27	4.3	-	0.22	298	4	4	0	9	9	-3	14	13	-6
DTC494A	N-C4		14	0.27	4.1	-	0.22	298	4	4	-2	9	9	-5	14	13	-7
DTC518A	N-C4		14	0.28	4.1	-	0.21	299	4	4	1	8	8	0	13	12	-4
DTC545A	N-C4		14	0.27	3.6	-	0.21	299	4	4	7	7	8	8	11	12	5
DTC555A	N-C4		14	0.24	3.9	-	0.20	299	4	4	11	8	8	8	11	12	7
DTC566A	N-C4		14	0.23	3.8	-	0.20	299	4	4	-10	8	8	-4	12	12	-3
DTC571A	N-C4		14	0.26	4.2	-	0.20	298	4	4	6	7	8	10	12	12	7
DTC587A	N-C4		14	0.27	5.5	-	0.19	297	7	4	-52	8	9	8	13	13	5
DTC473B	N-C4		15	0.29	4.2	-	0.23	297	4	3	-27	7	6	-21	11	9	-20
DTC482B	N-C4		15	0.27	4.3	-	0.22	298	3	4	9	7	7	3	11	11	-1
DTC494B	N-C4		15	0.27	4.1	-	0.22	298	4	3	-6	7	7	-7	11	10	-9
DTC518B	N-C4		15	0.28	4.1	-	0.21	299	3	3	6	7	7	-2	11	10	-7
DTC545B	N-C4		15	0.27	3.6	-	0.21	299	3	3	-10	6	6	-5	10	9	-4
DTC555B	N-C4		15	0.24	3.9	-	0.20	299	4	3	-9	7	7	-14	11	10	-15
CTC175A	N-C4		7	0.26	4.1	-	0.16	298	-	2		5	5	-1	-	8	
CTC175B	N-C4		7	0.26	4.0	-	0.16	298	3	2	-44	5	5	-7	-	8	
CTC189A	N-C4		7	0.26	4.0	-	0.16	297	3	3	-2	8	7	-2	-	12	
CTC189B	N-C4		7	0.26	4.0	-	0.16	297	3	3	-10	8	7	-9	-	12	
CTC200A	CO		8	0.24	39.7	-	0.15	299	2	1	-10	3	3	-3	-	5	
CTC200B	CO		8	0.24	39.6	-	0.15	299	2	1	-16	4	3	-12	-	5	
CTC206A	N-C4		8	0.25	4.5	-	0.15	298	4	3	-7	8	8	-8	-	13	

Table A-8 (continued)

Run	Run Type or VOC [a]	Rct'y Type [a]	Chr Set [b]	NOx (ppm)	VOC (ppm) [c]	Surg (ppmC) [d]	k_1 (min^{-1}) [e]	T (K) [f]	Δ (O_3-NO) Results (pphm)								
									2 Hour			4 Hour			6 Hour		
									Expt	Calc	Δ%	Expt	Calc	Δ%	Expt	Calc	Δ%
CTC206B	N-C4		8	0.25	4.5	-	0.15	298	4	3	-13	9	8	-12	15	13	-13
CTC213A	N-C4		8	0.26	4.7	-	0.15	297	4	3	-10	9	8	-9	14	13	-7
CTC213B	N-C4		8	0.26	4.7	-	0.15	297	4	3	-17	9	8	-14	-	13	
CTC224A	CO		8	0.25		-	0.15	298	1	1	-6	2	3	7	4	4	1
CTC224B	CO		8	0.25		-	0.15	298	1	1	-23	3	3	-11	-	4	
CTC230A	N-C4		9	0.28	4.4	-	0.14	302	2	3	29	4	6	29	7	9	23
CTC230B	N-C4		9	0.28	4.4	-	0.14	302	2	3	32	4	6	29	-	10	
CTC241A	N-C4		9	0.27	4.3	-	0.14	302	3	3	-3	8	7	-3	-	12	
CTC241B	N-C4		9	0.27	4.2	-	0.14	302	3	3	7	7	7	1	12	12	-5
Control Runs																	
DTC331A	PROPENE		11	0.55	1.02	-	0.21	296	24	27	13	72	83	14	97	100	3
DTC331B	PROPENE		11	0.54	1.01	-	0.21	296	23	27	13	71	82	14	100	101	2
DTC346A	PROPENE		11	0.58	0.98	-	0.20	299	29	24	-24	82	72	-14	98	100	2
DTC346B	PROPENE		11	0.59	0.99	-	0.20	299	30	23	-30	83	71	-17	99	100	1
DTC371A	PROPENE		11	0.57	0.63	-	0.20	299	28			82			100		
DTC371B	PROPENE		11	0.57	0.63	-	0.20	299	28			82			101		
DTC393A	PROPENE		11	0.57	0.89	-	0.19	296	23	18	-27	62	49	-27	94	84	-11
DTC393B	PROPENE		11	0.56	0.88	-	0.19	296	23	18	-29	62	49	-26	91	84	-9
DTC405A	PROPENE		11	0.56	0.95	-	0.19	299	29	20	-43	83	65	-28	103	98	-5
DTC405B	PROPENE		11	0.56	0.94	-	0.19	299	30	20	-46	82	63	-31	102	96	-6
DTC417A	PROPENE		11	0.53	1.14	-	0.19	297	27	29	7	83	92	10	105	100	-4
DTC417B	PROPENE		11	0.53	1.18	-	0.19	297	28	32	12	84	93	10	105	98	-7
DTC431A	PROPENE		11	0.56	1.07	-	0.18	297	31	25	-25	90	78	-15	104	98	-6
DTC431B	PROPENE		11	0.56	1.07	-	0.18	297	32	25	-28	91	78	-17	108	98	-10
DTC443A	PROPENE		11	0.53	1.15	-	0.17	297	26	29	8	83	90	7	103	96	-7
DTC443B	PROPENE		11	0.53	1.16	-	0.17	297	27	29	7	84	89	6	103	95	-9
DTC503A	PROPENE		14	0.52	1.05	-	0.22	299	38	31	-23	102	93	-10	114	105	-8
DTC503B	PROPENE		15	0.51	1.05	-	0.22	299	36	30	-19	101	93	-8	113	105	-7
DTC526A	PROPENE		14	0.51	1.06	-	0.21	300	42	31	-32	104	94	-11	112	102	-9
DTC526B	PROPENE		15	0.51	1.07	-	0.21	300	41	31	-35	104	94	-11	112	103	-8
CTC170A	PROPENE		7	0.54	1.29	-	0.17	299	35	22	-59	105	85	-22	-	99	
CTC170B	PROPENE		7	0.53	1.29	-	0.17	299	36	23	-56	104	89	-17	-	98	
CTC191A	PROPENE		7	0.48	1.23	-	0.16	298	29	21	-41	95	80	-20	-	91	
CTC191B	PROPENE		7	0.47	1.22	-	0.16	298	29	20	-42	96	80	-19	105	90	-17
CTC203A	PROPENE		8	0.48	1.30	-	0.15	298	30	22	-35	96	83	-16	-	89	
CTC203B	PROPENE		8	0.47	1.32	-	0.15	298	30	24	-26	96	84	-15	100	87	-16
CTC219A	PROPENE		8	0.49	1.20	-	0.15	297	31	17	-76	94	65	-44	-	90	
CTC219B	PROPENE		8	0.48	1.19	-	0.15	297	28	18	-54	93	72	-28	100	89	-12
CTC234A	PROPENE		9	0.51	1.50	-	0.14	302	25	27	8	90	90	0	-	86	
CTC234B	PROPENE		9	0.51	1.50	-	0.14	302	25	28	14	90	89	-1	96	85	-13
CTC176A	FORMALD		7	0.25	0.38	-	0.16	299	11	10	-12	18	17	-9	-	22	
CTC176B	FORMALD		7	0.25	0.38	-	0.16	299	11	10	-13	19	17	-11	-	22	
Single Ketone - NOx Runs																	
DTC337A	MEK		11	0.29	7.83	-	0.21	296	26	27	5	39	42	6	51	56	8
DTC337B	MEK		11	0.11	7.83	-	0.21	296	19	20	8	-	33		-	38	
DTC361A	MEK		11	0.10	9.18	-	0.20	298	21	22	4	33	34	3	36	38	5
DTC361B	MEK		11	0.23	9.49	-	0.20	298	27	29	7	43	45	4	59	59	1
CTC178A	MEK		7	0.24	9.06	-	0.16	298	24	23	-5	36	34	-6	-	44	
CTC178B	MEK		7	0.09	9.08	-	0.16	298	17	16	-7	28	26	-7	-	33	
DTC550A	CC6-KET		14	0.12	1.97	-	0.20	301	4	3	-57	8	6	-45	12	9	-36
DTC550B	CC6-KET		15	0.12	3.72	-	0.20	301	5	2	-154	10	5	-118	14	7	-100
CTC228A	CC6-KET		9	0.09	2.54	-	0.15	301	2	2	18	4	4	16	6	7	10
CTC228B	CC6-KET		9	0.09	4.79	-	0.15	301	2	2	-27	5	4	-14	8	7	-16
DTC422A	MIBK		11	0.21	3.49	-	0.19	297	10	12	20	19	21	10	27	28	5
DTC422B	MIBK		11	0.21	8.88	-	0.19	297	16	18	8	29	28	-3	42	37	-12
DTC437A	MIBK		11	0.16	4.99	-	0.18	298	14	14	-4	26	22	-18	38	30	-26
DTC437B	MIBK		11	0.19	4.86	-	0.18	298	17	17	1	31	27	-14	44	35	-24
CTC179A	MIBK		7	0.21	2.98	-	0.16	298	8	8	10	15	16	2	-	21	
CTC179B	MIBK		7	0.21	7.64	-	0.16	298	14	13	-8	26	22	-18	38	29	-31

Table A-8 (continued)

Run	Run Type or VOC [a]	Rct'y Type [a]	Chr Set [b]	NOx (ppm)	VOC (ppm) [c]	Surg (ppmC) [d]	k_1 (min^{-1}) [e]	T (K) [f]	Δ (O_3-NO) Results (pphm) 2 Hour Expt	2 Hour Calc	2 Hour Δ%	4 Hour Expt	4 Hour Calc	4 Hour Δ%	6 Hour Expt	6 Hour Calc	6 Hour Δ%
Incremental Reactivity Experiments: VOC Added to Standard Surrogate - NOx Run																	
DTC541A	CYCC6	MR3	14	0.38	0.95	5.42	0.21	299	8	9	13	24	25	5	44	45	2
DTC551A	CYCC6	MR3	14	0.38	1.71	4.93	0.20	300	8	7	-10	21	18	-13	37	32	-14
DTC543B	CYCC6	MR8	15	0.30	1.95	4.00	0.21	299	42	38	-8	65	61	-6	81	77	-5
DTC552B	CYCC6	MR8	15	0.31	1.25	3.73	0.20	300	36	26	-39	64	52	-21	81	69	-18
DTC544A	CYCC6	R8	14	0.13	0.86	3.82	0.21	299	40	38	-5	49	48	-3	52	50	-3
DTC553A	CYCC6	R8	14	0.13	1.41	3.83	0.20	300	41	40	-4	51	50	-3	54	53	-3
DTC395A	I-C3-OH	MR3	11	0.40	9.48	5.27	0.19	299	25	25	-3	64	57	-12	96	93	-3
DTC398B	I-C3-OH	MR3	11	0.43	2.51	5.35	0.19	297	19	15	-31	47	36	-30	80	61	-32
DTC396B	I-C3-OH	MR8	11	0.29	10.65	3.76	0.19	299	63	70	10	81	91	11	77	100	23
DTC399A	I-C3-OH	MR8	11	0.27	1.97	3.74	0.19	298	40	37	-10	62	55	-11	72	68	-6
DTC397A	I-C3-OH	R8	11	0.13	4.96	3.77	0.19	298	45	45	1	50	55	10	47	59	20
DTC400B	I-C3-OH	R8	11	0.11	2.09	3.86	0.19	298	39	37	-5	44	44	0	43	46	7
DTC508B	1-C8-OH	MR3	15	0.37	0.94	5.24	0.22	299	5	6	6	15	15	-1	30	28	-7
DTC529A	1-C8-OH	MR3	14	0.36	0.18	4.88	0.21	299	9	10	5	27	26	-2	49	46	-7
DTC509A	1-C8-OH	MR8	14	0.30	0.25	3.93	0.22	299	32	26	-23	55	49	-13	70	64	-10
DTC519B	1-C8-OH	R8	15	0.12	0.45	3.96	0.21	298	35	36	3	43	45	4	45	47	5
DTC517A	2-C8-OH	MR3	14	0.37	0.25	5.55	0.21	299	10	11	6	32	30	-6	60	54	-12
DTC521B	2-C8-OH	MR8	15	0.30	0.55	4.11	0.21	299	34	31	-11	59	57	-4	74	72	-2
DTC524B	2-C8-OH	R8	15	0.13	0.40	4.09	0.21	299	38	37	-1	45	46	1	46	48	4
DTC514B	3-C8-OH	MR3	15	0.38	0.26	5.36	0.21	299	9	10	9	28	27	-3	52	48	-7
DTC516B	3-C8-OH	MR8	15	0.32	0.29	4.08	0.21	299	34	33	-3	55	53	-3	70	68	-3
DTC520A	3-C8-OH	R8	14	0.13	0.45	3.95	0.21	299	38	38	0	46	47	3	46	49	7
DTC510B	ET-O-ET	MR3	15	0.39	0.68	5.48	0.22	299	19	21	11	53	56	4	99	97	-2
DTC522A	ET-O-ET	MR3	14	0.37	1.68	5.41	0.21	299	23	28	18	73	79	8	116	115	-1
DTC511A	ET-O-ET	MR8	14	0.31	1.79	4.09	0.21	299	78	88	11	107	114	6	109	120	10
DTC515A	ET-O-ET	MR8	14	0.31	0.56	3.84	0.21	299	57	49	-16	87	76	-15	101	93	-9
DTC513A	ET-O-ET	R8	14	0.13	0.68	3.86	0.21	298	49	50	2	57	59	3	57	60	5
DTC525A	ET-O-ET	R8	14	0.13	0.34	4.03	0.21	299	46	44	-3	53	53	-1	54	54	0
DTC358A	ET-ACET	MR3	11	0.33	5.88	5.56	0.20	298	13	13	-1	28	28	3	40	42	5
DTC362B	ET-ACET	MR3	11	0.30	4.29	5.95	0.20	298	11	13	14	25	29	12	39	45	12
DTC364B	ET-ACET	MR3	11	0.32	4.48	5.70	0.20	298	12	13	2	28	28	2	41	42	4
DTC359B	ET-ACET	MR8	11	0.27	5.91	4.15	0.20	298	28	30	6	42	46	8	51	58	11
DTC408B	ET-ACET	MR8	11	0.28	10.12	3.77	0.19	298	32	28	-12	45	43	-4	55	54	-2
DTC415B	ET-ACET	R3	11	0.20	4.24	5.62	0.19	297	12	11	-11	26	23	-13	42	37	-13
DTC394A	ET-ACET	R8	11	0.11	6.06	3.69	0.19	296	25	24	-2	31	33	5	33	36	8
DTC409A	ET-ACET	R8	11	0.11	9.03	3.57	0.19	298	25	23	-6	31	32	3	33	36	7
CTC195B	ET-ACET	R8	8	0.14	4.99	5.15	0.16	297	34	31	-8	40	37	-9	42	38	-8
DTC528B	ME-IBUAT	MR3	15	0.38	5.34	5.42	0.21	299	10	13	23	29	30	5	49	46	-5
DTC533A	ME-IBUAT	MR3	14	0.36	3.54	5.35	0.21	299	10	14	30	31	34	9	53	53	0
DTC530B	ME-IBUAT	MR8	15	0.31	5.20	3.95	0.21	299	33	33	-2	54	50	-9	71	64	-11
DTC534B	ME-IBUAT	MR8	15	0.29	7.75	3.94	0.21	299	32	35	8	56	53	-4	73	68	-9
DTC531A	ME-IBUAT	R8	14	0.12	5.34	3.95	0.21	299	34	33	-5	44	40	-9	47	42	-11
DTC539A	ME-IBUAT	R8	14	0.13	7.38	3.99	0.21	299	34	33	-1	44	42	-5	47	44	-6
DTC548A	ME-IBUAT	R8	14	0.13	9.99	3.76	0.20	299	34	32	-7	44	42	-5	48	46	-4
DTC365A	BU-ACET	MR3	11		5.88	5.55	0.20	298	9	9	2	20	21	5	33	35	7
DTC368B	BU-ACET	MR3	11		6.30	5.65	0.20	299	8	9	8	19	21	9	32	35	9
DTC402B	BU-ACET	MR3	11		3.79	5.28	0.19	299	9	10	5	24	24	0	39	39	0
CTC196A	BU-ACET	MR3	8	0.22	3.98	4.99	0.16	297	5	6	12	14	16	9	25	26	5
DTC403A	BU-ACET	MR8	11	0.29	5.15	4.05	0.19	299	37	40	7	58	62	7	70	76	8
DTC410B	BU-ACET	MR8	11	0.26	7.60	3.85	0.19	298	41	39	-5	61	60	-1	71	73	2
DTC406A	BU-ACET	R8	11	0.12	3.69	3.98	0.19	299	35	36	3	42	44	3	44	46	4
DTC411A	BU-ACET	R8	11	0.11	7.72	3.71	0.19	297	34	34	1	41	43	4	43	46	7
DTC532B	PGME-ACT	MR3	15	0.36	0.88	5.36	0.21	299	10	10	4	25	24	-2	40	39	-4
DTC537A	PGME-ACT	MR3	14	0.35	0.50	5.08	0.21	299	11	11	2	29	27	-8	48	43	-11
DTC549B	PGME-ACT	MR3	15	0.37	1.05	5.14	0.20	300	12	10	-18	28	23	-20	45	37	-23
DTC538B	PGME-ACT	MR8	15	0.29	0.99	3.85	0.21	299	36	35	-4	54	53	-1	68	68	1
DTC547B	PGME-ACT	MR8	15	0.30	1.53	3.87	0.20	300	39	35	-12	58	55	-5	72	70	-3
DTC540B	PGME-ACT	R8	15	0.13	0.96	3.90	0.21	299	35	34	-2	43	44	1	46	47	1
DTC338A	MEK	MR8	11	0.29	4.03	4.05	0.21	297	38	40	7	54	58	7	64	70	8
DTC345B	MEK	MRX	11	0.34	1.65	6.16	0.20	300	26	27	2	52	52	1	75	76	2

Table A-8 (continued)

Run	Run Type or VOC [a]	Rct'y Type [a]	Chr Set [b]	NOx (ppm)	VOC (ppm) [c]	Surg (ppmC) [d]	k_1 (min^{-1}) [e]	T (K) [f]	Δ (O_3-NO) Results (pphm)								
									2 Hour			4 Hour			6 Hour		
									Expt	Calc	Δ%	Expt	Calc	Δ%	Expt	Calc	Δ%
DTC363A	MEK	MRX	11	0.32	2.60	6.11	0.20	298	30	30	-1	54	54	1	75	75	1
CTC181A	MEK	MR3	7	0.23	3.01	5.48	0.16	298	24	22	-11	47	40	-16	62	55	-12
CTC180B	MEK	MR8	7	0.39	4.08	5.60	0.16	298	47	46	-1	67	66	-2	82	79	-4
DTC554B	CC6-KET	MR3	15	0.37	1.90	5.22	0.20	299	9	8	-21	22	19	-13	33	31	-7
DTC558A	CC6-KET	MR3	14	0.34	1.33	5.44	0.20	300	10	9	-7	23	23	-3	38	37	-3
DTC556A	CC6-KET	MR8	14	0.28	1.19	4.16	0.20	300	26	32	17	44	50	12	56	63	11
DTC559B	CC6-KET	MR8	15	0.28	1.95	4.23	0.20	299	26	32	17	43	50	15	54	64	15
DTC557B	CC6-KET	R8	15	0.12	2.20	4.09	0.20	300	28	31	12	37	39	6	39	41	6
DTC560B	CC6-KET	R8	15	0.12	1.12	4.16	0.20	299	30	31	6	37	37	2	38	38	1
CTC227A	CC6-KET	MR3	9	0.21	1.26	5.19	0.15	300	5	7	37	14	19	29	23	30	23
CTC229B	CC6-KET	MR8	9	0.39	2.43	5.57	0.15	301	24	28	15	47	55	16	49	69	28
CTC235A	CC6-KET	R8	9	0.16	1.79	5.96	0.14	301	31	35	12	38	41	8	-	42	
CTC238A	CC6-KET	R8	9	0.17	0.84	5.80	0.14	301	36	37	5	43	44	1	-	45	
DTC366B	MIBK	MR3	11	0.32	3.39	5.73	0.20	298	17	19	9	32	33	2	47	45	-3
DTC369A	MIBK	MR3	11	0.35	4.33	5.54	0.20	298	19	21	7	35	35	2	50	49	-4
DTC370B	MIBK	MR8	11	0.29	3.25	3.83	0.20	298	32	34	5	50	52	4	63	67	6
DTC414A	MIBK	MR8	11	0.27	9.32	4.04	0.19	298	37	36	-3	56	54	-4	67	68	1
DTC412B	MIBK	R8	11	0.11	9.02	3.82	0.19	297	27	26	-1	29	34	15	30	36	18
DTC418A	MIBK	R8	11	0.11	2.53	3.80	0.19	298	27	27	-1	32	34	5	33	36	6
CTC183A	MIBK	MR3	7	0.23	1.91	5.00	0.16	298	11	10	-9	22	19	-13	32	27	-20
CTC182B	MIBK	MR8	7	0.38	1.78	5.89	0.16	298	42	39	-9	63	60	-4	78	75	-3
Base Case Surrogate - NOx Runs									-			-			-		
DTC345A	SURG-m3M		11	0.34		6.21	0.20	300	14	14	4	38	38	-2	65	64	-1
DTC363B	SURG-m3M		11	0.32		6.22	0.20	298	14	14	0	37	36	-1	62	62	1
DTC358B	SURG-3M		11	0.33		5.61	0.20	298	15	16	4	39	40	3	64	67	3
DTC395B	SURG-3M		11	0.41		5.26	0.19	299	14	11	-29	37	30	-24	61	48	-27
DTC398A	SURG-3M		11	0.43		5.36	0.19	297	13	11	-20	35	29	-19	57	47	-21
DTC402A	SURG-3M		11	0.37		5.41	0.19	299	13	14	5	37	37	0	61	62	1
DTC508A	SURG-3M		14	0.37		5.19	0.22	299	13	16	17	40	40	1	71	69	-3
DTC510A	SURG-3M		14	0.39		5.50	0.22	299	17	16	-5	46	40	-14	79	68	-16
DTC512A	SURG-3M		14	0.38		5.33	0.21	299	14	14	6	40	36	-9	70	62	-14
DTC514A	SURG-3M		14	0.39		5.35	0.21	299	13	15	10	39	37	-7	71	61	-15
DTC517B	SURG-3M		15	0.37		5.49	0.21	299	12	14	15	37	37	1	68	65	-4
DTC522B	SURG-3M		15	0.37		5.37	0.21	299	12	14	10	36	36	-2	65	61	-5
DTC528A	SURG-3M		14	0.38		5.43	0.21	299	14	14	1	40	36	-10	71	62	-14
DTC529B	SURG-3M		15	0.36		4.91	0.21	299	12	12	-1	34	31	-11	63	54	-17
DTC532A	SURG-3M		14	0.36		5.35	0.21	299	11	14	24	34	37	7	64	65	2
DTC533B	SURG-3M		15	0.36		5.38	0.21	299	11	14	20	36	37	5	64	64	0
DTC537B	SURG-3M		15	0.35		5.17	0.21	299	10	13	20	33	34	2	61	59	-4
DTC541B	SURG-3M		15	0.38		5.40	0.21	299	11	13	17	35	34	-1	62	59	-6
DTC549A	SURG-3M		14	0.37		5.04	0.20	300	14	13	-8	39	33	-18	70	57	-23
DTC551B	SURG-3M		15	0.38		4.95	0.20	300	12	11	-4	35	29	-20	63	48	-31
DTC554A	SURG-3M		14	0.38		5.21	0.20	299	13	14	5	37	35	-4	66	60	-9
DTC558B	SURG-3M		15	0.34		5.45	0.20	300	11	13	18	33	35	8	61	63	3
CTC172A	SURG-3M		7	0.32		5.14	0.16	294	7	9	22	26	28	8	-	49	
CTC172B	SURG-3M		7	0.32		5.10	0.16	294	8	9	11	27	28	3	-	50	
CTC181B	SURG-3M		7	0.23		5.52	0.16	298	13	11	-19	39	33	-17	63	54	-16
CTC183B	SURG-3M		7	0.23		5.00	0.16	298	12	11	-8	37	34	-9	61	55	-11
CTC196B	SURG-3M		8	0.22		4.95	0.16	297	10	11	6	34	34	-1	-	54	
CTC227B	SURG-3M		9	0.21		5.23	0.15	300	8	16	53	28	42	34	51	54	5
DTC360A	SURG-3M		11	0.25		6.09	0.20	297	12	18	35	32	45	29	57	67	15
DTC360B	SURG-3M		11	0.24		6.10	0.20	297	11	18	39	31	45	30	57	67	15
DTC362A	SURG-3M		11	0.30		5.82	0.20	298	12	15	18	34	39	13	60	66	9
DTC364A	SURG-3M		11	0.32		5.61	0.20	298	14	14	-5	37	36	-5	63	62	-2
DTC365B	SURG-3M		11	0.32		5.69	0.20	298	13	15	12	35	38	6	61	65	5
DTC366A	SURG-3M		11	0.33		5.73	0.20	298	13	15	15	35	39	10	60	67	10
DTC368A	SURG-3M		11	0.35		5.59	0.20	299	13	14	6	35	35	0	61	60	-1
DTC369B	SURG-3M		11	0.35		5.64	0.20	298	12	14	10	34	35	3	59	60	2
DTC415A	SURG-3M		11	0.20		5.46	0.19	297	15	16	4	42	40	-5	61	58	-5
DTC338B	SURG-8M		11	0.29		4.14	0.21	297	24	28	14	40	44	10	50	57	11
DTC359A	SURG-8M		11	0.28		4.19	0.20	298	26	29	8	43	45	6	54	58	8

Table A-8 (continued)

Run	Run Type or VOC [a]	Rct'y Type [a]	Chr Set [b]	NOx (ppm)	VOC (ppm) [c]	Surg (ppmC) [d]	k_1 (min^{-1}) [e]	T (K) [f]	Δ (O_3-NO) Results (pphm)								
									2 Hour			4 Hour			6 Hour		
									Expt	Calc	Δ%	Expt	Calc	Δ%	Expt	Calc	Δ%
DTC370A	SURG-8M		11	0.28		3.82	0.20	298	24	24	2	40	40	1	50	52	3
DTC396A	SURG-8M		11	0.29		3.74	0.19	299	28	22	-26	44	37	-18	56	49	-15
DTC399B	SURG-8M		11	0.27		3.81	0.19	298	27	25	-7	42	39	-7	53	51	-5
DTC403B	SURG-8M		11	0.30		4.02	0.19	299	27	28	2	44	45	2	55	58	5
DTC408A	SURG-8M		11	0.28		3.73	0.19	298	30	24	-23	46	39	-18	57	51	-13
DTC410A	SURG-8M		11	0.28		3.79	0.19	298	29	26	-12	45	41	-10	56	53	-5
DTC414B	SURG-8M		11	0.27		4.04	0.19	298	28	27	-4	45	42	-6	56	53	-5
DTC488A	SURG-8M		14	0.30		4.11	0.22	298	32	23	-43	51	40	-26	66	53	-23
DTC488B	SURG-8M		15	0.30		4.10	0.22	298	32	22	-43	50	40	-25	64	53	-22
DTC509B	SURG-8M		15	0.30		3.96	0.22	299	32	27	-18	50	44	-15	64	57	-13
DTC511B	SURG-8M		15	0.31		4.03	0.21	299	32	28	-16	51	45	-14	65	58	-12
DTC515B	SURG-8M		15	0.31		3.82	0.21	299	31	25	-24	49	41	-20	63	53	-18
DTC516A	SURG-8M		14	0.32		4.08	0.21	299	31	28	-9	49	45	-10	64	59	-9
DTC521A	SURG-8M		14	0.30		4.06	0.21	299	32	28	-14	50	45	-12	64	58	-10
DTC530A	SURG-8M		14	0.31		3.91	0.21	299	29	26	-15	47	41	-13	60	54	-11
DTC534A	SURG-8M		14	0.29		3.92	0.21	299	29	27	-7	48	44	-9	62	57	-8
DTC538A	SURG-8M		14	0.29		3.82	0.21	299	28	27	-3	46	43	-6	59	56	-5
DTC547A	SURG-8M		14	0.31		3.75	0.20	300	31	25	-21	49	41	-18	63	54	-16
DTC552A	SURG-8M		14	0.31		3.79	0.20	300	32	26	-26	52	43	-21	67	56	-20
DTC556B	SURG-8M		15	0.28		4.18	0.20	300	26	33	20	44	50	11	58	63	9
CTC171A	SURG-8M		7	0.39		5.70	0.16	300	38	36	-5	61	60	-2	-	73	
CTC171B	SURG-8M		7	0.39		5.64	0.16	300	37	35	-6	61	59	-3	-	74	
CTC180A	SURG-8M		7	0.39		5.63	0.16	298	35	35	1	57	57	0	72	71	-2
CTC182A	SURG-8M		7	0.39		5.81	0.16	298	36	34	-5	58	56	-3	74	70	-5
CTC229A	SURG-8M		9	0.40		5.63	0.15	301	24	30	20	48	55	12	64	69	7
DTC394B	SURG-8		11	0.11		3.72	0.19	296	29	30	2	34	35	2	34	36	5
DTC397B	SURG-8		11	0.13		3.80	0.19	298	32	31	-3	38	39	3	38	41	8
DTC400A	SURG-8		11	0.12		3.85	0.19	298	31	30	-4	36	37	1	36	38	5
DTC406B	SURG-8		11	0.13		4.10	0.19	299	32	33	3	37	38	3	37	38	4
DTC409B	SURG-8		11	0.11		3.64	0.19	298	31	30	-3	35	36	2	34	37	7
DTC411B	SURG-8		11	0.11		3.76	0.19	297	30	29	-3	35	35	1	34	35	4
DTC412A	SURG-8		11	0.11		3.84	0.19	297	30	31	4	35	36	5	35	37	6
DTC418B	SURG-8		11	0.10		3.81	0.19	298	30	30	-1	34	34	-2	34	34	0
DTC513B	SURG-8		15	0.13		3.83	0.21	298	35	33	-8	42	40	-4	43	42	-2
DTC519A	SURG-8		14	0.13		3.17	0.21	298	35	32	-8	41	39	-6	42	40	-5
DTC520B	SURG-8		15	0.12		4.04	0.21	299	35	34	-4	41	40	-2	42	41	-2
DTC524A	SURG-8		14	0.13		4.06	0.21	299	36	34	-6	42	40	-5	43	41	-4
DTC525B	SURG-8		15	0.13		4.00	0.21	299	37	34	-8	44	42	-6	45	43	-4
DTC531B	SURG-8		15	0.12		3.88	0.21	299	35	33	-7	42	39	-7	43	40	-6
DTC539B	SURG-8		15	0.13		3.95	0.21	299	34	34	-2	41	41	-1	42	42	0
DTC540A	SURG-8		14	0.12		3.76	0.21	299	35	33	-6	40	40	-2	42	41	-1
DTC543A	SURG-8		14	0.30		4.05	0.21	299	31	29	-5	48	45	-7	62	58	-7
DTC544B	SURG-8		15	0.13		3.81	0.21	299	36	34	-7	43	41	-3	44	43	-2
DTC548B	SURG-8		15	0.13		3.76	0.20	299	35	32	-9	42	41	-3	43	43	0
DTC553B	SURG-8		15	0.13		3.81	0.20	300	36	33	-7	43	42	-3	44	44	-1
DTC557A	SURG-8		14	0.12		4.16	0.20	300	35	35	0	42	40	-5	43	41	-6
DTC559A	SURG-8		14	0.29		4.14	0.20	299	28	32	13	46	49	6	60	62	3
DTC560A	SURG-8		15	0.12		4.12	0.20	299	34	34	-1	40	38	-4	41	39	-4
CTC195A	SURG-8		8	0.14		5.14	0.16	297	39	36	-9	44	41	-7	44	41	-5
CTC235B	SURG-8		9	0.15		5.94	0.14	301	36	37	3	40	41	2	41	42	4
CTC238B	SURG-8		9	0.16		5.83	0.14	301	37	39	4	43	44	4	43	45	5

[a] See Table 5 for the definitions of the codes used to designate run type and incremental reactivity experiment category.

[b] Characterization set. Runs with the same chamber and characterization set number are assumed to have the same chamber effects and (for CTC runs) light spectrum.

[c] Initial concentration of the test VOC used in VOC - NO_x experiments and of the added test VOC in incremental reactivity experiments

[d] Total concentration (in ppmC) of the base case surrogate components in the incremental reactivity or surrogate - NO_x runs.

[e] NO_2 photolysis rate assigned for this experiment. See Section III.B.1.a and III.B.1.b.

[f] Average measured temperature for this experiment.

Table A-9. Summary of experimental incremental reactivity results.

Run	Type	VOC (ppm)	t=3 $\Delta(O_3\text{-NO})$ (ppm)			t=6 $\Delta(O_3\text{-NO})$ (ppm)			t=6 IntOH (10^{-6} min)		
			Base	Test	IR [a]	Base	Test	IR [a]	Base	Test	IR [a]
Cyclohexane											
DTC541A	MR3	0.95	0.23	0.15	-0.07	0.62	0.45	-0.19	17	7	-11
DTC551A	MR3	1.71	0.23	0.14	-0.06	0.63	0.37	-0.15	19	4	-9
DTC543B	MR8	1.95	0.41	0.55	0.07	0.62	0.81	0.10	29	11	-9
DTC552B	MR8	1.25	0.44	0.53	0.07	0.67	0.81	0.11	28	12	-13
DTC544A	R8	0.86	0.41	0.46	0.06	0.44	0.52	0.09	27	15	-14
DTC553A	R8	1.41	0.41	0.48	0.05	0.44	0.54	0.07	27	12	-11
Isopropyl Alcohol											
DTC395A	MR3	9.48	0.26	0.42	0.02	0.61	0.96	0.04	26	22	0
DTC398B	MR3	2.51	0.24	0.33	0.04	0.57	0.80	0.09	22	24	1
DTC396B	MR8	10.65	0.37	0.76	0.04	0.56	0.81	0.02	29	26	0
DTC399A	MR8	1.97	0.36	0.52	0.08	0.53	0.72	0.10	34	28	-3
DTC397A	R8	4.96	0.37	0.49	0.03	0.38	0.50	0.02	32	21	-2
DTC400B	R8	2.09	0.35	0.43	0.04	0.36	0.44	0.04	30	24	-3
1-Octanol											
DTC508B	MR3	0.94	0.27	0.09	-0.19	0.71	0.30	-0.44	21	4	-18
DTC529A	MR3	0.18	0.23	0.17	-0.30	0.63	0.49	-0.72	18	9	-47
DTC509A	MR8	0.25	0.42	0.46	0.15	0.64	0.70	0.24	28	19	-35
DTC519B	R8	0.45	0.39	0.40	0.02	0.42	0.45	0.06	27	14	-29
2-Octanol											
DTC517A	MR3	0.25	0.25	0.20	-0.17	0.68	0.60	-0.29	-57	16	292
DTC521B	MR8	0.55	0.42	0.49	0.13	0.64	0.74	0.18	29	17	-22
DTC524B	R8	0.40	0.40	0.43	0.07	0.43	0.46	0.08	26	14	-31
3-Octanol											
DTC514B	MR3	0.26	0.28	0.19	-0.33	0.72	0.53	-0.71	20	10	-38
DTC516B	MR8	0.29	0.41	0.46	0.17	0.64	0.70	0.22	29	20	-30
DTC520A	R8	0.45	0.39	0.43	0.09	0.42	0.46	0.09	27	12	-32
Diethyl Ether											
DTC510B	MR3	0.68	0.32	0.35	0.05	0.79	0.99	0.30	23	16	-10
DTC522A	MR3	1.68	0.24	0.44	0.12	0.65	1.16	0.30	17	13	-3
DTC511A	MR8	1.79	0.43	0.97	0.30	0.65	1.09	0.24	27	18	-5
DTC515A	MR8	0.56	0.41	0.75	0.59	0.63	1.01	0.67	27	23	-8
DTC513A	R8	0.68	0.40	0.55	0.22	0.43	0.57	0.21	29	17	-17
DTC525A	R8	0.34	0.42	0.51	0.27	0.45	0.54	0.26	27	21	-17
Ethyl Acetate											
DTC358A	MR3	5.88	0.27	0.21	-0.01	0.64	0.40	-0.04	22	7	-2
DTC362B	MR3	4.29	0.24	0.19	-0.01	0.62	0.40	-0.05	19	10	-2
DTC364B	MR3	4.48	0.26	0.21	-0.01	0.63	0.41	-0.05	20	9	-2
DTC359B	MR8	5.91	0.36	0.36	0.00	0.54	0.51	0.00	28	12	-3
DTC408B	MR8	10.12	0.39	0.40	0.00	0.57	0.55	0.00	36	16	-2
DTC394A	R8	6.06	0.33	0.29	-0.01	0.35	0.33	0.00	38	13	-4

Table A-9 (continued)

Run	Type	VOC (ppm)	t=3 Δ(O_3-NO) (ppm)			t=6 Δ(O_3-NO) (ppm)			t=6 IntOH (10^{-6} min)		
			Base	Test	IR [a]	Base	Test	IR [a]	Base	Test	IR [a]
DTC409A	R8	9.03	0.34	0.29	-0.01	0.35	0.33	0.00	-83	10	10
DTC415B	R3	4.24	0.28	0.19	-0.02	0.61	0.42	-0.05	30	22	-2
CTC195B	R8	4.99	0.43	0.39	-0.01	0.44	0.42	0.00	22	11	-2
Methyl Isobutyrate											
DTC528B	MR3	5.34	0.27	0.19	-0.02	0.71	0.49	-0.04	19	7	-2
DTC533A	MR3	3.54	0.23	0.20	-0.01	0.64	0.53	-0.03	17	9	-2
DTC530B	MR8	5.20	0.39	0.45	0.01	0.60	0.71	0.02	28	16	-2
DTC534B	MR8	7.75	0.40	0.46	0.01	0.62	0.73	0.01	28	12	-2
DTC531A	R8	5.34	0.40	0.41	0.00	0.43	0.47	0.01	27	13	-3
DTC539A	R8	7.38	0.39	0.40	0.00	0.42	0.47	0.01	26	-67	-13
DTC548A	R8	9.99	0.40	0.41	0.00	0.43	0.48	0.00	-70	7	8
n-Butyl Acetate											
DTC365A	MR3	5.88	0.24	0.14	-0.02	0.61	0.33	-0.05	21	3	-3
DTC368B	MR3	6.30	0.24	0.13	-0.02	0.61	0.32	-0.05	-58	-58	0
DTC402B	MR3	3.79	0.25	0.16	-0.02	0.61	0.39	-0.06	18	5	-4
DTC403A	MR8	5.15	0.37	0.50	0.02	0.55	0.70	0.03	29	10	-4
DTC410B	MR8	7.60	0.38	0.53	0.02	0.56	0.71	0.02	28	8	-3
DTC406A	R8	3.69	0.35	0.40	0.01	0.37	0.44	0.02	29	10	-5
DTC411A	R8	7.72	0.34	0.39	0.01	0.34	0.43	0.01	26	6	-3
CTC196A	MR3	3.98	0.22	0.09	-0.03	0.58	0.25	-0.08	19	3	-4
1-Methoxy-2-Propyl Acetate (Propylene Glycol Methyl Ether Acetate)											
DTC532B	MR3	0.88	0.22	0.17	-0.06	0.64	0.40	-0.27	18	5	-15
DTC537A	MR3	0.50	0.22	0.20	-0.03	0.61	0.48	-0.25	-51	9	120
DTC549B	MR3	1.05	0.21	0.20	-0.02	0.70	0.45	-0.23	20	6	-14
DTC538B	MR8	0.99	0.38	0.46	0.08	0.59	0.68	0.09	28	10	-17
DTC547B	MR8	1.53	0.41	0.50	0.06	0.63	0.72	0.06	25	8	-11
DTC540B	R8	0.96	0.39	0.40	0.01	0.42	0.46	0.05	24	9	-15
Methyl Ethyl Ketone											
DTC338A	MR8	4.03	0.33	0.47	0.03	0.50	0.64	0.03	26	22	-1
DTC345B	MRX	1.65	0.26	0.38	0.08	0.65	0.75	0.06	22	22	0
DTC363A	MRX	2.60	0.26	0.42	0.06	0.62	0.75	0.05	20	19	0
CTC181A	MR3	3.01	0.26	0.36	0.03	0.63	0.62	0.00	22	17	-2
CTC180B	MR8	4.08	0.48	0.58	0.02	0.72	0.82	0.02	25	19	-2
Cyclohexanone											
DTC554B	MR3	1.90	0.25	0.15	-0.05	0.66	0.33	-0.17	18	3	-8
DTC558A	MR3	1.33	0.22	0.16	-0.04	0.61	0.38	-0.17	18	7	-8
DTC556A	MR8	1.19	0.37	0.37	0.00	0.58	0.56	-0.02	26	13	-11
DTC559B	MR8	1.95	0.38	0.36	-0.01	0.60	0.54	-0.03	29	10	-10
DTC557B	R8	2.20	0.40	0.33	-0.03	0.43	0.39	-0.02	27	8	-9
DTC560A	R8	1.12	0.34	0.39	0.04	0.38	0.41	0.02	14	26	11
CTC227A	MR3	1.26	0.17	0.09	-0.06	0.51	0.23	-0.22	17	4	-10
CTC229B	MR8	2.43	0.39	0.38	0.00	0.64	0.49	-0.06	21	9	-5
CTC235A	R8	1.79	0.39	0.36	-0.02	0.41	-1.00	-0.78	21	9	-7

Table A-9 (continued)

Run	Type	VOC (ppm)	t=3 $\Delta(O_3$-NO) (ppm)			t=6 $\Delta(O_3$-NO) (ppm)			t=6 IntOH (10^{-6} min)		
			Base	Test	IR [a]	Base	Test	IR [a]	Base	Test	IR [a]
CTC238A	R8	0.84	0.41	0.41	-0.01	0.43	-1.00	-1.71	22	14	-10
4-Methyl-2-Pentanone (Methyl Isobutyl Ketone)											
DTC366B	MR3	3.39	0.24	0.25	0.00	0.60	0.47	-0.04	21	5	-5
DTC369A	MR3	4.33	0.23	0.27	0.01	0.59	0.50	-0.02	19	4	-3
DTC370B	MR8	3.25	0.33	0.42	0.03	0.50	0.63	0.04	25	5	-6
DTC414A	MR8	9.32	0.38	0.48	0.01	0.56	0.67	0.01	29	5	-3
DTC412B	R8	9.02	0.34	0.29	-0.01	0.35	0.30	-0.01	32	10	-2
DTC418A	R8	2.53	0.33	0.31	-0.01	0.34	0.33	0.00	37	10	-11
CTC183A	MR3	1.91	0.24	0.16	-0.04	0.61	0.32	-0.16	22	4	-10
CTC182B	MR8	1.78	0.50	0.54	0.03	0.74	0.78	0.02	25	8	-10

[a] Incremental Reactivity = (Test Results -Base Results)/(Test VOC Added).